SACLANTCEN Memorandum SM - 121

AD A067256

DDC FILE COPY

LEVEL II

SACLANTCEN Memorandum
SM -121

SACLANT ASW RESEARCH CENTRE MEMORANDUM

DDC
RECEIVED
APR 13 1979
C

SNAP: THE SACLANTCEN NORMAL-MODE ACOUSTIC PROPAGATION MODEL

by

FINN B. JENSEN and MELCHIORRE C. FERLA

Memorandum rept.,

12 109 p.

11 15 JANUARY 1979

This document has been approved for public release and sale; its distribution is unlimited.

NORTH ATLANTIC TREATY ORGANIZATION

LA SPEZIA, ITALY

This document is unclassified. The information it contains is published subject to the conditions of the legend printed on the inside cover. Short quotations from it may be made in other publications if credit is given to the author(s). Except for working copies for research purposes or for use in official NATO publications, reproduction requires the authorization of the Director of SACLANTCEN.

79 04 11 029

317 950

This document is released to a NATO Government at the direction of the SACLANTCEN subject to the following conditions:

1. The recipient NATO Government agrees to use its best endeavours to ensure that the information herein disclosed, whether or not it bears a security classification, is not dealt with in any manner (a) contrary to the intent of the provisions of the Charter of the Centre, or (b) prejudicial to the rights of the owner thereof to obtain patent, copyright, or other like statutory protection therefor.

2. If the technical information was originally released to the Centre by a NATO Government subject to restrictions clearly marked on this document the recipient NATO Government agrees to use its best endeavours to abide by the terms of the restrictions so imposed by the releasing Government.

Published by

STI

SACLANTCEN MEMORANDUM SM-121

NORTH ATLANTIC TREATY ORGANIZATION

SACLANT ASW Research Centre
Viale San Bartolomeo 400, I-19026 San Bartolomeo (SP), Italy.

tel: national 0187 503540
international + 39 187 503540

telex: 271148 SACENT I

DDC
RECEIVED
APR 13 1979
C

SNAP: THE SACLANTCEN NORMAL-MODE ACOUSTIC PROPAGATION MODEL

by

Finn B. Jensen and Melchiorre C. Ferla

15 January 1979

This memorandum has been prepared within the SACLANTCEN Underwater Research Division.

G.C. VETTORI
Division Chief

This document has been approved for public release and sale; its distribution is unlimited.

79 04 11 029

TABLE OF CONTENTS

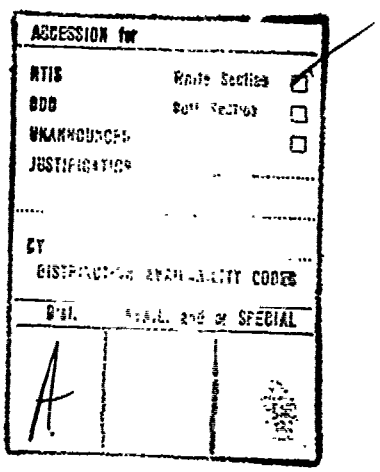

Available upon request as SACLANTCEN Special Report M-91

**Available upon request as SACLANTCEN Special Report M-92*

TABLE OF CONTENTS (Cont'd)

List of Figures

TABLE OF CONTENTS (Cont'd)

List of Tables

SNAP: THE SACLANTCEN NORMAL-MODE ACOUSTIC PROPAGATION MODEL

by

Finn B. Jensen and Melchiorre C. Ferla

ABSTRACT

A sound-propagation model based on normal mode theory is described. The model is designed to give a realistic treatment of the ocean environment, including arbitrary sound-speed profiles in both water column and bottom, compressional and shear wave attenuation, scattering at rough boundaries, and range dependence. Furthermore, the model has a flexible input/output structure that facilitates model handling and provides users with a wide choice of computational (output) options, ranging from plots of sound-speed profiles and individual mode functions to contoured transmission loss versus depth and range or versus frequency and range. The computer code is written in FORTRAN V with a few routines in NUALGOL. The version documented here runs on a UNIVAC 1106.

INTRODUCTION

This report represents the end of a major modelling project started at SACLANTCEN in 1974 with the objective of developing an acoustic model particularly suited for handling propagation in shallow water.

The SACLANTCEN Normal-mode Acoustic Propagation model (SNAP) is based on mode theory, which is just one of several wave theoretic solutions employed in acoustic modelling today *[1,2]*. The reasons for choosing the modal solution as basis for a SACLANTCEN standard shallow-water model were many. First of all, some major U.S. naval laboratories were already using mode models intensively with good results *[3]*. Secondly, the U.S. Naval Research Laboratory, Washington, D.C., made available to SACLANTCEN their normal-mode model, which provided a good starting point for creating a version particularly suited for modelling needs at SACLANTCEN. Finally, as was apparent from the NRL version, a mode program can be easily automated, which is an important factor for prospective model users.

Even if considerable effort has been put into the development of the SNAP model, it was realised at an early stage that a normal-mode model would not be a universal answer to all modelling needs *[2]*. Thus, even if SNAP is an accurate and versatile model, it cannot handle propagation in, for instance, a strongly range-dependent environment. Likewise, the SNAP model is an impractical tool for propagation in deep water at high frequencies ($f > 1$ kHz) due to the excessive computation times involved. Therefore alternative propagation models are needed, and work has been done on both the Parabolic Equation (PE) model *[1]* and on a ray-trace model *[4]*. Recently, also a Fast Field Program (FFP) was implemented at SACLANTCEN *[5]*.

However, in spite of the need for several acoustic models to cover all possible propagation cases, the great majority of shallow-water environments can be handled adequately by the SNAP model, and it is exactly for that reason the model has been developed. In fact, the SNAP model has already proved to be an excellent research tool, mainly due to its flexible input/output system and to its versatility in handling a variety of propagation conditions.

Two different program versions are documented in this memorandum: (1) a general-purpose range-dependent version (SNAP), and (2) a smaller and faster range-independent version (SNAP1).

1 ENVIRONMENT HANDLED BY SNAP

The SNAP model has been designed to treat a shallow-water ocean environment as realistically as possible. As shown in Fig. 1, the environment is a half space subdivided into three layers: a water column of depth H_o, a sediment layer of thickness H_1, and a semi-infinite subbottom. In the water column the sound speed $c_o(z)$ is allowed to vary arbitrarily with depth, while density ρ_o and volume attenuation β_o are taken to be constant over depth. The sediment layer is treated in exactly the same way: an arbitrary sound-speed profile $c_1(z)$, a constant density ρ_1, and a constant volume attenuation β_1. The subbottom, on the other hand, is treated as a solid with depth-independent properties: c_{2S} is the shear speed and β_{2S} the shear attenuation; c_2 is the compressional speed, ρ_2 the density, and β_2 the compressional attenuation.

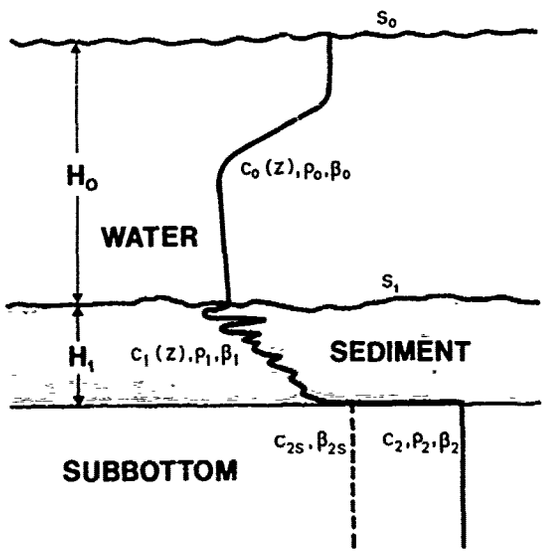

FIG. 1 ENVIRONMENT HANDLED BY SNAP

Furthermore, both sea surface (pressure release) and sea floor are treated as rough boundaries with the rms roughness heights given by the parameters s_o and s_1, respectively.

Finally, in the general-purpose SNAP model all environmental parameters given in Fig. 1 are allowed to vary with range. Such a range-dependent environment is simulated by dividing the full range into a certain number of segments, all with different but range-independent properties.

2 THEORETICAL BASIS

2.1 Introductory

We first consider the simplified geometry given in Fig. 2. Here all three layers are taken to be lossless ($\beta_o = \beta_1 = \beta_2 = 0$), and both sea surface and sea floor are taken to be smooth ($s_o = s_1 = 0$). Furthermore, shear properties of the subbottom are omitted. Then the acoustic field from a harmonic point source of unit strength at position $(0,z_o)$ can be written in terms of normal modes as

$$P(r,z) = \frac{\omega\rho_o^2}{4} \sum_{n=1}^{N} u_n(z_o)\, u_n(z)\, \mathcal{H}_o^{(1)}(k_n r) \quad , \qquad \text{(Eq. 1)}$$

where ω is the source frequency ($\omega = 2\pi f$), u_n the normalized modal eigenfunction, k_n the modal eigenvalue (wave number), and $\mathcal{H}_o^{(1)}$ the zeroth-order Hankel function of the first kind *[6,7]*. In arriving at Eq. 1, the propagation geometry has been assumed to be range independent and cylindrically symmetric around the vertical z-axis. Moreover, a time dependence of $\exp(-i\omega t)$ has been omitted from the formula.

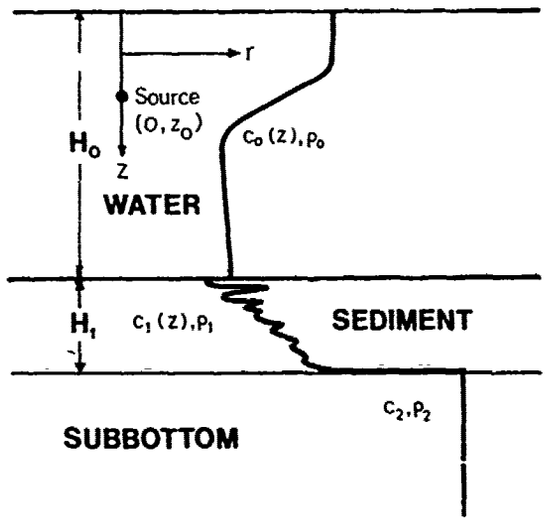

FIG. 2 SIMPLIFIED GEOMETRY FOR MODE CALCULATIONS

In Eq. 1 the summation is done only over the discrete set of normal modes. Actually, the acoustic field is composed of both a continuous and a discrete part, but it can be shown that the continuous spectrum generally gives a negligible contribution beyond the nearfield of the source,

particularly if any loss mechanism (bottom loss) is introduced into the system.

As shown in [7], the mode functions $u_n(z)$ are solutions to the depth-dependent Helmholtz equation

$$\frac{d^2u_n(z)}{dz^2} + \left[\left(\frac{\omega}{c(z)}\right)^2 - k_n^2 \right] u_n(z) = 0 \quad , \qquad \text{(Eq. 2)}$$

which poses an eigenvalue problem with a finite number N of discrete eigenfunctions for k_n in the interval

$$\frac{\omega}{c_2} < k_n < \max \left[\frac{\omega}{c_o(z)} , \frac{\omega}{c_1(z)} \right] \quad . \qquad \text{(Eq. 3)}$$

This last inequality imposes a bound on the speed c_2 in the subbottom. Thus, for discrete modes to exist, the bottom speed must be higher than the minimum speed encountered in water column and sediment, i.e.

$$c_2 > \min [c_o(z), c_1(z)] \quad . \qquad \text{(Eq. 4)}$$

Equation 2 is the fundamental equation to be solved by the SNAP computer program. Before passing to a description of the numerical solution technique, it should be emphasized that the modal solution obtained from Eq. 2 applies only to a lossless environment. Several loss factors will, however, be introduced later as perturbations to the lossless case.

2.2 Modal computations

The ordinary, second-order differential equation, Eq. 2, together with appropriate boundary conditions poses an eigenvalue problem with solutions $u_n(z)$ for only a discrete set of k_n values. The eigenfunctions $u_n(z)$ are the mode-amplitude functions, while the eigenvalues k_n are the horizontal wave numbers. A solution is found by a finite-difference technique. Thus, both water column and sediment layer are subdivided into a number of incremental layers, LIØ and LI1, respectively. The

sound-speed profile $c(z)$ is entered as a discrete set of points, and linear interpolation is performed between the profile depths in order to assign sound speeds to all incremental layers.

The boundary conditions for continuity of acoustic pressure and of the vertical particle velocity are matched at both the subbottom/sediment interface and at the sediment/water interface. At the sea surface (pressure release) it is required that the pressure be zero to within a designated epsilon. Trial solutions for k_n are made to find the wave numbers corresponding to the discrete set of modes. When a solution is bracketed, a false-position technique proceeds to find the acceptable solution, and the mode amplitude function $u_n(z)$ is calculated and normalized. For details of the mode solution technique, see *[8]* and *[9]*.

Even though the basic solution technique used in the SNAP program is identical to the one described in the above references, the actual numerical routines are different and so is the program structure. Actually, the SNAP model can be considered as an improved version of the model described in *[9]*, with substantial improvements in computational speed as well as in program size.

As mentioned earlier, if discrete modes exist, the number of modes is finite, and the number will generally be dependent on both source frequency and environmental parameters. In the special case of isovelocity water of depth H_o and speed c_W overlying a semi-infinite bottom with constant speed c_B, the number of modes is given by the integer part of

$$N = \frac{2H_o f}{c_W} \sqrt{1 - \left(\frac{c_W}{c_B}\right)^2} + 0.5 \quad , \qquad \text{(Eq. 5)}$$

where f is the source frequency (*[10]*, p. 372). From this formula we can also derive the cut-off frequency f_c below which there are no discrete modes. Thus, by inserting $N = 1$ we find for isovelocity water

$$f_c = \frac{c_W}{4H_o \sqrt{1 - \left(\frac{c_W}{c_B}\right)^2}} \quad . \qquad \text{(Eq. 6)}$$

In the general case where the water speed changes with depth, the exact number of modes N can be obtained only from the computer program. However, by substituting for c_W the average water speed $\bar{c}_W$, an approximation to the actual number of modes may be obtained from Eq. 5. It is found, however, that the formula always gives too high numbers.

An empirical formula established on the basis of a variety of test cases with different sound-speed profiles determines the number of modes as the integer part of

$$N = \frac{2Hf}{\bar{c}_W} \cdot \frac{\ell n\left(\sqrt{1 - \frac{\bar{c}_W}{c_B}} + 1\right)}{\ell n\ 2} + 0.5 \quad . \qquad \text{(Eq. 7)}$$

This formula is generally more accurate than Eq. 5, and it gives N to within ±5% for both shallow and deep-water environments. If a sediment layer exists, the speed $\bar{c}_W$ should include averaging over both water and sediment. Also the depth H should in that case include the sediment layer, i.e. $H = H_o + H_1$. The cut-off frequency is found from Eq. 7 to be

$$f_c = \frac{\bar{c}_W \cdot \ell n\ 2}{4H \cdot \ell n\left(\sqrt{1 - \frac{\bar{c}_W}{c_B}} + 1\right)} \quad . \qquad \text{(Eq. 8)}$$

We see from Eqs. 5 and 7 that the number of modes is directly proportional to both water depth and source frequency.

2.3 Modal loss computations

If some kind of loss is introduced into the system, the modal wave numbers become complex with a small imaginary part. By substituting $k_n + i\alpha_n$ for k_n in Eq. 1, we obtain

$$P(r,z) = \frac{\omega\rho_o^2}{4} \sum_{n=1}^{N} u_n(z_o)\ u_n(z)\ \mathcal{H}_o^{(1)}(k_n r + i\alpha_n r) \quad . \qquad \text{(Eq. 9)}$$

At sufficiently long range the asymptotic form of the Hankel function can be used

$$H_o^{(1)}(k_n r + i\alpha_n r) \simeq \sqrt{\frac{2}{\pi k_n r}}\, e^{i(k_n r + i\alpha_n r - \frac{\pi}{4})} \qquad \text{(Eq. 10)}$$

leading to the following expression for the acoustic field *[6,7]*:

$$P(r,z) = \omega\rho_c^2 \sqrt{\frac{i}{8\pi r}} \sum_{n=1}^{N} \frac{u_n(z_o)\, u_n(z)}{\sqrt{k_n}} \cdot e^{-\alpha_n r} \cdot e^{i(k_n r - \frac{\pi}{4})} . \qquad \text{(Eq. 11)}$$

In SNAP the modal attenuation coefficient α_n is written as a sum of individual loss terms:

$$\alpha_n = \alpha_n^{(0)} + \alpha_n^{(1)} + \begin{Bmatrix} \alpha_n^{(2)} \\ \alpha_n^{(2S)} \end{Bmatrix} + \alpha_n^{(OS)} + \alpha_n^{(OB)} \qquad \text{(Eq. 12)}$$

each corresponding to a particular loss mechanism, as given below:

$\alpha_n^{(0)}$: Compressional-wave attenuation in water,

$\alpha_n^{(1)}$: Compressional-wave attenuation in sediment,

$\alpha_n^{(2)}$: Compressional-wave attenuation in subbottom,

$\alpha_n^{(2S)}$: Compressional and shear losses in subbottom,

$\alpha_n^{(OS)}$: Scattering loss at sea surface,

$\alpha_n^{(OB)}$: Scattering loss at sea floor.

The choice between the use of $\alpha_n^{(2)}$ or $\alpha_n^{(2S)}$ depends on the bottom properties. Thus, if the subbottom is taken to be a fluid (no shear waves), the coefficient $\alpha_n^{(2)}$ is used; if, on the other hand, the subbottom is considered a solid, $\alpha_n^{(2S)}$ is used.

Before giving the various formulas for calculating the attenuation coefficients, a useful general notation is introduced:

$$u_n(z) = \begin{cases} u_n^{(0)}(z) & \text{for water} \\ u_n^{(1)}(z) & \text{for sediment} \\ u_n^{(2)}(z) & \text{for subbottom} \end{cases}$$

$$k_{n,z}^{(0)}(z) = \sqrt{\left(\frac{\omega}{c_o(z)}\right)^2 - k_n^2}$$

$$k_{n,z}^{(1)}(z) = \sqrt{\left(\frac{\omega}{c_1(z)}\right)^2 - k_n^2}$$

$$k_{n,z}^{(2)} = \left| \sqrt{\left(\frac{\omega}{c_2}\right)^2 - k_n^2} \right|$$

$$H_2 = H_o + H_1 \quad .$$

The modal attenuation coefficients arising from compressional-wave attenuation in the various layers are given by the following expressions *[6,7]*:

$$\alpha_n^{(0)} = \frac{\beta_o f}{\bar{c}_o \cdot (20 \log e)} \frac{\omega \rho_o}{k_n} \int_0^{H_o} \frac{[u_n^{(0)}(z)]^2}{c_o(z)} dz \quad , \qquad \text{(Eq. 13)}$$

$$\alpha_n^{(1)} = \frac{\beta_1 f}{\bar{c}_1 \cdot (20 \log e)} \frac{\omega \rho_1}{k_n} \int_{H_1}^{H_2} \frac{[u_n^{(1)}(z)]^2}{c_1(z)} dz \quad , \qquad \text{(Eq. 14)}$$

$$\alpha_n^{(2)} = \frac{\beta_2 f}{c_2 \cdot (20 \log e)} \frac{\omega \rho_2}{k_n} \int_{H_2}^{\infty} \frac{[u_n^{(2)}(z)]^2}{c_2} dz \quad , \qquad \text{(Eq. 15)}$$

where β_o, β_1, and β_2 are the plane-wave attenuation coefficients of compressional waves in water, sediment, and subbottom, respectively. The attenuation coefficient β_o for water is currently computed in the SNAP program from a formula, given in *[11]*,

$$\beta_o = \frac{\bar{c}_o}{f}\left(0.007\ f^2 + 0.155\ \frac{1.7\ f^2}{1.7^2+f^2\cdot 10^{-6}}\right)10^{-9} \quad \left[\frac{dB}{\lambda}\right], \quad \text{(Eq. 16)}$$

where $\bar{c}_o$ is the average sound speed in the water column in m/s and f the source frequency in Hz. The unit is dB/λ, i.e. dB per wavelength. Equation 16 has been established on the basis of experimental data collected in the Mediterranean Sea. The factor $f/(\bar{c}_o\ 20 \log e)$, multiplying β_o in Eq. 13, converts the unit dB/λ into nepers/m.

The two bottom attenuation coefficients β_1 and β_2 are input parameters to the program and should be given in dB/λ. By using this unit we are implying that the attenuation in dB/m increases linearly with frequency, which is in agreement with results reported in *[12]*. Thus, β_1 and β_2 are independent of frequency.

The modal attenuation coefficient arising from compressional and shear losses in the subbottom is taken from *[13]* and *[14]*:

$$\alpha_n^{(2S)} = \rho_1 \frac{[u_n^{(1)}(H_2)]^2 \cdot k_{n,z}^{(1)}(H_2)}{8k_n}\left[1 + \left(\frac{\rho_1 \cdot k_{n,z}^{(2)}}{\rho_2 \cdot k_{n,z}^{(1)}(H_2)}\right)^2\right] Q(\theta_n) \ , \quad \text{(Eq. 17)}$$

where $Q(\theta_n) = 1 - |R|^2$ for $\cos\theta_n \leq 1$

$Q(\theta_n) = 2R_i$ for $\cos\theta_n > 1$.

Here $R = R_r + iR_i$ is the complex plane-wave reflection coefficient at the interface between sediment and subbottom. θ_n is the grazing angle at the same interface, determined from

$$\cos\theta_n = \frac{k_n}{\omega/c_1(H_2)} \quad \text{(Eq. 18)}$$

We see from Eq. 17 that the expression used for $Q(\theta_n)$ depends on the grazing angle. Thus, for real angles ($\cos \theta_n \leq 1$), Q is a function of the modulus of the complex reflection coefficient, while for non-real angles ($\cos \theta_n > 1$) Q is proportional to only the imaginary part of R. In the latter case the modes are evanescent at the interface between sediment and subbottom.

The reflection coefficient R is calculated from the following expression, which may be derived from the formula given in *[10]*, p. 31:

$$R = \frac{A + B - C}{A + B + C} \quad , \qquad \text{(Eq. 19)}$$

where

$$A = \frac{\rho_2 c_2}{\sqrt{1 - \left(\frac{c_2}{c_1(H_2)} \cdot \cos \theta_n\right)^2}} \left[1 - 2\left(\frac{c_{2S}}{c_1(H_2)} \cdot \cos \theta_n\right)^2\right]^2$$

$$B = \frac{\rho_2 c_{2S}}{\sqrt{1 - \left(\frac{c_{2S}}{c_1(H_2)} \cdot \cos \theta_n\right)^2}} \left\{1 - \left[1 - 2\left(\frac{c_{2S}}{c_1(H_2)} \cdot \cos \theta_n\right)^2\right]^2\right\}$$

$$C = \frac{\rho_1 c_1(H_2)}{\sin \theta_n} \quad .$$

The computer code corresponding to Eq. 19 was obtained from *[15]*.

Since Eq. 17 is based on a perturbation approach, its validity is limited to small reflection losses, i.e.

$$RB \equiv Q(\theta_n) << 1 \quad . \qquad \text{(Eq. 20)}$$

This criterion must be fulfilled at least for the most important modes, which in general are the lower-order modes.

The two modal attenuation coefficients arising from surface and bottom scattering losses are taken from *[7]*:

$$\alpha_n^{(OS)} = \frac{\rho_o s_o^2 \cdot k_{n,z}^{(0)}(0)}{2k_n} \left(\frac{du_n^{(0)}(z)}{dz} \right)^2_{z=0} \qquad \text{(Eq. 21)}$$

$$\alpha_n^{(OB)} = \frac{\rho_o s_1^2 \cdot k_{n,z}^{(0)}(H_o)}{2k_n} \left\{ \left(\frac{du_n^{(0)}(z)}{dz} \right)^2_{z=H_o} + \left[u_n^{(0)}(H_o) \cdot k_{n,z}^{(0)}(H_o) \right]^2 \right\} \quad , \qquad \text{(Eq. 22)}$$

where s_o and s_1 are the rms roughness heights of sea surface and sea floor, respectively. Note that the more general expression for reflection loss at the sea floor (Eq. 22) reduces to the sea-surface formula (Eq. 21) for $u_n = 0$, which is exactly the boundary condition imposed at the free surface.

The above formulas are both derived on the basis of a boundary perturbation method, and their validity is limited to small wave heights, as given by the following expressions:

$$SS \equiv 2s_o^2 \cdot \left[k_{n,z}^{(0)}(0) \right]^2 << 1 \qquad \text{(Eq. 23)}$$

$$SB \equiv 2s_1^2 \cdot \left[k_{n,z}^{(0)}(H_o) \right]^2 << 1 \quad . \qquad \text{(Eq. 24)}$$

It should also be pointed out that Eqs. 21 and 22 are valid only for scattering in the Kirchhoff approximation, and that the formulas deal only with the coherent component of the scattered field. Thus, by using Eqs. 21 and 22 we are neglecting contributions from the non-specularly reflected energy, a fact that generally leads to an overestimation of modal scattering losses in the SNAP model.

2.4 Transmission loss

The acoustic field from a point source of unit source strength is given as a function of range and depth by Eq. 11. By introducing the abbreviations

$$A_n = \frac{u_n(z_o)\, u_n(z)}{\sqrt{k_n}}\, e^{-\alpha_n r} \qquad \text{(Eq. 25)}$$

$$\gamma_n = k_n r - \frac{\pi}{4} \qquad \text{(Eq. 26)}$$

Equation 11 takes the form

$$P(r,z) = \omega\rho_o^2 \sqrt{\frac{i}{8\pi r}} \sum_{n=1}^{N} A_n \cdot e^{i\gamma_n} \quad . \qquad \text{(Eq. 27)}$$

Since the pressure amplitude at a distance of 1 m from a point source of unit strength is given by

$$P_1 = \frac{\omega\rho_o}{4\pi} \qquad \text{(Eq. 28)}$$

the transmission loss in dB re 1 m may be calculated from the expression

$$TL = -20 \log \frac{P}{P_1} \quad , \qquad \text{(Eq. 29)}$$

leadirg to

$$TL = -20 \log \left| \left[\rho_o \sqrt{\frac{2\pi}{r}} \sum_{n=1}^{N} A_n \cdot e^{i\gamma_n} \right] \right| \quad . \qquad \text{(Eq. 30)}$$

From the above summation we obtain the following expression for transmission loss by coherent addition of modes:

$$TL_{COH} = -20 \log \left[\rho_o \sqrt{\frac{2\pi}{r}} \sqrt{\left(\sum_{n=1}^{N} A_n \cdot \cos \gamma_n \right)^2 + \left(\sum_{n=1}^{N} A_n \cdot \sin \gamma_n \right)^2} \right] . \qquad \text{(Eq. 31)}$$

Modes may also be added incoherently, which mathematically means that they are assigned a uniformly-distributed random phase. We then obtain

$$TL_{INC} = -20 \log \left[\rho_o \sqrt{\frac{2\pi}{r}} \sqrt{\sum_{n=1}^{N} A_n^2} \right] \qquad \text{(Eq. 32)}$$

The SNAP model generally allows transmission loss calculations to be carried out by both coherent and incoherent addition of modes. However, it should be pointed out that only results obtained by coherent addition of modes (Eq. 31) are true deterministic representations of the acoustic field from a harmonic point source. On the other hand, by adding modes incoherently, an average acoustic field intensity is obtained. In fact, it can be shown that the incoherent result can be obtained by averaging the coherent result either in space or in frequency. Finally, while incoherent results make good sense in shallow water, they should never be applied to deep-water propagation, since characteristic features, such as caustics and shadow zones, will be averaged out by an incoherent addition of the modes.

The SNAP model also provides depth-averaged transmission loss computed from

$$TL_{AVR} = -10 \log \left[\frac{1}{H_o} \int_0^{H_o} 10^{-\frac{TL}{10}} dz \right] . \qquad \text{(Eq. 33)}$$

In the program the averaging over the water column is done numerically by means of a Simpson integration scheme. We see that computed transmission losses are converted to pressure squared (P^2) before the averaging is performed. Thus it is an energy averaging that is done in the SNAP model.

Three more formulas will be given here. The first two are related to the output option ANGLE, which gives field intensity versus arrival angle. The angle asssociated with each mode at a given point in space is calculated from

$$\theta_n = \cos^{-1}\left(\frac{k_n}{\omega / c_o(z)} \right) , \qquad \text{(Eq. 34)}$$

while the amount of energy carried by the individual modes is given by

$$TL_n = -20 \log\left|\left[\rho_o \sqrt{\frac{2\pi}{r}} A_n\right]\right| \quad . \qquad \text{(Eq. 35)}$$

It may happen for lower-order modes that $k_n > \omega/c_o(z)$ in certain parts of the water column. In that case no real angle can be associated with the modes, which are evanescent in that particular region. Evanescent modes generally carry very little energy and can therefore be neglected.

The third formula is associated with the output option PHASE, which provides phase distribution over the water column of the acoustic field. The phase is normalized to zero at the surface and given by the expression

$$\psi(z) = \tan^{-1}\left(\frac{\sum_{n=1}^{N} A_n \cdot \sin \gamma_n}{\sum_{n=1}^{N} A_n \cdot \cos \gamma_n}\right) - \psi(0) \quad , \qquad \text{(Eq. 36)}$$

which may be derived from Eq. 27.

2.5 Range dependence

A range-dependent environment is simulated in the SNAP model by dividing the full range into a number of segments, each with different range-independent properties. The mode set corresponding to each segment is then computed together with wave numbers, k_n, and attenuation coefficients, α_n. Hence there is no significant difference between computing modal properties for a range-independent and a range-dependent environment. The difference arises when summing the modes, since several parameters change from segment to segment. In the SNAP model the modes are summed in the adiabatic approximation (*[16]*, p. 48) leading to the following expression for the acoustic field:

$$P(r,z) = \omega\rho_o^2 \sqrt{\frac{1}{8\pi r}} \sum_{n=1}^{N^*} \frac{u_n'(z_o)\, u_n''(z)}{\sqrt{k_n}} \cdot e^{-\bar{\alpha}_n r} \cdot e^{i(\bar{k}_n r - \frac{\pi}{4})} \quad ,$$

(Eq. 37)

where

u'_n : normalized mode amplitude at source

u''_n : normalized mode amplitude at receiver

$\bar{k}_n$: range-averaged wave number $\left(= \frac{1}{r} \int_o^r k_n(r)\, dr\right)$

$\bar{\alpha}_n$: range-averaged att. coef. $\left(= \frac{1}{r} \int_o^r \alpha_n(r)\, dr\right)$

and n^* denotes the lowest number of modes existing in any given segment between source and receiver. Thus if, for instance, five segments are considered with the following number of discrete modes: 12, 14, 15, 11, and 14, the summation within each segment would be over the following number of modes: 12, 12, 11, 11, and 11. Note that Eq. 37 reduces to Eq. 11 for a range-independent environment.

To avoid discontinuities in the pressure field at the segment interfaces, all range-dependent variables such as u_n, k_n, and α_n are interpolated in range before Eq. 37 is evaluated. Finally, transmission losses are calculated from formulas similar to the ones given by Eqs. 31 and 32.

Strictly speaking, a solution for the acoustic field in terms of normal modes can be obtained only for a horizontally-stratified environment. Therefore, any attempt to handle a range-dependent environment by mode theory has to be an approximate solution with a limited range of validity. Actually, the adiabatic approximation works well only for slight changes in environmental parameters with range. According to [17], the following two inequalities have to be satisfied:

$$f << \frac{\Delta k^2_{1,2} \cdot \langle c_o^2 \rangle}{4\pi \left| \left\langle \frac{\partial c_o}{\partial r} \right\rangle \right|} \qquad \text{(Eq. 38)}$$

$$\left| k^2_{n,p} - k^2_{n,p+1} \right| << \left| k^2_{n,p} - k^2_{n+1,p} \right| \ . \qquad \text{(Eq. 39)}$$

Here c_o denotes the sound speed in the water column, which is generally

a function of both range and depth, i.e. $c_o = c_o(r,z)$. The symbol $\langle\rangle$ indicates averaging over the water column, while $\Delta k_{1,2}$ is the wave number difference between first and second mode.

In Eq. 39, n denotes the mode number and p the segment number. This inequality essentially says that no overlap in wave-number space is allowed from segment to segment, i.e. the wave number corresponding to mode n in segment p cannot correspond to modes $n-1$ or $n+1$ in segment $p+1$, but only to the same mode n.

We see that Eq. 38 limits the range of frequencies that can be considered for a given environment, while Eq. 39 imposes a lower limit on the number of segments that can be used.

3 INPUT DATA

A summary of the data input structure is given in Tables 1 to 5. The first part of the input (Table 1) deals primarily with the environment, while the second part (Tables 2 to 5) deals with the available computational and output options.

3.1 Environmental input

The environment handled by the SNAP model was described in Ch. 1 (Fig. 1). Here the environmental input to the computer program will be discussed in detail. Table 1 gives a summary of the input, with each line corresponding to a card in the data deck. All inputs are in free format, which means that parameters on the same card should be separated by either commas or blanks. The following is a line-by-line comment on the environmental inputs of Table 1.

TITLE A string of no more than 80 alphanumeric characters that will will appear as the heading on all plots.

NF Number of source frequencies (≤ 25).

F Source frequency in hertz. The frequencies can be entered in any order, but the program will start execution from the lowest frequency.

MMIN First mode to be calculated.

MMAX Last mode to be calculated. Since the program is set up to calculate a maximum of 500 modes, an appropriate input is [MMIN,MMAX] = [1,500], meaning that all modes will be computed. However, for particular studies it can be of interest to investigate the properties of individual modes or of certain mode sets. This can be obtained by specifying for instance:

[MMIN,MMAX] = [5,5] : only mode 5 computed.
[MMIN,MMAX] = [7,20]: only modes 7 to 20 computed.

LIØ Number of discretization points in the water column.

TABLE 1 SUMMARY OF SNAP INPUTS (PART I)

INPUT PARAMETER	EXPLANATION	UNIT	LIMITS
TITLE	Text on plots	-	≤ 50 characters
NF	No. of source frequencies	-	NF ≤ 25
F(1),·····F(NF)	Source frequencies	Hz	F > 0
MMIN,MMAX	MMIN: First mode to be calculated MMAX: Last mode to be calculated	- -	1 ≤ MMIN ≤ MMAX ≤ 500
LI0,LI1	LI0: No. of discretization points in water LI1: No. of discretization points in sediment	- -	0 < LI0+LI1 ≤ 2500
NSEG	No. of segments in range	-	NSEG ≥ 1
SEGL(1)	Length of first segment	km	SEGL > 0
H0,S0,S1	H0: Water depth in first segment S0: RMS roughness of sea surface S1: RMS roughness of sea bottom	m m m	H0 > 0 S0 ≥ 0 S1 ≥ 0
Z0(1),C0(1)	Z0(1): First sound-speed profile depth (= 0) C0(1): First sound-speed profile value in water	m m/s	- -
⋮	⋮	⋮	⋮
Z0(n),C0(n)	Z0(n): Last sound-speed profile depth (= H0) C0(n): Last sound-speed profile value in water	m m/s	2 ≤ n ≤ 100
H1,R1,B1	H1: Thickness of sediment layer R1: Density of sediment B1: Compressional wave attenuation in sediment	m g/cm³ dB·λ	H1 ≥ 0 R1 > 0 B1 ≥ 0
Z1(1),C1(1)	Z1(1): First sound-speed profile depth (= 0) C1(1): First sound-speed profile value in sediment	m m/s	- -
⋮	⋮	⋮	⋮
Z1(m),C1(m)	Z1(m): Last sound-speed profile depth (= H1) C1(m): Last sound-speed profile value in sediment	m m/s	2 ≤ m ≤ 100
R2,B2,C2	R2: Density of subbottom B2: Compressional attenuation in subbottom C2: Compressional speed in subbottom	g/cm³ dB/λ m/s	R2 > 0 B2 ≥ 0 C2 > 0
B2S,C2S	B2S: Shear attenuation in subbottom C2S: Shear speed in subbottom	dB·λ m/s	$0 \le B2S < 0.75\,B2\left(\frac{C2}{C2S}\right)^2$ 0 ≤ C2S << C1(H1)

*To be repeated for all segments ("NSEG" times).

TABLE 2 SUMMARY OF SNAP INPUTS (PART II)

1) ANGLE,PLT,PRT XAXIS x_1,x_2,x_3,x_4 YAXIS y_1,y_2,y_3,y_4 rmin,rmax,delr sd(1),rd(1) ⋮ sd(n),rd(n)	2) CONDR,INC,COH,PLT rmin,rmax,delr zmin,zmax,delz sd(1) ⋮ sd(n)	3) CONFR,INC,COH,PLT rmin,rmax,delr zmin,zmax,delz sd(1),rd(1) ⋮ sd(n),rd(n)	4) MODES,PLT,PRT
5) PHASE,PLT,PRT rmin,rmax,delr sd(1) ⋮ sd(n)	6) PROFL,PLT	7) TLAVF,INC,COH,PLT,PRT rmin,rmax,delr sd(1) ⋮ sd(n)	8) TLAVR,INC,COH,PLT,PRT rmin,rmax,delr sd(1) ⋮ sd(n)
9) TLDEP,INC,COH,PLT,PRT rmin,rmax,delr sd(1) ⋮ sd(n)	10) TLRAN,INC,COH,PLT,PRT rmin,rmax,delr sd(1),rd(1) ⋮ sd(n),rd(n)		

TABLE 3 DEFINITION OF INPUT CODES USED IN PART II

INPUT CODE	EXPLANATION
ANGLE	Field intensity vs arrival angle
CONDR*	Contoured transmission loss vs depth and range
CONFR	Contoured transmission loss vs frequency and range
MODES	Individual mode functions vs depth
PHASE	Phase of acoustic field vs depth
PROFL	Sound speed vs depth
TLAVF	Depth-averaged transmission loss vs frequency
TLAVR	Depth-averaged transmission loss vs range
TLDEP	Transmission loss vs depth
TLRAN	Transmission loss vs range
INC	Incoherent addition of modes
COH	Coherent addition of modes
PLT	Plotted output
PRT	Printed output
XAXIS	Identifier for horizontal axis
YAXIS	Identifier for vertical axis

*This option can be executed only for constant water depth

TABLE 4 DEFINITION OF INPUT PARAMETERS USED IN PART II

INPUT PARAMETER	EXPLANATION	UNIT	LIMITS
x_1, x_2, x_3, x_4	x_1: Lowest data value on horizontal axis[1] x_2: Highest data value on horizontal axis[1] x_3: No. of data units per centimeter[2] x_4: Distance between tick marks in data units[3]	see Table 5	
y_1, y_2, y_3, y_4	y_1: Lowest data value on vertical axis[1] y_2: Highest data value on vertical axis[1] y_3: No. of data units per centimeter[2] y_4: Distance between tick marks in data units[3]	see Table 5	
rmin, rmax, delr	rmin: Minimum range for loss calculation rmax: Maximum range for loss calculation delr: Range increment[4]	km km km	$\emptyset \leq$ rmin $\leq$ rmax delr $\geq \emptyset$
zmin, zmax, delz	zmin: Minimum contour level zmax: Maximum contour level delz: Level increment[5]	dB dB dB	$\emptyset \leq$ zmin $\leq$ zmax delz $\geq \emptyset$
sd(1), rd(1)	sd(1): First source depth rd(1): First receiver depth	m m	$\emptyset <$ sd $\leq H\emptyset$ $\emptyset <$ rd $\leq H\emptyset$
⋮	⋮	⋮	⋮
sd(n), rd(n)	sd(n): Last source depth rd(n): Last receiver depth	m m	n $\leq 1\emptyset$

[1] Axis directions can be changed as compared to the standard ones given in Figs. B3-B20 by assigning highest data values to (x_1, y_1) and lowest data values to (x_2, y_2).

[2] For logarithmic frequency axes this argument indicates the length of an octave in centimeters.

[3] For logarithmic frequency axes this argument indicates the number of subdivisions per octave ($x_4 \geq 1$). Ex: x_4=3 results in tick marks every 1/3 of an octave.

[4] No. of range steps per segment cannot exceed 500.

[5] No. of contour level steps cannot exceed 51.

TABLE 5 DEFAULT AXIS VALUES

OPTION	X-AXIS								Y-AXIS							
	x_1		x_2		x_3		x_4		y_1		y_2		y_3		y_4	
ANGLE	Ø	deg	4Ø	deg	2	deg/cm	5	deg	4Ø	dB	14Ø	dB	5	dB/cm	2Ø	dB
CONDR	rmin	km	rmax	km	2	km/cm	5	km	Ø	m	[illegible]		5	m/cm	2Ø	m
CONFR*	rmin	km	rmax	km	2	km/cm	5	km	F_{min}	Hz	F_{max}	Hz	2	cm/oct	1	-
MODES	-Ø.2	**	Ø.2	**	.12	**/cm	Ø.2	**	[illegible]	m	HØ+Hi	m	5	m/cm	2Ø	m
PHASE	-18Ø	deg	18Ø	deg	18	deg/cm	45	deg	[illegible]	m	[illegible]	m	5	m/cm	2Ø	m
PROFL	145Ø	m/s	165Ø	m/s	1Ø	m/s/cm	25	m/s	Ø	m	HØ+[illegible]	m	5	m/cm	2Ø	m
TLAVF*	F_{min}	Hz	F_{max}	Hz	3	cm/oct	1	-	4Ø	dB	14Ø	dB	5	dB/cm	2Ø	dB
TLAVR	rmin	km	rmax	km	2	km/cm	5	km	4Ø	dB	14Ø	dB	5	dB/cm	2Ø	dB
TLDEP	Ø	dB	16Ø	dB	8	dB/cm	2Ø	dB	Ø	m	HØ	m	5	m/cm	2Ø	m
TLRAN	rmin	km	rmax	km	2	km/cm	5	km	4Ø	dB	14Ø	dB	5	dB/cm	2Ø	dB

*Option with logarithmic frequency axis.

** $(m^2/kg)^{\frac{1}{2}}$.

NB: The unit for loss is dB re 1 meter.

LI1 Number of discretization points in the sediment layer. These parameters refer to the number of layers into which water (LIØ) and sediment (LI1) have been subdivided for doing modal computations by a finite-difference technique (Sect. 2.2). Hence the accuracy with which modes are calculated increases with increasing number of discretization points. In the program, LIØ+LI1 cannot exceed 2500, which, on the other hand, has turned out to be an appropriate upper limit for calculating 500 modes sufficiently accurately. The division of discretization points between water and sediment should be according to depth, i.e. LIØ/LI1 = HØ/H1. However, since sound-speed gradients are generally much higher in the sediment than in the water, a relatively denser sampling is often needed for the sediment. For a standard shallow-water case the recommended input is [LIØ,LI1] = [2000,200], which assures accurate calculation in most cases. Naturally, such a high number of points results in long running times for the program, and if a faster and less accurate execution is desired, the number of sample points can be diminished. However, LIØ+LI1 should never be less than three times the maximum number of modes.

NSEG Number of segments into which a range-dependent environment is divided. Each segment has range-independent properties, but from segment to segment all input parameters given below may vary arbitrarily.

SEGL Length of segment in kilometres. For a range-independent environment only one segment is needed, and the length then becomes a dummy parameter.

HØ Water depth in metres.

SØ rms roughness of sea surface in metres.

S1 rms roughness of sea floor in metres. Scattering loss due to rough boundaries can be neglected by putting both SØ and S1 equal to zero.

ZØ,CØ Sound-speed profile in water column. The first value given has to be at the sea surface (ZØ = 0) and the last value at the sea floor (ZØ = HØ). Thus, the minimum number of profile values is two and the maximum is 100.

H1 Thickness of sediment layer in metres. This layer can be omitted by putting H1 equal to zero. In that case both R1 and B1 should be omitted from the input, together with the profile [Z1,C1].

R1 Density of sediment in g/cm^3.

B1 Compressional-wave attenuation in sediment in dB/wavelength.

Z1,C1 Sound-speed profile in sediment layer. The first value given has to be at the water/sediment interface (Z1 = 0), and the last value at the sediment / subbottom interface (Z1 = H1). Normally, there will be a discontinuity in the profile at the water/sediment interface, i.e. $C\emptyset_{Z\emptyset=H\emptyset} \neq C1_{Z1=0}$. If H1 is equal to zero, the profile has to be omitted. Otherwise the minimum number of profile values is 2.

R2 Density of subbottom in g/cm^3.

B2 Compressional-wave attenuation in subbottom in dB/wavelength.

C2 Compressional speed in subbottom in m/s. For discrete modes to exist, this speed must be higher than the minimum speed in water and sediment, i.e. C2 > min [C$\emptyset$,C1]. This is a necessary but not sufficient criterion for the existence of discrete modes.

B2S Shear-wave attenuation in subbottom in dB/wavelength. By treating the subbottom as a "Voigt" solid *[18]*, we impose upper limits on both shear attenuation ($B2S < 0.75\ B2(C2/C2S)^2$) and shear speed ($C2S < \sqrt{0.75}\ C2$). If these limits are exceeded, the solid becomes non-real with negative compressibility.

C2S Shear speed in subbottom in m/s. Shear waves can be neglected by putting C2S equal to zero. In that case the attenuation B2S becomes a dummy parameter. Since the effect of shear waves is introduced in a perturbation approach, C2S has to be small compared to the compressional speed C1(H1) for results to be accurate.

N.B. In the case of a range-dependent environment, the part of the input indicated by an asterisk in Table 1 has to be repeated for all segments, i.e. NSEG times.

3.2 Computational input

The second part of the input (Table 2) deals with the kinds of calculation to be performed. Here there is no rigid structure determining the sequence in which numerical values have to be entered. Instead, several code words are used, as for instance option identifiers (ANGLE, CONDR, CONFR, etc.), calculation-type codes (INC, COH), output-type codes (PLT, PRT), and axis codes (XAXIS, YAXIS). These codes are given in upper-case letters in Table 2, and are explained in Table 3.

While code words have to be typed in full in the input, all parameters given by lower-case letters in Table 2 should be replaced by numerical values. Thus the input shown here is a mixed system of code words and parameters: a procedure that has been chosen to facilitate the use of the model.

A standard input data structure is used in all options, see Table 2. On the first line appears the option identifier (ANGLE, CONDR, etc.), followed by calculation-type identifiers (INC, COH) and output-type identifiers (PLT, PRT). This is the general structure, but some options (e.g. ANGLE and PHASE) do not have calculation-type identifiers, since the choice between coherent and incoherent addition of modes does not apply to these options. Likewise, some options (e.g. PROFL and CONDR) do not have the print option, either because a printout generates an enormous and partly useless set of numbers (CONDR) or because a printout is already part of the standard printout (PROFL). Anyhow, if a certain type of calculation is wanted, the first line should contain the option identifier followed by at least one of the calculation-type identifiers (INC, COH), whenever these codes apply, and at least one of the output-type identifiers (PLT, PRT). The sequence in which the 3-letter codes are entered is arbitrary. Hence all of the following combinations are acceptable: [INC,COH,PLT], [PRT,PLT,COH], [INC,PLT,PRT], [PLT,INC], etc.

The first line is followed by the axis definitions. These are surrounded by dashed lines to indicate that these instructions may be omitted completely and the default axis values given in Table 5 used instead. If a change of one or both axes is desired, the axis identifiers (in

upper-case letters) followed by four parameter values should appear immediately after the first line. The significance of the axis parameters $[x_1,x_2,x_3,x_4]$ and $[y_1,y_2,y_3,y_4]$ is given in Table 4. As an example, we might want a 25 cm long range axis going from 10 to 60 km with tick marks every 10 km. This is obtained by specifying [XAXIS 10.,60.,2.,10.]. As shown here, the identifier XAXIS should always be separated from the first parameter x_1 by a blank. For logarithmic frequency axes, arguments 3 and 4 (x_3,x_4 or y_3,y_4) take a special meaning, as indicated by the footnotes to Table 4. Thus, if we want the y-axis for option CONFR to cover the frequency range 50 to 1600 Hz (5 octaves) with tick marks every octave and with a total length of 25 cm, we specify [YAXIS 50.,1600.,5.,1.].

Generally, the axis definitions provide full flexibility for plotted output. Not only can axis directions be changed from the standard ones (see footnote 1 of Table 4) but any part of the calculated data can be displayed. Thus, even if calculations are requested from 0 to 30 km, say, the range axis can cover any interval, for instance 0 to 50 km, 20 to 100 km, 10 to 25 km, etc. This means that axis specifications can be given independently of computational specifications.

Next are given the parameters [rmin,rmax,delr] to indicate that computations should be made from range rmin to range rmax in steps of delr kilometres. One limitation is introduced here; the number of range steps per segment cannot exceed 500. However, if a denser sampling in range is needed, this limitation can be overcome by dividing a given segment into several segments all with the same properties.

For the two contour options CONDR and CONFR, the next input is a specification of contour levels given by [zmin,zmax,delz]. Thus if, for instance, contouring is wanted from 50 dB to 150 dB in steps of 10 dB, we input [50.,150.,10.].

The last input is a specification of the source/receiver depths for which calculations are wanted (max. 10). We see that for some options (MODES and PROFL) neither source nor receiver depth should be specified. For other options (CONDR, PHASE, etc.) only a source depth needs to be specified, although a receiver depth can be given as a dummy input.

As shown in Table 2, the SNAP model allows for ten different outputs. Any one, or all, of these options can be chosen, and the sequence in which calculations are requested is arbitrary. The program has an established internal routine for performing calculations, depending on the looping of parameters. A detailed description of each of the ten output options is given in the next chapter.

4 OUTPUT OPTIONS

The SNAP model provides both printed and plotted output for the ten options given in Table 2. However, since the printed output of loss versus depth, range, or frequency is self-explanatory, only the plotted output will be described in detail in the following. Preceding the plotted output is a standard printout of environmental inputs and some essential modal properties. This standard printout will first be described.

4.1 Printed output

A deep-water test is used in this chapter to illustrate the various output options. A sample printout of this test is given in Fig. 3. We see that the heading is followed by a table indicating which output options have been requested, whether printed or plotted output is wanted, and whether calculations should be done by coherent or incoherent addition of modes.

Next comes a printout, segment by segment, of environmental inputs and of some basic modal properties. First are given the segment number and the segment length, then the number of sample points. MSP is the stored modal sample points in the water column used for calculating the acoustic field over depth. This number can be 51, 101, or 201, depending on which program version has been executed, see Appendix A. Thus version A5Ø gives a sample point every $H_o/50$ metres, with a total of 51 sample points in the water column. The other program versions are A1ØØ and A2ØØ. MSP is followed by the number of discretization points in water (LIØ) and in sediment (LI1). Next are given the inputted depths, densities, attenuation coefficients, and rms roughnesses; finally sound speeds for water, sediment, and subbottom are given. In this particular example, no sediment layer is considered, and the sound-speed profile for the sediment is therefore missing.

Some basic modal properties are given next. For a source frequency of 10 Hz the number of modes is 13. The table gives for each mode the horizontal wave number k_n followed by the modal attenuation coefficient α_n (ALPHA), both in nepers/m. As shown by Eq.12 in Sect. 2.3,

THIS PAGE IS BEST QUALITY PRACTICABLE
FROM COPY FURNISHED TO DDC

```
**********************************************************

DEEP WATER CASE

**********************************************************

OUTPUT OPTIONS:

          PRT      PLT      CON      INC
ANGLE      0.       1.
CONDR      0.       1.       1.       0.
MODES      0.       1.
PHASE      0.       1.
PROFL      0.       1.
TLAVR      0.       1.       1.       0.
TLDEP      0.       1.       1.       0.
TLRAN      0.       1.       1.       0.


 SEGMENT NO.  1
 ************

 SEGMENT LENGTH  =  500.00 KM


 SAMPLE POINTS:
 NSP             =   101
 WATER           =  1000
 SEDIMENT        =     0


 DEPTHS (M):
 WATER           =  5000.00
 SEDIMENT        =     .00


 DENSITIES (G/CM**3):
 WATER           =    1.00
 SEDIMENT        =     .00
 SUBBOTTOM       =    1.00


 ATTENUATION COEFFICIENTS (DB/WL):
 SEDIMENT        =     .00
 SUBBOTTOM       =     .10
 SHEAR           =     .50


 RMS ROUGHNESSES (M):
 SEA SURFACE     =     .10
 SEA FLOOR       =     .10


    SOUND SPEED PROFILE

          WATER

   DEPTH (M)   SPEED (M/S)
      .00       1524.00
     400.00     1522.00
     650.00     1520.00
     825.00     1516.70
    1000.00     1490.00
    1500.00     1492.00
    3500.00     1520.00
    5000.00     1545.00


 BOTTOM SOUND SPEED   = 1545.00 M/S
 SHEAR SPEED          =  500.00 M/S


 SOURCE FREQUENCY     =   10.00 HZ
 MAXIMUM NO. OF MODES =   13

                 WAVE NUMBER          ALPHA          A0          A1          A2          A2S          A0S          A0B          RB      SS      SB
 MODE =  1 *  .9206325313-01   .11315-08   .11335-08   .00000   .81390-27   .15998-26   .00000   .00000   .09   .00   .00
 MODE =  2 *  .9189384565-01   .11536-08   .11336-08   .00000   .53368-23   .60131-23   .00000   .00000   .09   .00   .00
 MODE =  3    .9175024964-01   .11351-08   .11351-08   .00000   .10423-19   .13457-19   .00000   .00000   .09   .00   .00
 MODE =  4    .9159926000-01   .11364-08   .11364-08   .00000   .56296-17   .68779-17   .00000   .00000   .09   .00   .00
 MODE =  5    .9147232675-01   .11376-08   .11376-08   .00000   .10392-14   .10599-14   .00000   .00000   .09   .00   .00
 MODE =  6    .9135652553-01   .11387-08   .11386-08   .00000   .82881-13   .75250-13   .00000   .00000   .10   .00   .00
 MODE =  7    .9124306701-01   .11423-08   .11396-08   .00000   .32865-11   .26679-11   .00000   .00000   .10   .00   .00
 MODE =  8    .9114559356-01   .11992-08   .11407-08   .00000   .75998-10   .55274-10   .16514-11   .00000   .11   .00   .00
 MODE =  9    .9104777738-01   .19732-08   .11419-08   .00000   .12578-08   .82215-09   .46042-11   .00000   .13   .00   .00
 MODE = 10    .9095143373-01   .10934-07   .11430-08   .00000   .16625-07   .97957-08   .72907-11   .00000   .15   .00   .00
 MODE = 11    .9085820111-01   .32698-07   .11420-08   .00000   .17673-06   .91535-07   .10046-10   .00000   .21   .00   .00
 MODE = 12    .9075716345-01   .67149-06   .11706-08   .00000   .16465-05   .67755-06   .12314-10   .00000   .34   .00   .00
 MODE = 13    .9067044505-01   .32308-06   .63683-09   .00000   .33149-04   .32242-06   .60136-11   .00000   .28   .00   .00
```

FIG. 3 SAMPLE PRINTOUT

α_n is composed of several loss contributions: $\alpha_n^{(0)}$, $\alpha_n^{(1)}$, $\alpha_n^{(2)}$, $\alpha_n^{(2S)}$, $\alpha_n^{(OS)}$, and $\alpha_n^{(OB)}$, which are given in the following columns in that order. The last three columns give some check numbers, which all have to be smaller than unity for the associated loss calculations to be correct. RB is the quantity given by Eq. 20, and is related to bottom reflection loss in the presence of shear waves (A2S). SS and SB are given by Eqs. 23 and 24, respectively, and are related to surface-scattering loss (AOS) and bottom-scattering loss (AOB).

The asterisks appearing just after modes 1 and 2 indicate that these two modes have been artificially zeroed at the surface, a fact associated solely with the numerical solution procedure *[8,9]*, and thus without consequences for the accuracy of the transmission-loss calculations. Finally, if there is more than one segment, the type of printout shown in Fig. 3 will be repeated for all segments.

4.2 Plotted output

The various output options are described on the following pages, with one page allocated to each option. All examples given are for the same deep-water environment as described above (Fig. 3).

ANGLE

```
ANGLE,PLT,PRT
XAXIS x1,x2,x3,x4
YAXIS y1,y2,y3,y4
rmin,rmax,delr
sd(1),rd(1)
    :
sd(n),rd(n)
```

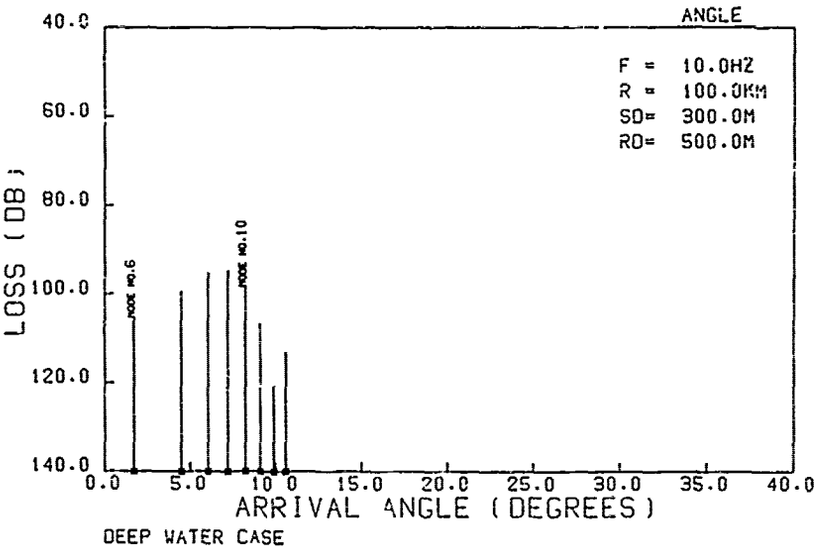

This option gives *field intensity versus arrival angle* calculated as specified by Eqs. 34 and 35 in Sect. 2.4. Since there is no range axis, a new plot will be generated for each range specified by the parameters [rmin,rmax,delr]. If only one plot is wanted, at range R_o say, the proper input would be $[R_o,R_o,\emptyset]$. One plot will be generated also for each source/receiver combination [sd,rd] specified in the input (max. 10), and for each source frequency.

The legend in the upper right corner of the plot gives frequency (10 Hz), range (100 km), source depth (300 m), and receiver depth (500 m). Using the ray/mode analogy, which associates up and downgoing rays, each having a specific grazing angle, with each normal mode at a given depth, we see that energy arrives at the receiver within an angle of ±10° to the horizontal. We also see that the energy is distributed on eight discrete modes, with most energy carried by modes 8 and 9. Actually, the number of modes is 13, but the first five modes are evanescent at the receiver, which means that no real angle can be associated with these modes. On the other hand, evanescent modes generally carry very little energy and can therefore be neglected.

CONDR

```
CONDR,INC,COH,PLT
XAXIS x1,x2,x3,x4
YAXIS y1,y2,y3,y4
rmin,rmax,delr
zmin,zmax,delz
sd(1)
  :
  :
sd(n)
```

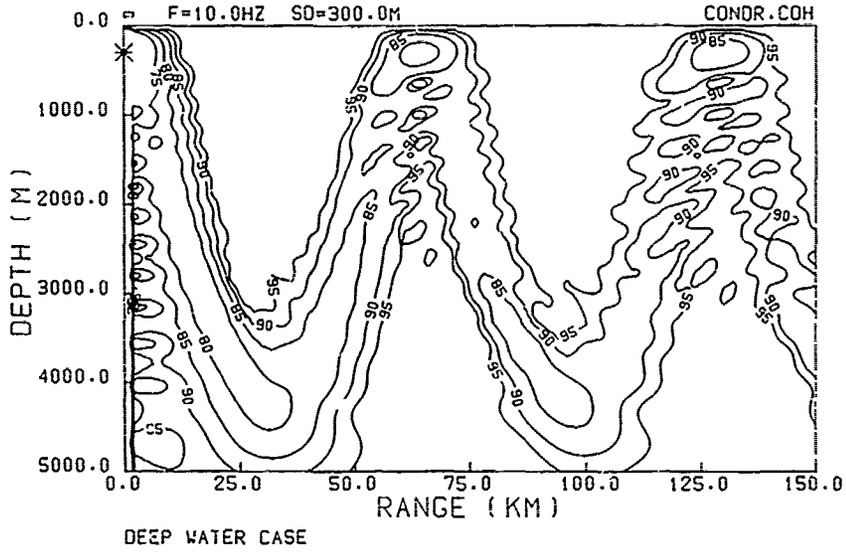

DEEP WATER CASE

This option gives *contoured transmission loss versus depth and range*. The number of sample points in range is determined by the parameters [rmin,rmax,delr], while the number of sample points in depth is 51. If a denser sampling in depth is desired, the standard program version (A5Ø) should be replaced by one of the alternative versions: A1ØØ or A2ØØ. The parameters [zmin,zmax,delz] give the contour levels in dB, and [sd] is the source depth. One contour plot will be generated for each source depth specified in the input (max. 10), and also for each source frequency and calculation type specification [INC,COH].

In the upper left corner of the plot is shown a small rectangle illustrating the grid size used for the contouring. The grid size can be changed either by changing the range step size (delr) or by changing the program version, e.g. from A5Ø to A1ØØ. On the upper frame is also given frequency (10 Hz) and source depth (300 m), and we see that calculations have been done by coherent addition of modes (COH). The position of the source is also indicated by a cross on the vertical axis.

The example shown here is a typical deep-water case, with convergence zones at 65 and 130 km. The contouring has been done between 75 and 95 dB in steps of 5 dB, leaving the high-loss shadow zones blank. Note the similarity between this contour plot and a standard ray-trace plot for a convergence-zone case.

CONFR

```
CONFR,INC,COH,PLT
XAXIS x1,x2,x3,x4
YAXIS y1,y2,y3,y4
rmin,rmax,delr
zmin,zmax,delz
sd(1),rd(1)
    :
sd(n),rd(n)
```

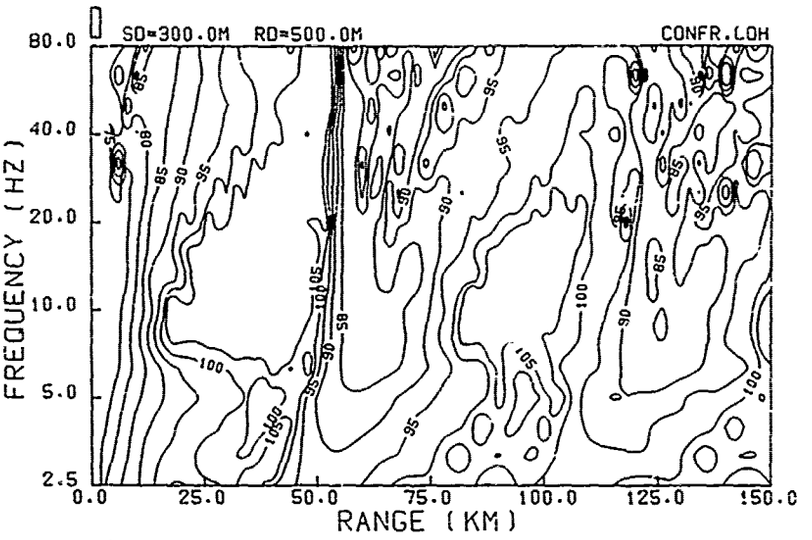

DEEP WATER CASE

This option gives *contoured transmission loss versus frequency and range*. The number of sample points in range is determined by the parameters [rmin,rmax,delr], while the number of sample points in frequency is equal to the number of source frequencies. The parameters [zmin,zmax,delz] give the contour levels in dB, and [sd,rd] are source and receiver depths. One contour plot will be generated for each source/receiver combination specified in the input (max. 10), and also for each calculation type specification [INC,COH].

In the upper left corner of the plot is shown a small rectangle illustrating the grid size used for the contouring. The grid size can be changed either by changing the range step size (delr) or by changing the number of frequencies. If input frequencies are not equally spaced on a logarithmic scale, an equidistant grid is established by interpolation. The grid size is then given by $(F_{max} - F_{min})/(NF - 1)$, where NF is the number of input frequencies. On the upper frame is also given source depth (300 m) and receiver depth (500 m), and we see that calculations have been done by coherent addition of modes (COH).

The example given here is a typical deep-water case with the first convergence zone clearly showing up in the plot around 50 km. We see that the convergence zone is very weak below 5 Hz, and that it moves slightly out in range with increasing frequency.

MODES

MODES,PLT,PRT

XAXIS x_1,x_2,x_3,x_4

YAXIS y_1,y_2,y_3,y_4

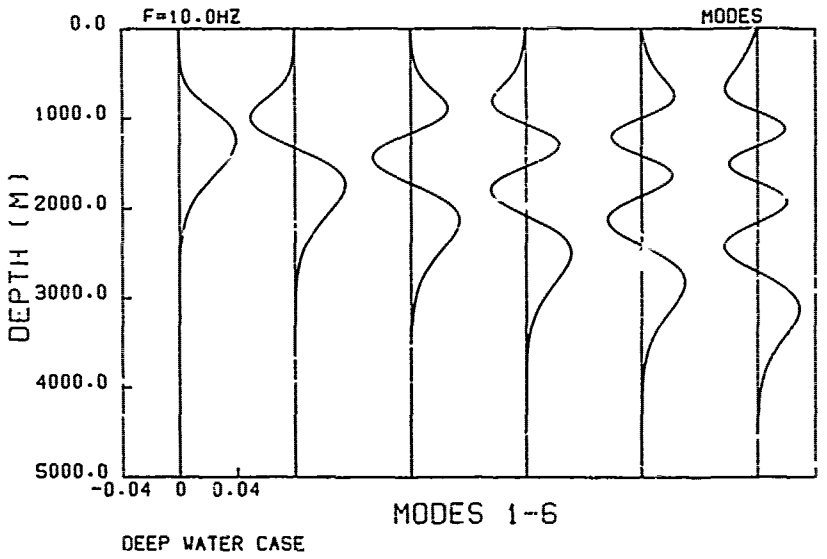

This option gives *normalized mode amplitudes versus depth*. Since the modes are plotted in groups of six, several plots will normally be generated in order to display all modes. In case of a range-dependent environment, a particular mode set exists for each segment, leading to a generation of even more plots.

The deep-water example given here is for a frequency of 10 Hz, as shown in the upper left corner of the plot. The total number of modes is thirteen, but only the first six modes are shown. If a sediment layer exists, the modal behaviour here can also be displayed, and the interface between water and sediment will then be shown as a horizontal line in the plot.

PHASE

```
PHASE,PLT,PRT
XAXIS x1,x2,x3,x4
YAXIS y1,y2,y3,y4
rmin,rmax,delr
sd(1)
  :
sd( )
```

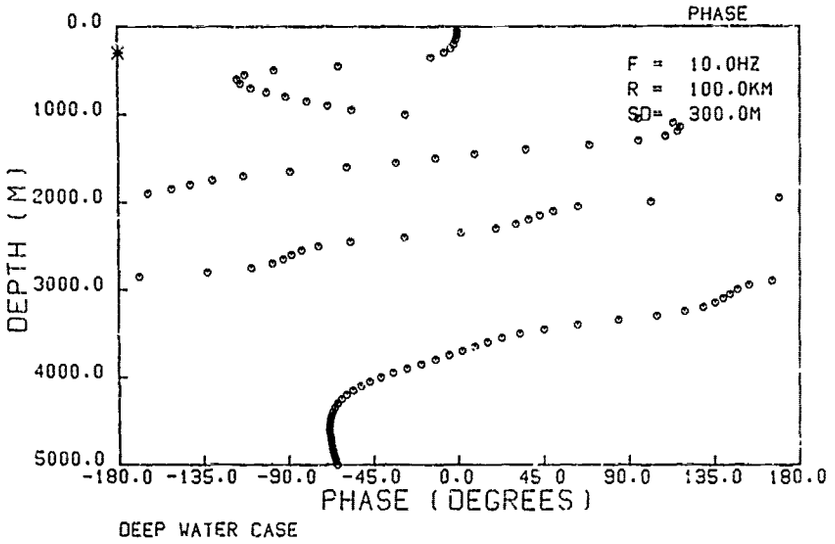

DEEP WATER CASE

This option gives the *phase of the acoustic field versus depth*, calculated from Eq. 36 in Sect. 2.4. The phase is normalized to zero at the surface, and computations are carried out in 51 equidistant points over the water column. If a denser sampling is desired, the standard program version (A5Ø) should be replaced by one of the alternative versions: A1ØØ or A2ØØ. Since there is no range axis, a new plot will be generated for each range specified by the parameters [rmin,rmax,delr]. If only one plot is wanted, at range R_o say, the proper input would be $[R_o,R_o,Ø]$. One plot will be generated also for each source depth [sd] specified in the input (max. 10), and for each source frequency.

The legend in the upper right corner of the plot gives frequency (10 Hz), range (100 km), and source depth (300 m). The position of the source is also indicated by a cross on the vertical axis. The deep-water example given here shows a complicated phase structure over depth (13 modes).

PROFL

PROFL,PLOT

XAXIS x_1,x_2,x_3,x_4

YAXIS y_1,y_2,y_3,y_4

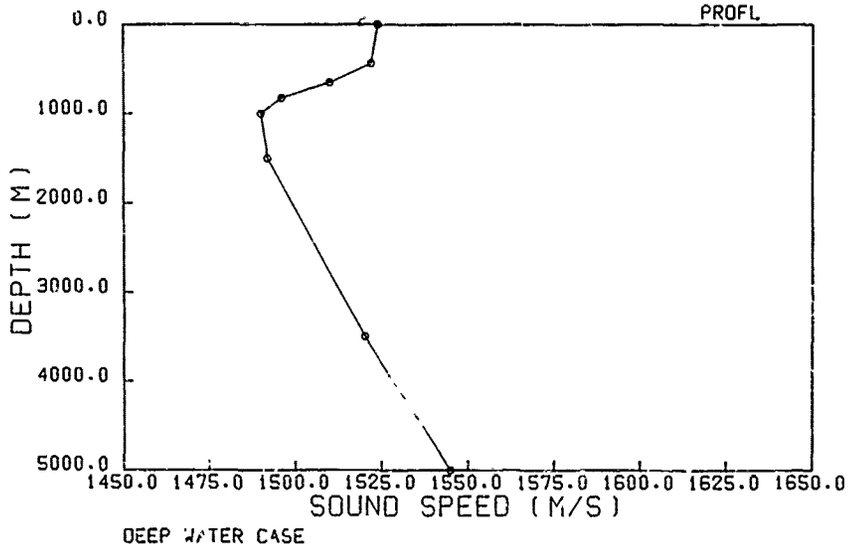

This option gives *sound speed versus depth*. If a sediment layer exists, the sound-speed profile within it can also be displayed, and the interface between water and sediment will then be shown as a horizontal line in the plot. In a range-dependent environment, a profile plot will be generated for each segment, and the segment number will be indicated on the upper frame to the left.

TLAVF

```
TLAVF,INC,COH,PLT,PRT
XAXIS x1,x2,x3,x4
YAXIS y1,y2,y3,y4
rmin,rmax,delr
sd(1)
  :
sd(n)
```

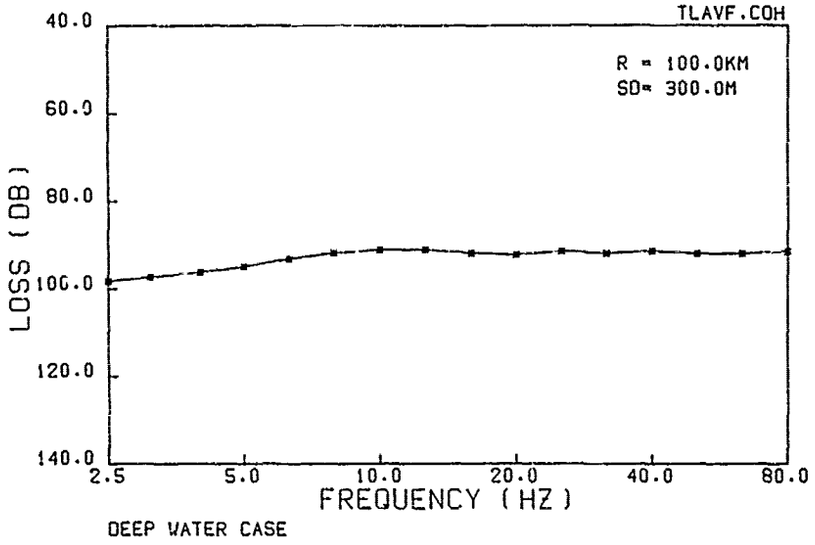

This option gives *depth-averaged transmission loss versus frequency*. The averaging is done over 51 equidistant sample points covering the whole water column (Eq. 33). If a denser sampling is desired, the standard program version (A5Ø) should be replaced by one of the alternative versions: A1ØØ or A2ØØ. Since there is no range axis, a new plot will be generated for each range specified by the parameters [rmin,rmax,delr]. If only one plot is wanted, at range R_o say, the proper input would be [R_o,R_o,Ø]. One plot will be generated also for each source depth [sd] specified in the input (max. 10), and for each calculation type specification [INC,COH].

The legend in the upper right corner of the plot gives range (100 km) and source depth (300 m). Furthermore, we see that calculations have been done by coherent addition of modes (COH). The number of frequency samples is equal to the number of source frequencies specified ... the input. The example given here shows that the average propagation is better at the higher frequencies.

```
TLAVR,INC,COH,PLT,PRT
XAXIS x1,x2,x3,x4
YAXIS y1,y2,y3,y4
rmin,rmax,delr
sd(1)
  :
sd(n)
```

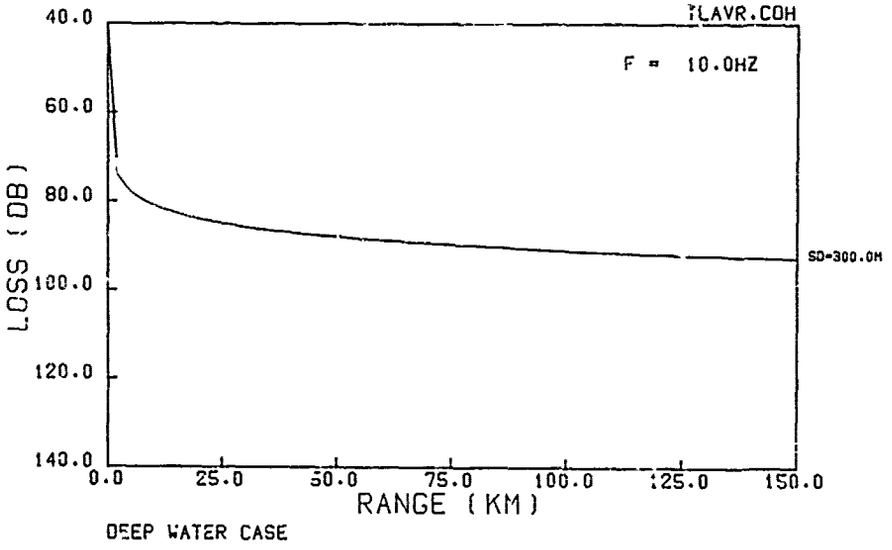

This option gives *depth-averaged transmission loss versus range*. The averaging is done over 51 equidistant sample points covering the whole water column (Eq. 33). If a denser sampling is desired, the standard program version (A5Ø) should be replaced by one of the alternative versions: A1ØØ or A2ØØ. The number of sample points in range is determined by the parameters [rmin,rmax,delr]. Results for up to ten different source depths are plotted in the same frame. However, a new plot will be generated for each source frequency and calculation type specification [INC,COH] given in the input.

The legend in the upper right corner of the plot indicates that calculations have been made for a frequency of 10 Hz by coherent addition of modes (COH). The source depth (300 m) for the loss curve presented is given to the right of the frame.

TLDEP

TLDEP,INC,COH,PLT,PRT

XAXIS x_1,x_2,x_3,x_4

YAXIS y_1,y_2,y_3,y_4

rmin,rmax,delr

sd(1)

⋮

sd(n)

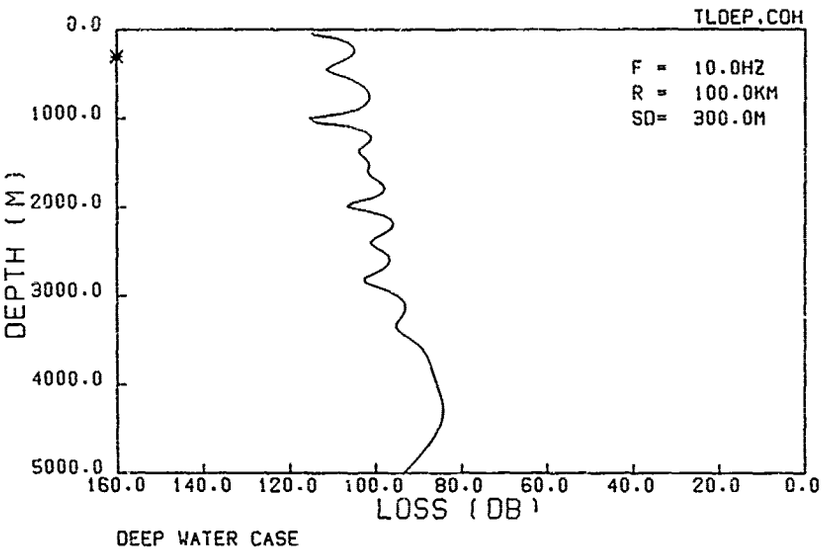

DEEP WATER CASE

This option gives *transmission loss versus depth* sampled in 51 equidistant points over the water column. If a denser sampling is desired, the standard program version (A5Ø) should be replaced by one of the alternative versions: A1ØØ or A2ØØ. Since there is no range axis, a new plot will be generated for each range specified by the parameters [rmin,rmax,delr]. If only one plot is wanted, at range R_o say, the proper input would be $[R_o,R_o,Ø]$. One plot will be generated for each source depth [sd] specified in the input (max. 10), and also for each source frequency and calculation type specification [INC,COH].

The legend in the upper right corner of the plot gives frequency (10 Hz), range (100 km), and source depth (300 m). The position of the source is also indicated by a cross on the vertical axis. Furthermore, we see that calculations have been made by coherent addition of modes (COH). The example given here shows the highest field intensity in the lower part of the water column.

TLRAN

```
TLRAN,INC,COH,PLT,PRT
XAXIS x1,x2,x3,x4
YAXIS y1,y2,y3,y4
rmin,rmax,delr
sd(1),rd(1)
    :
sd(n),rd(n)
```

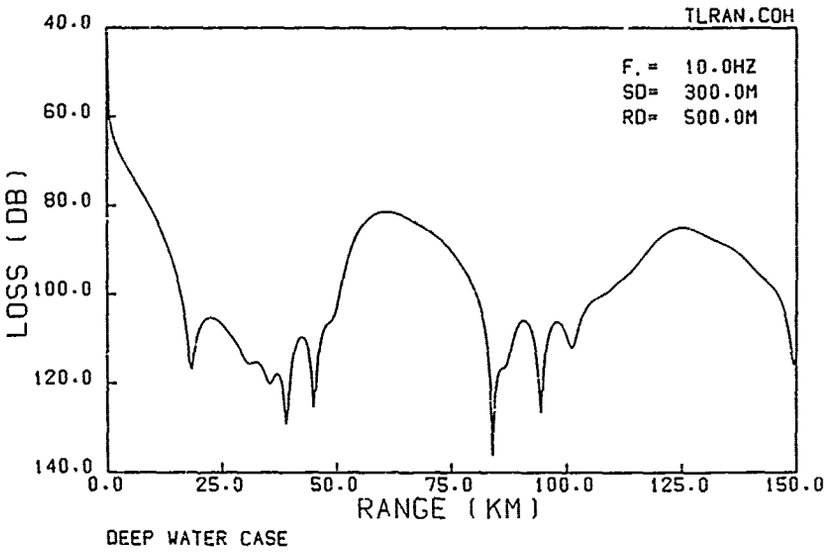

DEEP WATER CASE

This option gives *transmission loss versus range*. The number of sample points in range is determined by the parameters [rmin,rmax,delr], with a maximum of 500 range steps per segment. Since the number of segments handled by the program is unlimited, any density of range sample points can be obtained by dividing the full range into several segments, all with the same properties and each containing a maximum of 500 sample points. A new plot will be generated for each source/receiver combination specified in the input (max. 10), and also for each source frequency and calculation type specification [INC,COH].

The legend in the upper right corner of the plot gives frequency (10 Hz), source depth (300 m), and receiver depth (500 m). Furthermore, we see that calculations have been done by coherent addition of modes (COH). The example given here is a typical deep-water case with convergence zones at 65 and 130 km.

5 MODEL VALIDATION

A first version of the SNAP model was operational as early as 1974, and a continuous validation program has been going on since then. Thus, SNAP outputs have been compared with both synthetic and experimental data, the synthetic data comprising both exact analytical solutions for simplified environments and approximate numerical solutions for realistic environments.

An exact analytical solution for the acoustic field can be obtained only for an isovelocity waveguide with perfectly reflecting boundaries. Two types of simple waveguides have been considered in our tests.

1) A pressure-release/pressure-release waveguide, which can be simulated in the SNAP model by omitting the sediment layer and letting density and compressional speed in the subbottom approach the limits: $\rho_2 \to 0$ (10^{-38}) and $c_2 \to \infty$ (10^{+38}). In parentheses are given the actual numbers used.

2) A pressure-release/rigid waveguide, which can be simulated by letting both ρ_2 and c_2 approach infinity, i.e. $\rho_2 = c_2 = 10^{+38}$.

For these two waveguides, the modes are simple sine functions, which can be calculated from formulas given in *[10]*. The agreement found between the analytical solutions and the SNAP output was excellent and within the numerical accuracy of the computer used (UNIVAC 1106).

For more realistic environments, the SNAP output has been compared with results obtained from other propagation models. In fact, a thorough testing of the SNAP model against all other propagation models in use at SACLANTCEN *[2]* has been carried out, and good agreement was found in many cases. However, while most other models failed to provide accurate field predictions under certain circumstances, we never detected serious problems with the SNAP model, which passed all tests in an excellent way and turned out to be the most reliable propagation model available at SACLANTCEN *[19]*.

The final and crucial test for an acoustic propagation model is a comparison with experimental data. The SNAP model has been applied to

three major data sets collected in different shallow-water areas under various environmental conditions *[20,21,22]*. In all cases we have used high-quality broadband data from explosive sources, with a good sampling of the acoustic field in both range and depth. As pointed out in *[22]*, it is important for any model validation that the experimental data represent as broad a frequency range as possible. Concerning the field sampling, it is particularly important to have experimental data well sampled close to the surface and bottom, where the effects of the various loss mechanisms are most pronounced. The data sets mentioned above all cover the 50 to 3200 Hz frequency range, and the most recent data *[22]* were sampled at 1 m intervals close to both the surface and the bottom.

The results of the comparison between SNAP predictions and experimental data may be summarized as follows: For a nearly range-independent environment good agreement was obtained over a wide frequency range, not only for the acoustic field in the middle of the water column, but also for the field close to the surface and the bottom. Some discrepancies in absolute levels were detected, but the average behaviour of the acoustic field versus depth, range, and frequency was accurately predicted by the SNAP model in all cases. Thus, for such important features as optimal propagation frequency, optimal source / receiver depths, optimal season, etc. the SNAP predictions were in perfect agreement with the experimental data. We may therefore conclude that the SNAP model seems to handle diffraction and reflection processes as well as bottom-loss processes in an accurate frequency-dependent fashion. This in turn means, that with some confidence, we can continue to use the SNAP model to predict acoustic propagation in complicated ocean environments.

Three features implemented recently in SNAP were not tested during the aforementioned comparisons, namely shear losses in the subbottom, scattering losses at rough boundaries, and range dependence. The validation of these SNAP features are described separately below.

Since shear losses are included in SNAP in an approximate way, one would expect results to become inaccurate for high shear speeds. A validation of the shear-loss features has been carried out by comparison with the FFP model *[5]*, which is the only wave theoretic model at SACLANTCEN that

handles absorption losses in an exact way. It was found that SNAP and FFP predictions are in good agreement for shear speeds lower than 500 m/s, while the SNAP model predicts too high losses for higher shear speeds. At the same time the effect of compressional-wave attenuation was also tested. Here it was found that SNAP and FFP predictions agree well for $\beta_2 < 1$ dB/λ, while again SNAP predicts too high losses for high β_2 values. Thus, with high bottom losses, SNAP generally seems to overestimate the bottom-loss effects. It should be pointed out, however, that for realistic sedimentary bottoms ($\beta_2 < 1$ dB/λ and $c_{2S} < 500$ m/s), SNAP handles all bottom losses sufficiently accurately.

The boundary-scattering losses are also included in an approximate way, and we furthermore neglect all contributions to the acoustic field from the non-specularly reflected energy, a fact that definitely leads to an overestimation of predicted scattering losses. Since no other wave theoretic model was available for comparison with SNAP concerning scattering losses, experimental data were used for the validation. Unfortunately, SACLANTCEN possesses very few shallow-water propagation data for rough sea states in which there was a simultaneous monitoring of the wave height. The experimental data, however, confirm that the model predicts too high losses even for small wave heights. It is clear that no detailed validation of this feature can be carried out until a more complete theory has been developed and implemented.

SNAP handles a range-dependent environment in an approximate way, which leads to limitations on both frequency and the number of segments to be used for a given environment (see Sect. 2.5). Comparisons with the PE model *[1]*, which is a truly range-dependent wave model, show that such limitations do exist. Thus, strong range dependence cannot be handled adequately by the SNAP model. However, certain types of range dependence are handled better than others. For instance, SNAP should include changes in bottom losses with range quite well, while changes in speed or water depth are more difficult problems, since a change in the number of modes with range is then likely to occur. In any event, more testing of the range-dependent feature has to be done before definite conclusions about its validity can be drawn. Comparisons with experimental data should also be carried out.

It was mentioned in Ch. 2 that the SNAP model does not include the continuous mode spectrum. This fact is generally without importance except in the nearfield of the source. In order to establish the extension of the nearfield for various environmental conditions, some comparisons have been made between SNAP and the FFP model *[5]*, the latter including also the continuous spectrum. It was found that beyond a range of a few water depths, the contribution of the continuous spectrum to the acoustic field is generally negligible. This fact has also been confirmed by comparing SNAP predictions with experimental data, and we may conclude that the field solution given by SNAP is valid at least for ranges greater than two to five times the water depth.

In conclusion, the SNAP model has shown to provide an accurate description of the acoustic field, including both compressional and shear losses in the bottom. Two features of SNAP should however be handled with caution. One is the boundary-scattering loss, which is handled only in a first-order approximation, and thus always results in too high losses. The other is the range-dependent feature, which has not yet been sufficiently tested for drawing definite conclusions about its validity.

SUMMARY

The SNAP model has been created in response to present and future modelling needs at SACLANTCEN. A first version of SNAP became operational in 1974, and by now the model has already proved to be an excellent research tool. The success of the model is due both to its flexible input/output system and to its versatility in handling a variety of propagation cases. Furthermore, high computational accuracy in conjunction with an outstanding performance reliability has made SNAP the most powerful acoustic propagation model available at SACLANTCEN today.

ACKNOWLEDGMENT

SACLANTCEN wishes to thank the U.S. Naval Research Laboratory, Washington, D.C., for making their normal-mode model available for this work.

REFERENCES

1. JENSEN, F.B. and KROL, H.R The use of the parabolic equation method in sound propagation modelling, SACLANTCEN SM-72. La Spezia, Italy, SACLANT ASW Research Centre, 1975.

2. JENSEN, F.B. Acoustic propagation modelling: why several models? *In*: SACLANTCEN CP-19. La Spezia, Italy, SACLANT ASW Research Centre, 1976. *[AD CO 10187]*

3. INGENITO, F., FERRIS, R., KUPERMAN, W.A. and WOLF, S.N. Shallow-water acoustics, summary report (first phase), NRL Rpt 8179. Washington, D.C., U.S. Naval Research Laboratory, 1978.

4. BACHMANN, W. and RAIGNIAC, B. de. Calculations of reverberation and average intensity of broadband acoustic signals in the ocean by means of the RAIBAC computer model. *Journal Acoustical Society America* 59, 1976: 31-38.

5. KUTCHALE, H.W. Rapid computation by wave theory of propagation loss in the Arctic Ocean, Rpt. CU-8-73. Palisades, N.Y., Columbia University, 1973.

6. INGENITO, F. Measurement of mode attenuation coefficients in shallow water. *Journal Acoustical Society America* 53, 1973: 858-863.

7. KUPERMAN, W.A. and INGENITO, F. Attenuation of the coherent component of sound propagation in shallow water with rough boundaries. *Journal Acoustical Society America* 61, 1977: 1178-1187.

8. NEWMAN, A.V. and INGENITO, F. A normal mode computer program for calculating sound propagating in shallow water with an arbitrary velocity profile, NLR Memorandum Rpt. 2381. Washington, D.C., U.S. Naval Research Laboratory, 1972.

9. MILLER, J.F. and INGENITO, F. Normal mode FORTRAN programs for calculating sound propagation in the ocean, NRL Memorandum Rpt. 3071. Washington, D.C., U.S. Naval Research Laboratory, 1975.

10. BREKHOVSKIKH, L.M. Waves in layered media. New York, Academic Press, 1960.

11. SKRETTING, A. and LEROY, C.C. Sound attenuation between 200 Hz and 10 kHz, SACLANTCEN TR-156. La Spezia, Italy, SACLANT ASW Research Centre, 1969. *[AD 861 117]*

12. HAMILTON, E.L. Compressional-wave attenuation in marine sediments. *Geophysics* 37, 1972: 620-646.

13. INGENITO, F. and WOLF, S.N. Acoustic propagation in shallow water overlying a consolidated bottom. *Journal Acoustical Society America* 60, 1976: 611-617.

14. INGENITO, F. US Naval Research Laboratory, Washington, D.C. Private communication.

15. KUPERMAN, W.A. SACLANT ASW Research Centre, La Spezia, Italy. Private communication.

16. WILLIAMS, A.O. Normal-mode methods in propagation of underwater sound. *In*: Stephens, R.W.B. *ed.* Underwater Acoustics. London, Wiley-Interscience, 1970: 23-56.

17. NAGL, A., UBERALL, H., HAUG, A.J., and ZARUR, G.L. Adiabatic mode theory of underwater sound propagation in a range-dependent sound propagation in a range-dependent environment. *Journal Acoustical Society America* 63, 1978: 739-749.

18. KOLSKY, H. Stress waves in solids. New York, Dover Publications, 1963.

19. WOOD, D. US Naval Underwater Systems Center, New London, CT. Private Communication.

20. JENSEN, F.B. Comparison of transmission loss data for different shallow-water areas with theoretical results provided by a three-fluid normal-mode propagation model. *In*: HASTRUP, O.F. and OLESEN, O.V. *eds*. Sound propagation in shallow water, Vol. II: Unclassified papers, SACLANTCEN CP-14. La Spezia, Italy, SACLANT ASW Research Centre, 1974: 79-92. *[AD AO 04805]*

21. MURPHY, E., WASILJEFF, A., and JENSEN, F.B. Frequency-dependent influence of the sea bottom on the near-surface sound field in shallow water. *Journal Acoustical Society America* 59, 1976: 839-845.

22. JENSEN, F.B. Sound propagation in shallow water: a detailed description of the acoustic field close to surface and bottom. Paper presented at 9th International Congress on Acoustics, Madrid, 1977. SACLANTCEN SM in preparation.

APPENDIX A

HOW TO RUN THE SNAP PROGRAM

This appendix serves as a short user's manual to the range-dependent SNAP model. For ease of reference, all important tables from Ch. 3 are repeated here as Tables A1-A5. By following the instructions given below, any user, whether familiar with mode theory or not, should be able to have the model working without difficulties.

All executable program versions are stored on file SNAP*SNAP. Three versions are available:

SNAP*SNAP.A5Ø
SNAP*SNAP.A1ØØ
SNAP*SNAP.A2ØØ

The only difference between these versions is the number of points used for sampling the acoustic field over the water column. Thus version A5Ø is the standard one, which samples the field every $H_o/50$ m, with H_o being the water depth. Likewise, version A1ØØ samples the field every $H_o/100$ m, etc. While version A5Ø, the smallest and fastest program version, gives sufficient sampling for most shallow-water environments, it might be necessary to use more sample points when dealing with extremely deep water. Then versions A1ØØ and A2ØØ are available. It should however be recognized that these latter versions need longer execution times.

The standard program version SNAP.A5Ø can be executed by preparing a run stream, as shown in Fig. A1. The @RUN card is followed by two instructions for copying the contents of file SNAP*SNAP into file OWNPROJID*SNAP. This is done to avoid interference with other users of the model. The copying should be done only once, hence the dashed lines around the two

statements. Now the executable program versions are catalogued under the user's own project identifier (OWNPROJID), but the file name is still SNAP. In fact, *it is essential to the automatic program execution that the file name SNAP is kept unchanged*. As seen from Fig. A1 the @XQT statement is followed directly by the input data prepared according to the directions given in Tables A1-A5. Finally, an @EOF card indicates termination of the data stream.

An example of a full run stream for a shallow-water environment is given in Appendix B, together with illustrations of all possible outputs from the SNAP model.

New users of the model often have difficulties assessing certain environmental parameters, particularly those related to the ocean bottom *[A.1]*. Some guidance will therefore be given here concerning the choice of appropriate values for the bottom parameters. By limiting our considerations to unconsolidated sedimentary bottoms, the compressional speed, density, and attenuation coefficient will be determined by:

$$c_B = 1470 \text{ to } 1800 \text{ m/s}$$

$$\rho_B = 1 \text{ to } 2 \text{ g/cm}^3$$

$$\beta_B = 0 \text{ to } 1 \text{ dB}/\lambda$$

These values have been taken from *[A.2]*, and subscript B refers to both sediment and subbottom (see Fig. A2).

Shear properties for the bottom are more difficult to assess than compressional properties, and very few measurements have been reported in the literature. However, following *[A.3]* and *[A.4]*, we find for shear speed and shear attenuation

$$c_{2S} = 0 \text{ to } 500 \text{ m/s}$$

$$\beta_{2S} = 1 \text{ to } 10\ \beta_B$$

Finally, it should be emphasized that since propagation in shallow water is dominated by bottom losses, it is very important that all bottom parameters are carefully chosen *[A.1]*.

REFERENCES

A.1 JENSEN, F.B. The effect of the ocean bottom on sound propagation in shallow water. *In*: Sound propagation and underwater systems. Proceedings of British Institute of Acoustics Meeting. London, Imperial College, 1978.

A.2 HAMILTON, E.L. Compressional-wave attenuation in marine sediments. *Geophysics* 37, 1972: 620-646.

A.3 HAMILTON, E.L. Shear-wave velocity versus depth in marine sediments: a review. *Geophysics* 41, 1976: 334-338.

A.4 Hamilton, E.L. Attenuation of shear waves in marine sediments. *Journal Acoustical Society America* 60, 1976: 334-338.

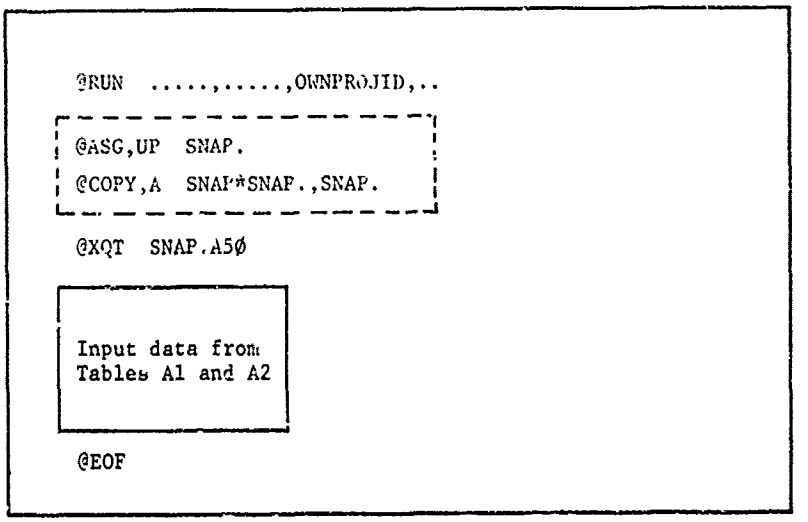

FIG. A1 RUN STREAM FOR PROGRAM EXECUTION

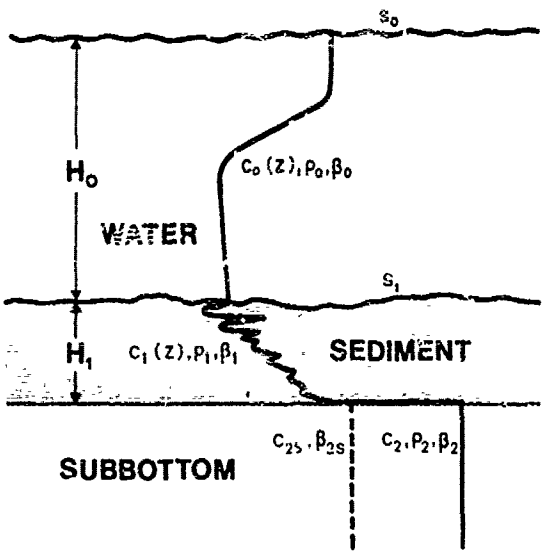

FIG. A2 ENVIRONMENT HANDLED BY SNAP MODEL

TABLE A1 SUMMARY OF SNAP INPUTS (PART I)

INPUT PARAMETER	EXPLANATION	UNIT	LIMITS
TITLE	Text on plots	-	≤ 30 characters
NF	No. of source frequencies	-	NF ≤ 25
F(1),·····F(NF)	Source frequencies	Hz	F > 0
MMIN,MMAX	MMIN: First mode to be calculated MMAX: Last mode to be calculated	- -	1 ≤ MMIN ≤ MMAX ≤ 500
LIØ,LI1	LIØ: No. of discretization points in water LI1: No. of discretization points in sediment	- -	Ø < LIØ+LI1 ≤ 2500
NSEG	No. of segments in range	-	NSEG ≥ 1
SEGL(1)	Length of first segment	km	SEGL > Ø
HØ,SØ,S1	HØ: Water depth in first segment SØ: RMS roughness of sea surface S1: RMS roughness of sea bottom	m m m	HØ > Ø SØ ≥ Ø S1 ≥ Ø
ZØ(1),CØ(1)	ZØ(1): First sound-speed profile depth (= Ø) CØ(1): First sound-speed profile value in water	m m/s	- -
⋮	⋮	⋮	⋮
ZØ(n),CØ(n)	ZØ(n): Last sound-speed profile depth (= HØ) CØ(n): Last sound-speed profile value in water	m m/s	2 ≤ n ≤ 100
H1,R1,B1	H1: Thickness of sediment layer R1: Density of sediment B1: Compressional wave attenuation in sediment	m g/cm³ dB/λ	H1 ≥ Ø R1 > Ø B1 ≥ Ø
Z1(1),C1(1)	Z1(1): First sound-speed profile depth (= Ø) C1(1): First sound-speed profile value in sediment	m m/s	- -
⋮	⋮	⋮	⋮
Z1(m),C1(m)	Z1(m): Last sound-speed profile depth (= H1) C1(m): Last sound-speed profile value in sediment	m m/s	2 ≤ m ≤ 100
R2,B2,C2	R2: Density of subbottom B2: Compressional attenuation in subbottom C2: Compressional speed in subbottom	g/cm³ dB/λ m/s	R2 > Ø B2 ≥ Ø C2 > Ø
B2S,C2S	B2S: Shear attenuation in subbottom C2S: Shear speed in subbottom	dB/λ m/s	Ø ≤ B2S < Ø.75 B2 $\left(\frac{C2}{C2S}\right)^2$ Ø ≤ C2S << C1(H1)

*To be repeated for all segments ("NSEG" times).

TABLE A2 SUMMARY OF SNAP INPUTS (PART II)

1) ANGLE, PLT, PRT XAXIS x_1, x_2, x_3, x_4 YAXIS y_1, y_2, y_3, y_4 rmin, rmax, delr sd(1), rd(1) ⋮ sd(n), rd(n)	2) CONDR, INC, COH, PLT rmin, rmax, delr zmin, zmax, delz sd(1) ⋮ sd(n)	3) CONFR, INC, COH, PLT rmin, rmax, delr zmin, zmax, delz sd(1), rd(1) ⋮ sd(n), rd(n)	4) MODES, PLT, PRT
5) PHASE, PLT, PRT rmin, rmax, delr sd(1) ⋮ sd(n)	6) PROFL, PLT	7) TLAVF, INC, COH, PLT, PRT rmin, rmax, delr sd(1) ⋮ sd(n)	8) TLAVR, INC, COH, PLT, PRT rmin, rmax, delr sd(1) ⋮ sd(n)
9) TLDEP, INC, COH, PLT, PRT rmin, rmax, delr sd(1) ⋮ sd(n)	10) TLRAN, INC, COH, PLT, PRT rmin, rmax, delr sd(1), rd(1) ⋮ sd(n), rd(n)		

TABLE A3 DEFINITION OF INPUT CODES USED IN PART II

INPUT CODE	EXPLANATION
ANGLE	Field intensity vs arrival angle
CONDR*	Contoured transmission loss vs depth and range
CONFR	Contoured transmission loss vs frequency and range
MODES	Individual mode functions vs depth
PHASE	Phase of acoustic field vs depth
PROFL	Sound speed vs depth
TLAVF	Depth-averaged transmission loss vs frequency
TLAVR	Depth-averaged transmission loss vs range
TLDEP	Transmission loss vs depth
TLRAN	Transmission loss vs range
INC	Incoherent addition of modes
COH	Coherent addition of modes
PLT	Plotted output
PRT	Printed output
XAXIS	Identifier for horizontal axis
YAXIS	Identifier for vertical axis

*This option can be executed only for constant water depth

TABLE A4 DEFINITION OF INPUT PARAMETERS USED IN PART II

INPUT PARAMETER	EXPLANATION	UNIT	LIMITS
x_1, x_2, x_3, x_4	x_1: Lowest data value on horizontal axis[1] x_2: Highest data value on horizontal axis[1] x_3: No. of data units per centimeter[2] x_4: Distance between tick marks in data units[3]	see Table A5	
y_1, y_2, y_3, y_4	y_1: Lowest data value on vertical axis[1] y_2: Highest data value on vertical axis[1] y_3: No. of data units per centimeter[2] y_4: Distance between tick marks in data units[3]	see Table A5	
rmin, rmax, delr	rmin: Minimum range for loss calculation rmax: Maximum range for loss calculation delr: Range increment[4]	km km km	$0 \leq$ rmin $\leq$ rmax delr ≥ 0
zmin, zmax, delz	zmin: Minimum contour level zmax: Maximum contour level delz: Level increment[5]	dB dB dB	$0 \leq$ zmin $\leq$ zmax delz ≥ 0
sd(1), rd(1)	sd(1): First source depth rd(1): First receiver depth	m m	$0 <$ sd ≤ 80 $0 <$ rd ≤ 80
⋮	⋮	⋮	⋮
sd(n), rd(n)	sd(n): Last source depth rd(n): Last receiver depth	m m	$n \leq 10$

[1] Axis directions can be changed as compared to the standard ones given in Figs. B3-B20 by assigning highest data values to (x_1, y_1) and lowest data values to (x_2, y_2).

[2] For logarithmic frequency axes this argument indicates the length of an octave in centimeters.

[3] For logarithmic frequency axes this argument indicates the number of subdivisions per octave ($x_4 \geq 1$). Ex: $x_4 = 3$ results in tick marks every 1/3 of an octave.

[4] No. of range steps per segment cannot exceed 500.

[5] No. of contour level steps cannot exceed 51.

TABLE A5 DEFAULT AXIS VALUES

OPTION	X-AXIS								Y-AXIS							
	x_1		x_2		x_3		x_4		y_1		y_2		y_3		y_4	
ANGLE	0	deg	40	deg	2	deg/cm	5	deg	40	dB	140	dB	8	dB/cm	20	dB
CONDR	rmin	km	rmax	km	2	km/cm	5	km	0	m	H0	m	8	m/cm	20	m
CONFR*	rmin	km	rmax	km	2	km/cm	5	km	F_{min}	Hz	F_{max}	Hz	2	cm/oct	1	-
MODES	-0.2	**	0.2	**	.12	**/cm	0.2	**	0	m	H0+H1	m	8	m/cm	20	m
PHASE	-180	deg	180	deg	18	deg/cm	45	deg	0	m	H0	m	8	m/cm	20	m
PROFL	1450	m/s	1650	m/s	10	m/s/cm	25	m/s	0	m	H0+H1	m	8	m/cm	20	m
TLAVF*	F_{min}	Hz	F_{max}	Hz	3	cm/oct	1	-	.40	dB	140	dB	8	dB/cm	20	dB
TLAVR	rmin	km	rmax	km	2	km/cm	5	km	40	dB	140	dB	8	dB/cm	20	dB
TLDEP	0	dB	160	dB	8	dB/cm	20	dB	0	m	H0	m	8	m/cm	20	m
TLRAN	rmin	km	rmax	km	2	km/cm	5	km	40	dB	140	dB	8	dB/cm	20	dB

*Option with logarithmic frequency axis.

** $(m^2/kg)^{\frac{1}{2}}$.

NB: The unit for loss is dB re 1 meter.

APPENDIX B

SHALLOW-WATER SAMPLE RUN

To illustrate the full capability of the SNAP model, a range-dependent shallow-water example with complete documentation of both input and output is given. Since the example also serves to illustrate the default axes used by the model, all plots are reproduced in scale 1:1. To limit the number of illustrations, only results for 100 Hz will be shown, except for options TLAVF and CONFR, which both give transmission loss versus frequency. The total running time on the UNIVAC 1106 for producing the 18 plots shown in this example was 1½ h, where most of the computer time was spent in producing the four frequency plots (Figs. B15, B16, B19, and B20). Thus, the remaining twelve plots took less than 10 min of CPU time, and a simple loss calculation versus range (Fig. B9) takes only around 30 seconds.

The following gives the complete run stream (Fig. B1), the standard printout (Fig. B2), and all possible plotted outputs (Figs. B3-B20).

A short comment to the various outputs will be given here in order to point out features of general interest to users of the SNAP model.

PROFL Figures B3 and B4 give sound-speed profiles for first and second segment, respectively. Both are downward-refracting profiles in 100 m of water; in segment 2 (Fig. B4) there is also a sediment layer of 10 m thickness. The interface between water and sediment is given by the horizontal line at 100 m depth, and we see that there is a discontinuity in the sound-speed profile at the interface.

MODES Figures B5 and B6 give mode amplitudes versus depth for a source frequency of 100 Hz. We see that the mode functions in segment 2 (Fig. B6) are discontinuous at the water/sediment interface, a fact caused by the density difference between the two layers.

ANGLE Figure B7 gives field intensity versus arrival angle for all four modes. For the specific source/receiver combination considered here and for a range of 20 km, the intensity decreases with increasing mode number.

PHASE Figure B8 gives the phase distribution over depth. We see that the phase structure is relatively simple for this 4-mode case.

TLRAN Figures B9 and B10 give transmission loss versus range by coherent and incoherent addition of modes, respectively. The dashed line at 15 km range indicates transition from segment 1 to segment 2. The coherent loss curve (Fig. B9) shows the effect of modal interference, with the most complicated interference pattern at short ranges where all modes are present. At long ranges the higher-order modes have been attenuated out (mode stripping) with a much simpler interference pattern as the result. As pointed out in Sect. 2.4, coherent addition of modes is the mathematically correct way of computing the acoustic field. However, incoherent addition of modes (Fig. B10) also makes sense in shallow water, where it represents a kind of average loss curve, with averaging done over either range or frequency.

TLDEP Figures B11 and B12 give transmission loss over depth by coherent and incoherent addition of modes, respectively. As described under option TLRAN, coherent addition of modes (Fig. B11) gives a correct field description in all details. On the other hand, incoherent addition of modes (Fig. B12) gives an average field intensity with averaging done over either range or frequency. We see from Fig. B12 that the field intensity is almost constant over the water column.

TLAVR Figures B13 and B14 give depth-averaged loss versus range by coherent and incoherent addition of modes, respectively. We see that the two methods give almost identical results, which will generally be the case when losses are averaged over the water column. We also see that propagation is better for the deep source (75 m) than for the shallow source (25 m).

TLAVF Figures B15 and B16 give depth-averaged loss versus frequency by coherent and incoherent addition of modes, respectively. Also here the two methods give almost identical results: we see that the optimal

propagation frequency is around 60 Hz for a range of 40 km and a source depth of 25 m.

CONDR Figures B17 and B18 give contoured loss versus depth and range by coherent and incoherent addition of modes, respectively. It is clear that no useful information can be extracted from the coherent contour plot (Fig. B17). On the other hand, the incoherent plot (Fig. B18) gives smooth and simple contours. Thus we see that the field intensity is almost constant over depth at short ranges, while energy tends to be trapped in the lower part of the water column at longer ranges.

N.B. It should be emphasized that contrary to the results given above, only coherent contour plots make sense in deep water, since incoherent plots average out both caustics and shadow zones.

CONFR Figures B19 and B20 give contoured loss versus frequency and range by coherent and incoherent addition of modes, respectively. Here again it is difficult to interprete the coherent plot (Fig. B19), while the incoherent plot (Fig. B20) gives simple, smooth contour lines. We see that all frequencies propagate equally well at short ranges, while optimal propagation at longer ranges is obtained for frequencies around 75 Hz. Actually, optimal propagation seems to occur at higher and higher frequencies for increasing range. The NB given under option CONDR obviously also applies here.

THIS PAGE IS BEST QUALITY PRACTICABLE
FROM COPY FURNISHED TO DDC

```
@XQT SNAP.A50
SNAP TEST
1
100.
1,500
1000,100
2
15.
100.,0.,0.
0.,1525.
20.,1530.
40.,1500.
100.,1502.
0.
2.,.5,1600.
0.,0.
50.
100.,.1,.25
0.,1530.
15.,1525.
25.,1525.
35.,1505.
45.,1500.
100.,1501.
10.,1.5,.15
0.,1550.
10.,1560.
2.,.5,1650.
1.,350.
PROFL,PLT
MODES,PLT
XAXIS -.1,.2,.12,.2
YAXIS 0.,110.,8.,20.
ANGLE,PLT
20.,20.,0.
25.,50.
PHASE,PLT
20.,20.,0.
25.
TLRAN,INC,COH,PLT
0.,40.,.1
25.,50.
TLDEP,INC,COH,PLT
20.,20.,0.
25.
TLAVR,INC,COH,PLT
0.,40.,.5
75.
75.
CONDR,INC,COH,PLT
0.,40.,.5
50.,140.,5.
25.
@EOF
```

WATER / SEDIMENT / SUBBOTTOM — SEGMENT NO.1

WATER / SEDIMENT / SUBBOTTOM — SEGMENT NO.2

OUTPUT OPTIONS

FIG. B1 RUN STREAM FOR SHALLOW-WATER CASE

SNAP TEST

THIS PAGE IS BEST QUALITY PRACTICABLE
FROM COPY FURNISHED TO DDC

OUTPUT OPTIONS:

	PRT	PLT	COH	INC
ANGLE	0.	1.		
COHDR	0.	1.	1.	1.
MODES	0.	1.		
PHASE	0.	1.		
PROFL	0.	1.		
TLAVR	0.	1.	1.	1.
TLDEP	0.	1.	1.	1.
TLRAN	0.	1.	1.	1.

SEGMENT NO. 1

SEGMENT LENGTH = 15.0 KM

SAMPLE POINTS:
RSP = 53
WATER = 1000
SEDIMENT = 0

DEPTHS (M):
WATER = 100.00
SEDIMENT = .00

DENSITIES (G/CM**3):
WATER = 1.00
SEDIMENT = .00
SUBBOTTOM = 2.00

ATTENUATION COEFFICIENTS (DB/WL):
SEDIMENT = .00
SUBBOTTOM = .50
SHEAR = .00

RMS ROUGHNESSES (M):
SEA SURFACE = .00
SEA FLOOR = .00

SOUND SPEED PROFILE

WATER

DEPTH (M)	SPEED (M/S)
.00	1529.00
20.00	1530.00
40.00	1500.00
100.00	1502.00

BOTTOM SOUND SPEED = 1600.00 M/S
SHEAR SPEED = .00 M/S

SOURCE FREQUENCY = 100.00 HZ
MAXIMUM NO. OF MODES = 4

	WAVE NUMBER	ALPHA	A0	A1	A2	A2S	A0S	A0R	RB	SS	SB
MODE = 1	.41728965A2+000	.21109-04	.11227-06	.000000	.20997-04		.000000	.000000		.00	.00
MODE = 2	.41329970?5+000	.69707-04	.11153-06	.000003	.69545-04		.000000	.000000		.00	.00
MODE = 3	.407343896?+000	.10687-03	.11175-06	.000001	.10674-03		.000000	.000000		.00	.00
MODE = 4	.4003716155+000	.16726-03	.11142-06	.000000	.16715-03		.000000	.000000		.00	.00

FIG. B2 STANDARD PRINTOUT FOR SHALLOW-WATER TEST CASE

THIS PAGE IS BEST QUALITY PRACTICABLE
FROM COPY FURNISHED TO DDC

SEGMENT NO. 2
****

SEGMENT LENGTH = 50.0 KM

SAMPLE POINTS:
MSP = 51
WATER = 1000
SEDIMENT = 100

DEPTHS (M):
WATER = 100.00
SEDIMENT = 10.00

DENSITIES (G/CM**3):
WATER = 1.00
SEDIMENT = 1.50
SUBBOTTOM = 2.00

ATTENUATION COEFFICIENTS (DB/WL):
SEDIMENT = .15
SUBBOTTOM = .50
SHEAR = 1.00

RMS ROUGHNESSES (M):
SEA SURFACE = .10
SEA FLOOR = .25

SOUND SPEED PROFILE

WATER

DEPTH (M)	SPEED (M/S)
.00	1530.00
15.00	1525.00
25.00	1525.00
35.00	1505.00
45.00	1500.00
100.00	1501.00

SEDIMENT

DEPTH (M)	SPEED (M/S)
.00	1550.00
10.00	1560.00

BOTTOM SOUND SPEED = 1650.00 M/S
SHEAR SPEED = 350.00 M/S

SOURCE FREQUENCY = 100.00 HZ
MAXIMUM NO. OF MODES = 6

	WAVE NUMBER	ALPHA	A0	A1	A2	A2S	A0S	A0W	RB	SS	SB
MODE = 1	.913740A0634+000	.12523-04	.11178-06	.10919-04	.17503-05	.14881-05	.00000	.52599-07	.08	.00	.00
MODE = 2	.913471311 3+000	.91125-04	.10995-06	.38721-04	.69063-05	.58990-05	.00000	.62485-06	.08	.00	.00
MODE = 3	.907719832 7+000	.65585-04	.10992-06	.52703-04	.14472-04	.10987-04	.38222-07	.11051-05	.08	.00	.00
MODE = 4	.901 0140016+000	.11163-03	.10774-06	.74758-04	.31387-04	.32046-04	.21505-06	.21466-05	.12	.00	.00

FIG. B2 STANDARD PRINTOUT FOR SHALLOW-WATER TEST CASE (Cont'd)

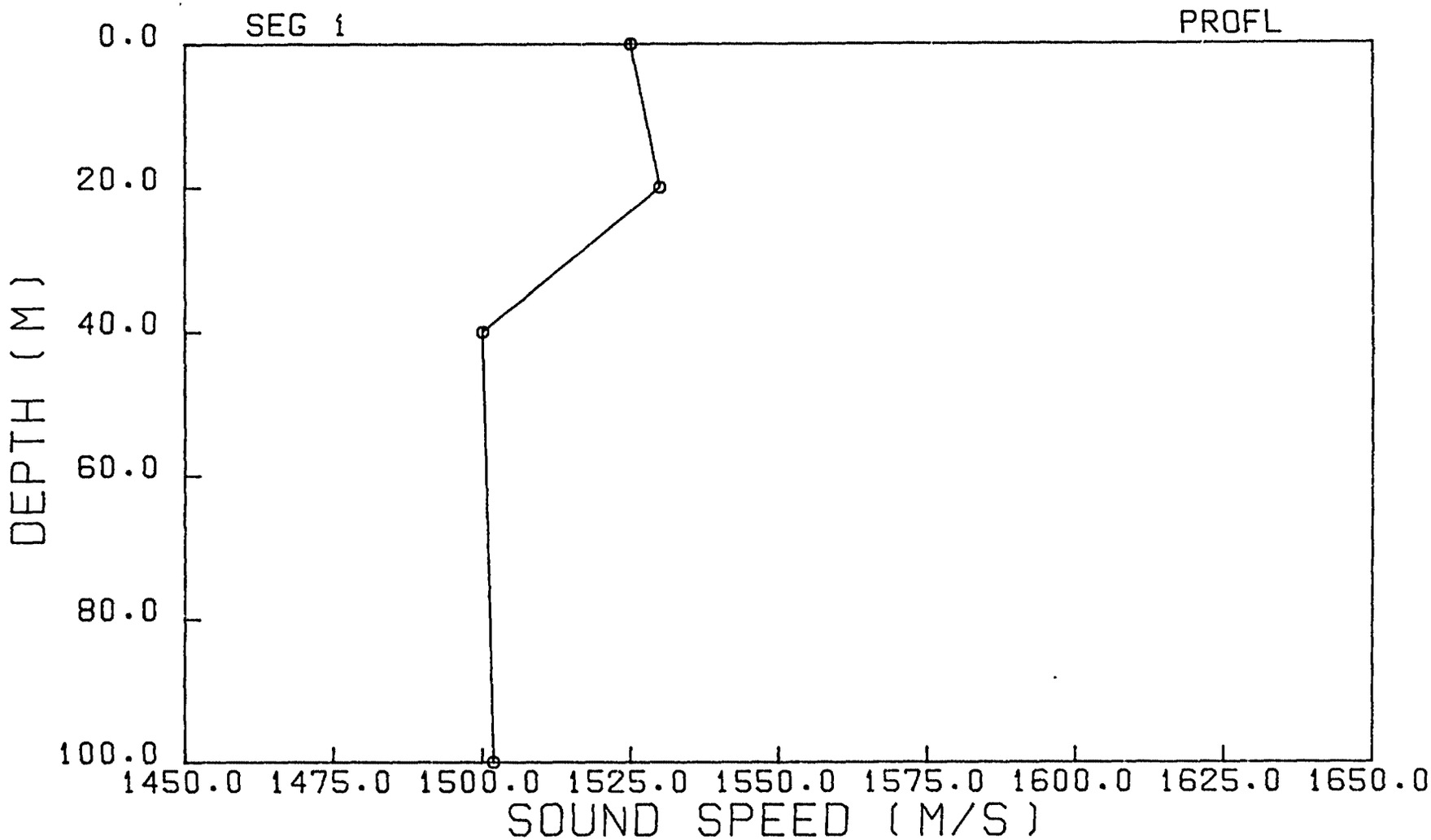

FIG. B3 SOUND-SPEED PROFILE IN SEGMENT No. 1

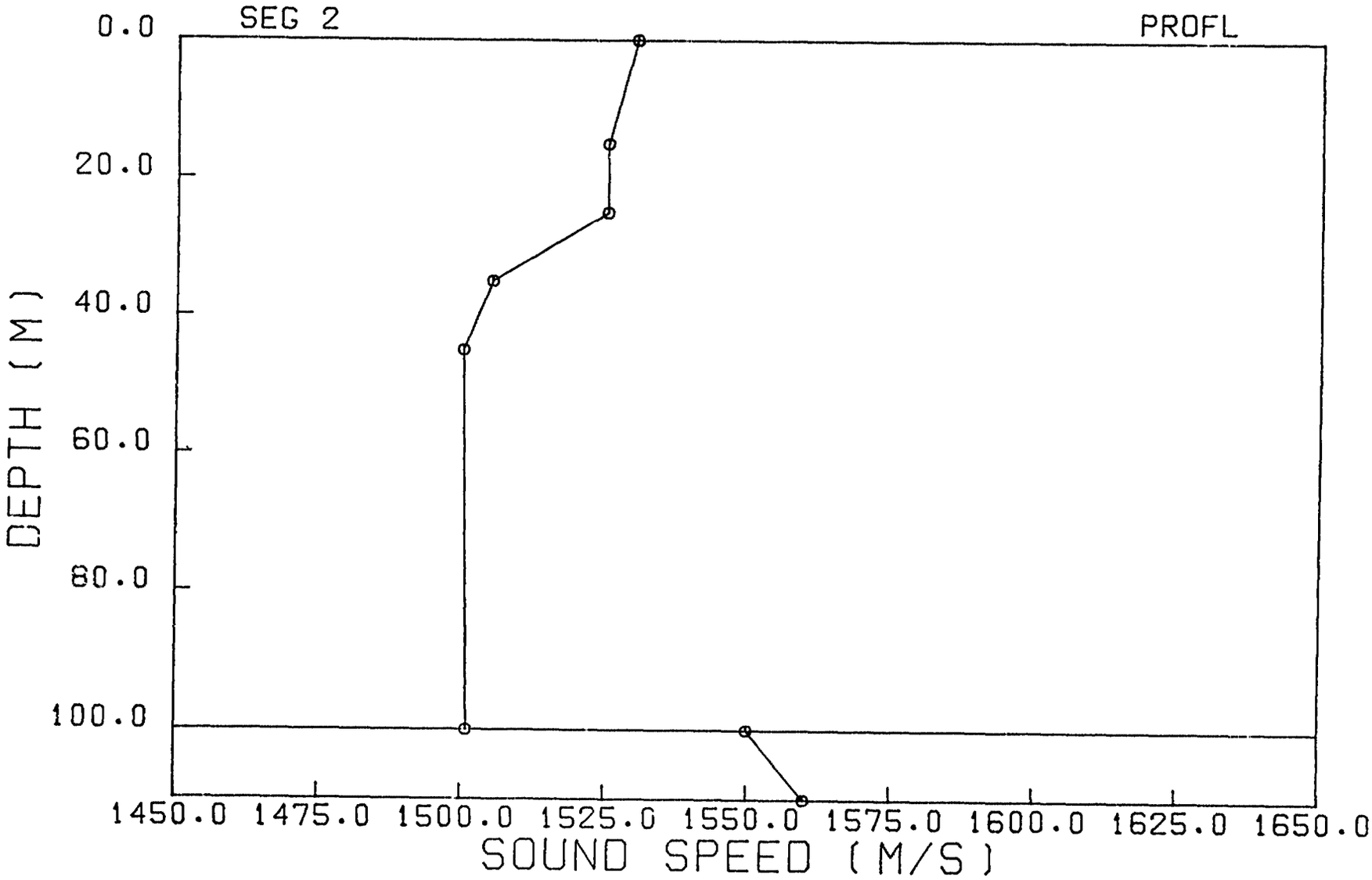

FIG. B4 SOUND-SPEED PROFILE IN SEGMENT No. 2

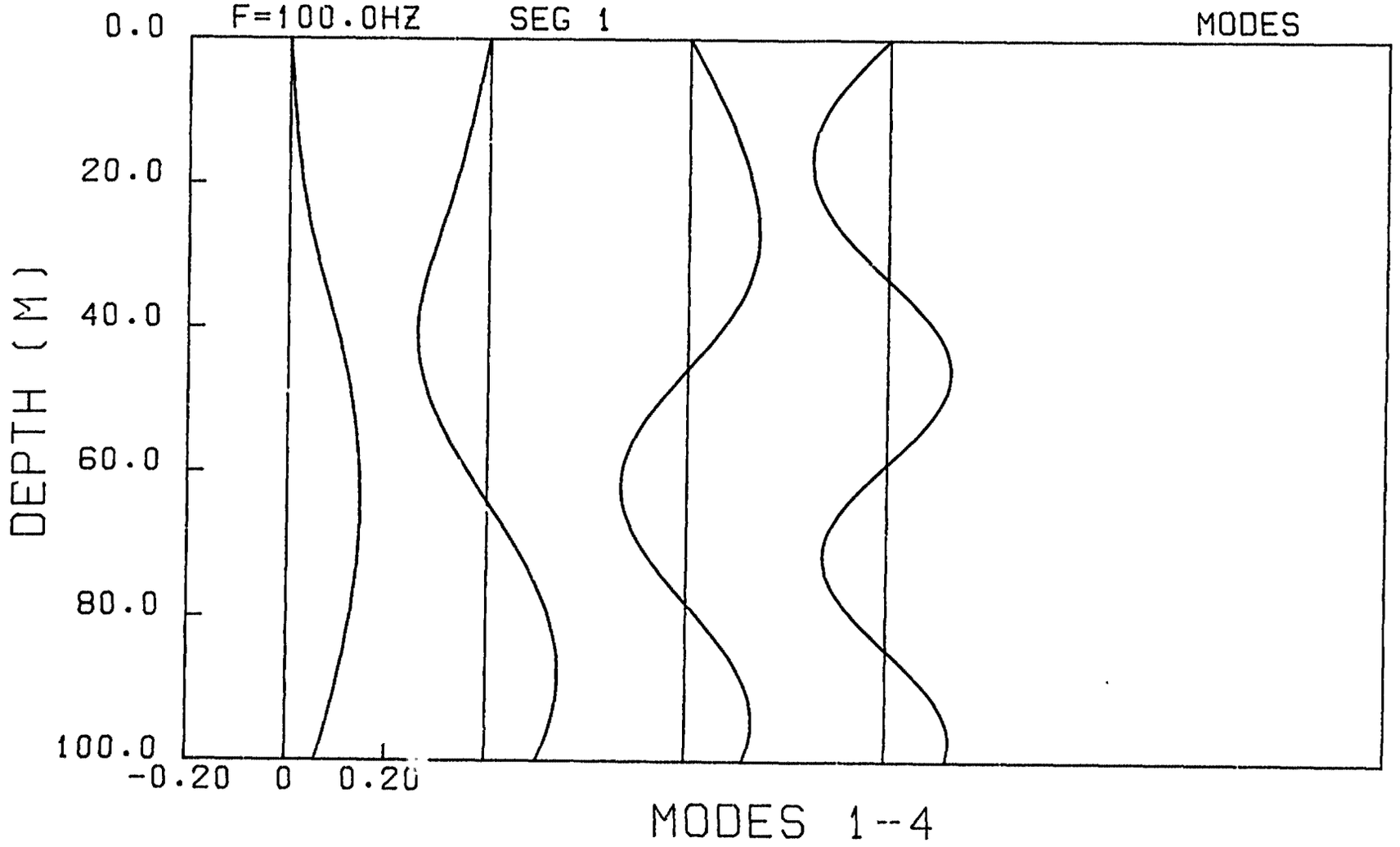

FIG. B5 MODE FUNCTIONS IN SEGMENT No. 1

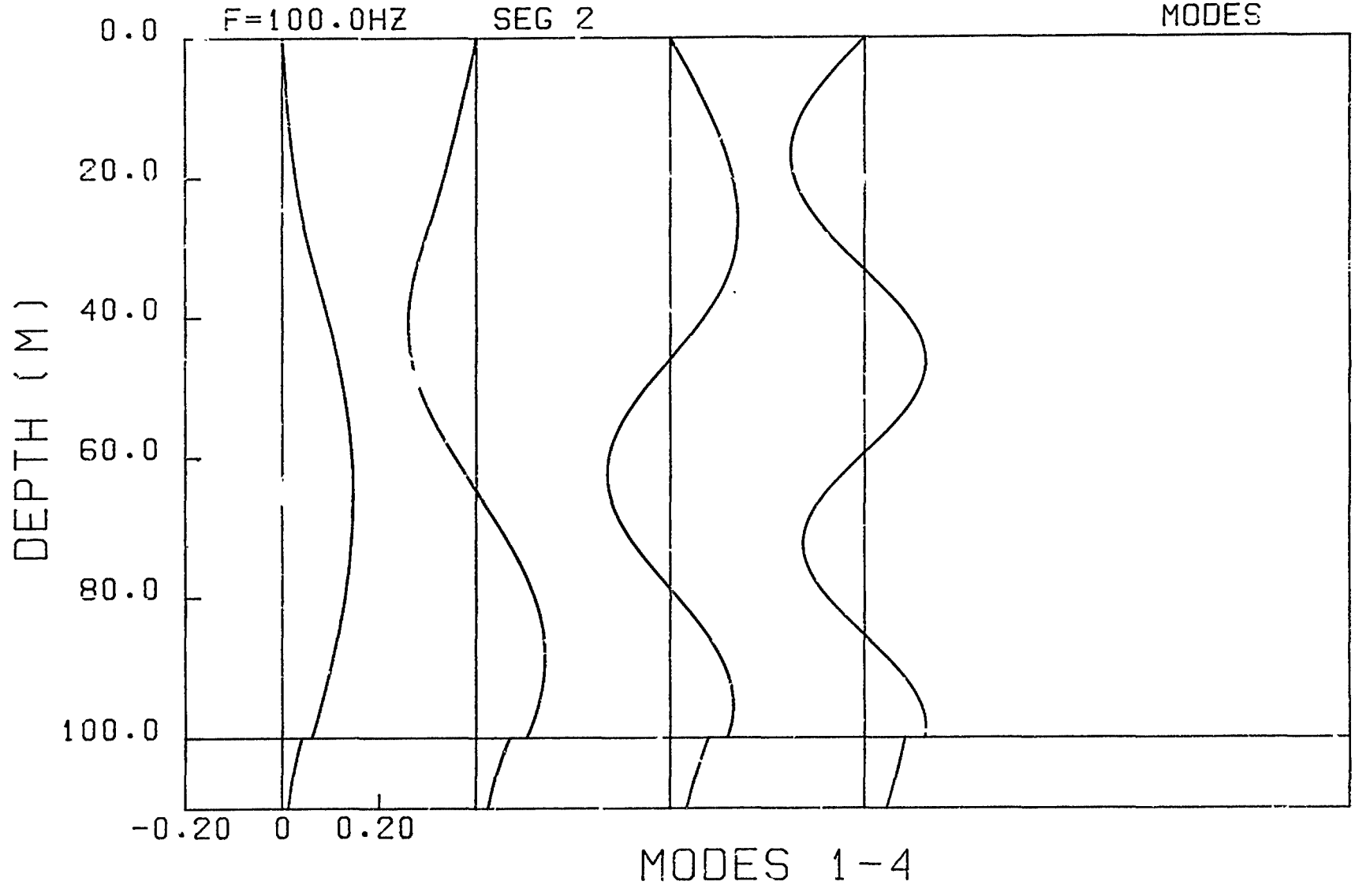

FIG. B6 MODE FUNCTIONS IN SEGMENT No. 2

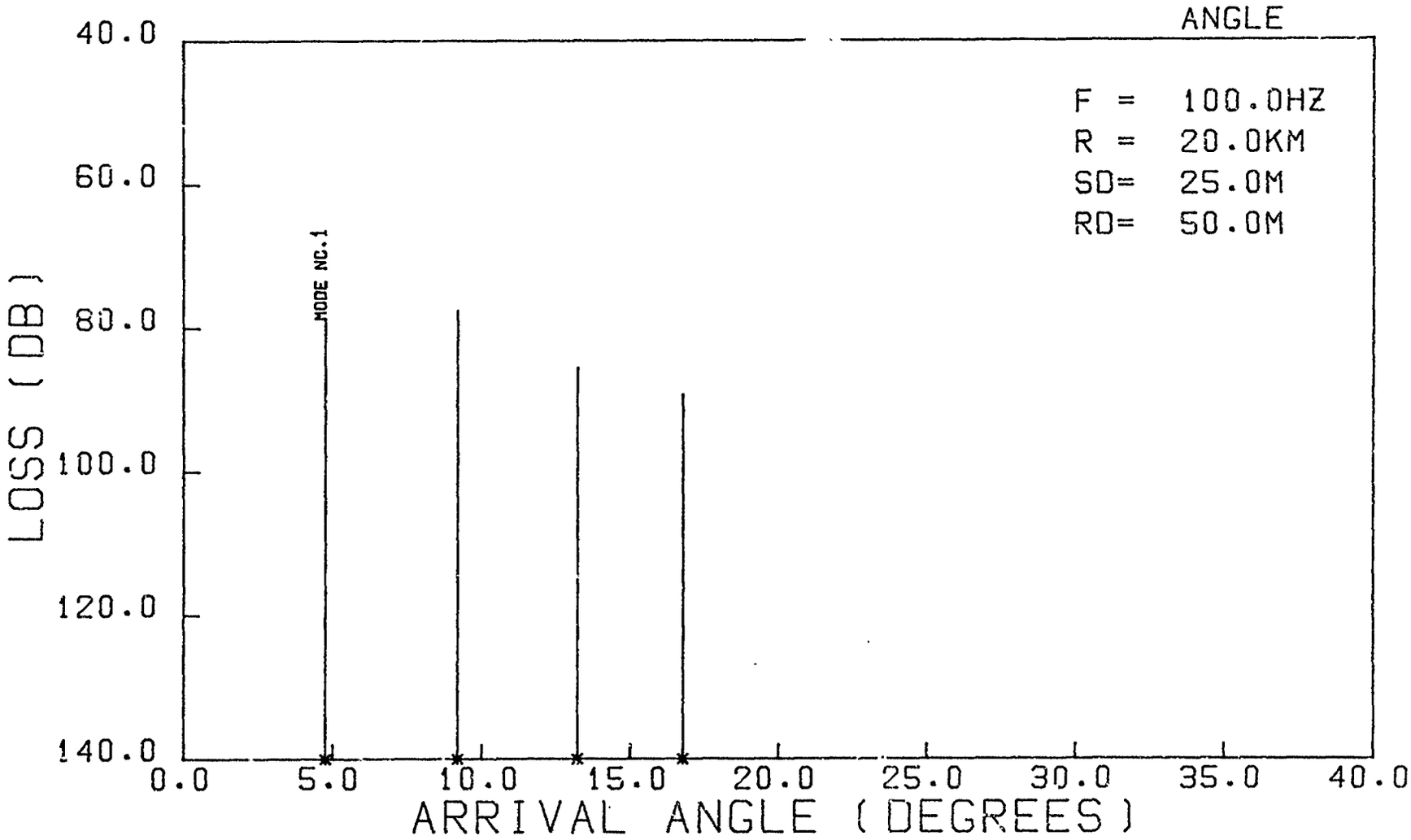

FIG. B7 FIELD INTENSITY VERSUS ARRIVAL ANGLE

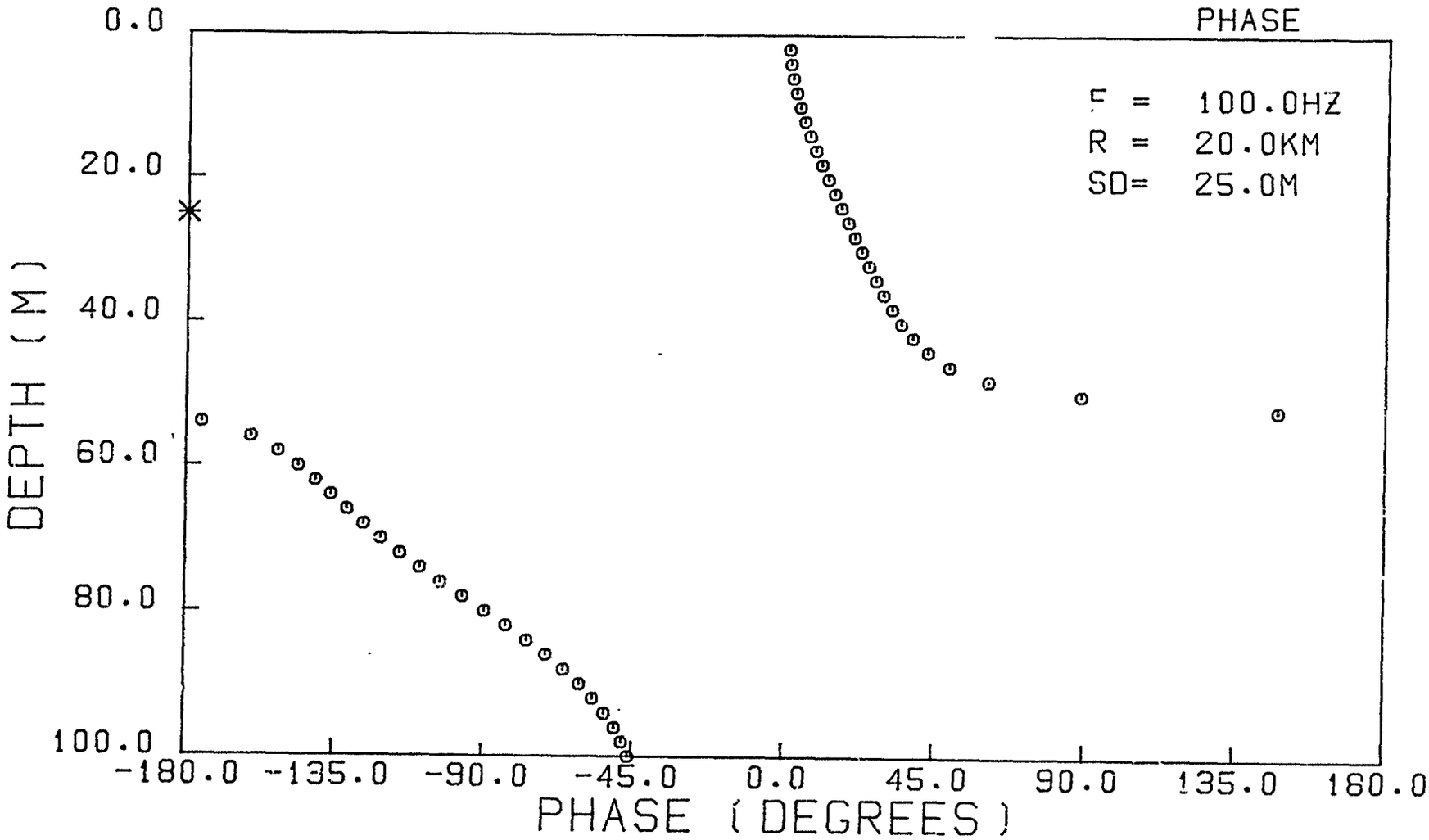

FIG. B8 PHASE DISTRIBUTION OVER DEPTH

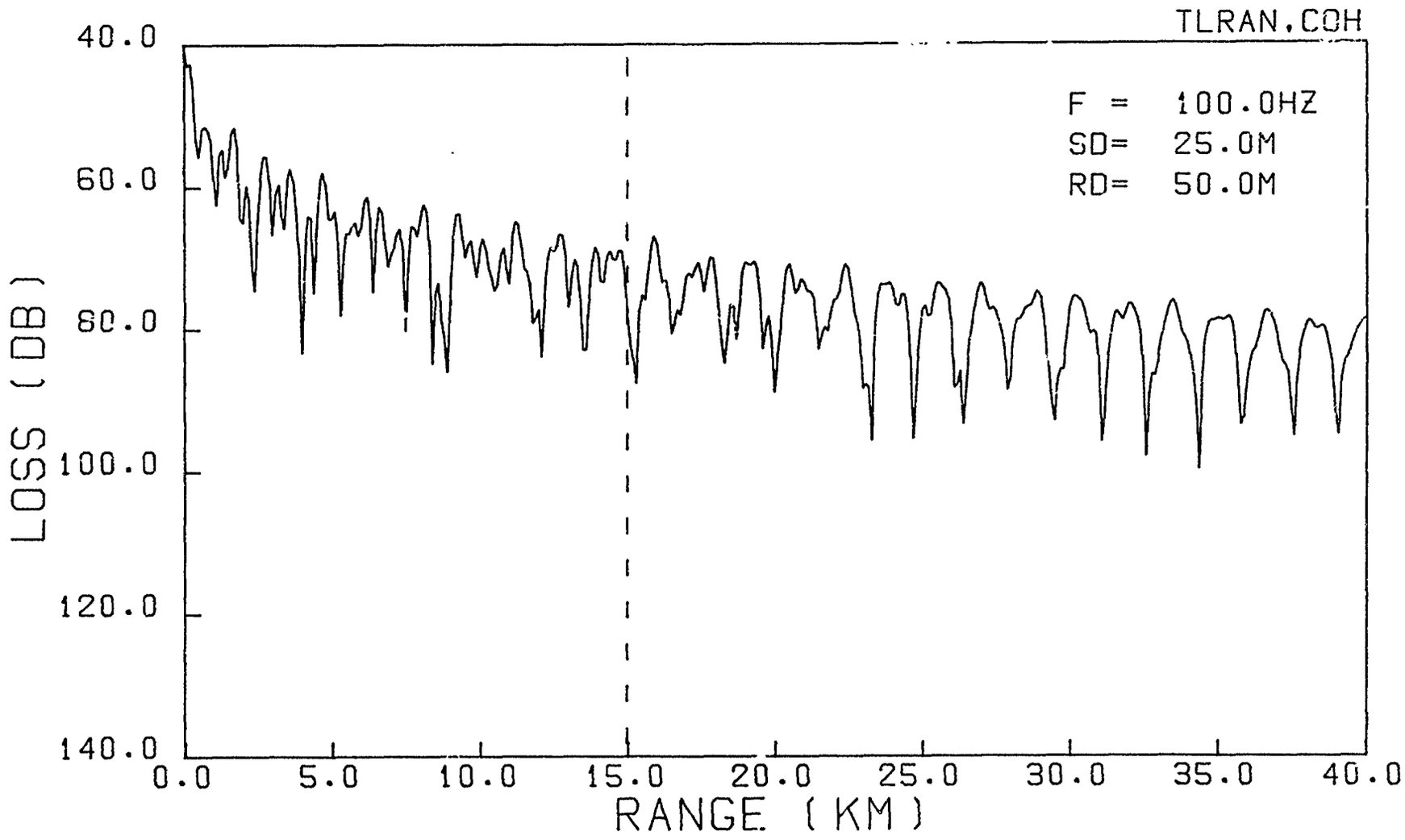

FIG. B9 TRANSMISSION LOSS VERSUS RANGE BY COHERENT ADDITION OF MODES

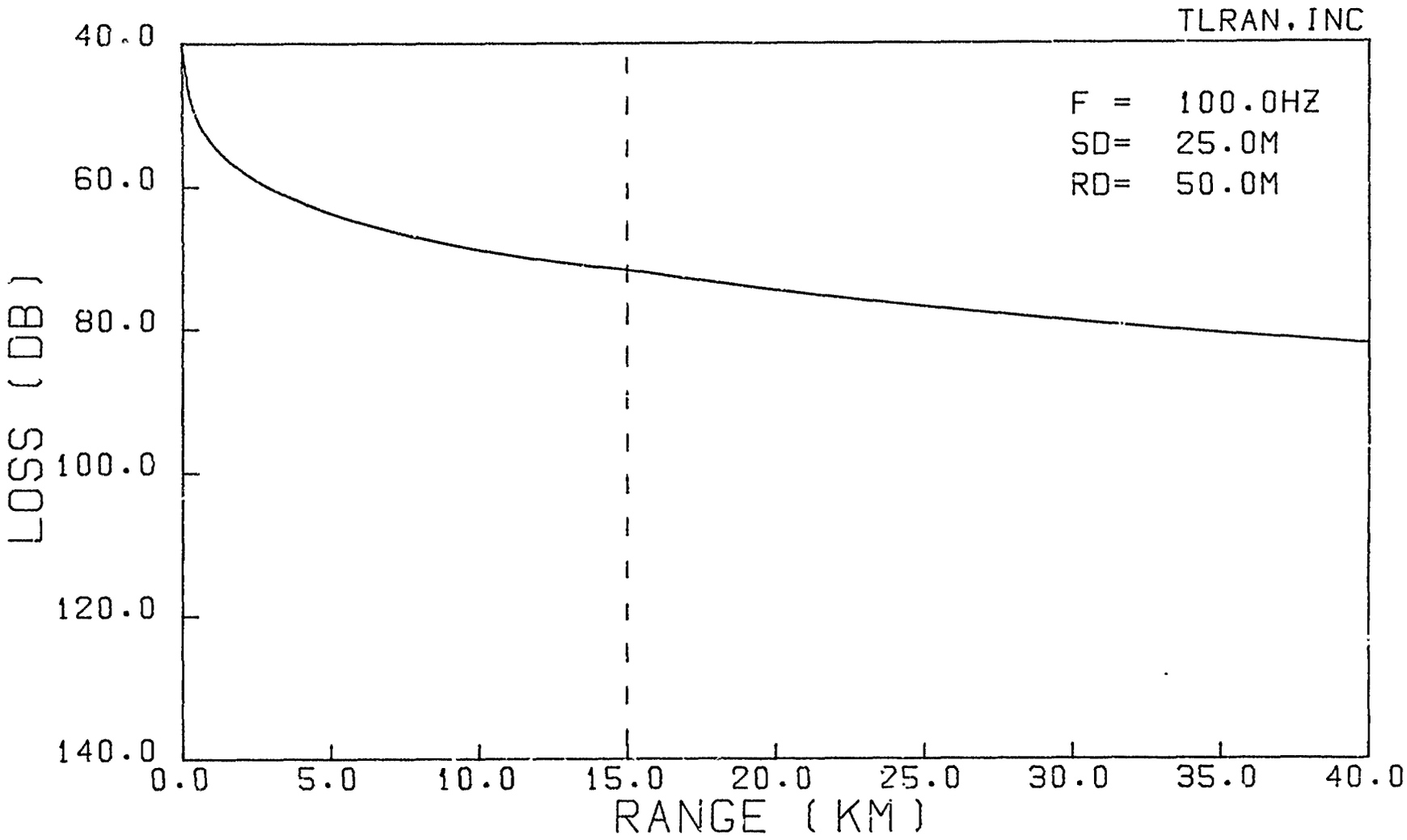

FIG. 310 TRANSMISSION LOSS VERSUS RANGE BY INCOHERENT ADDITION OF MODES

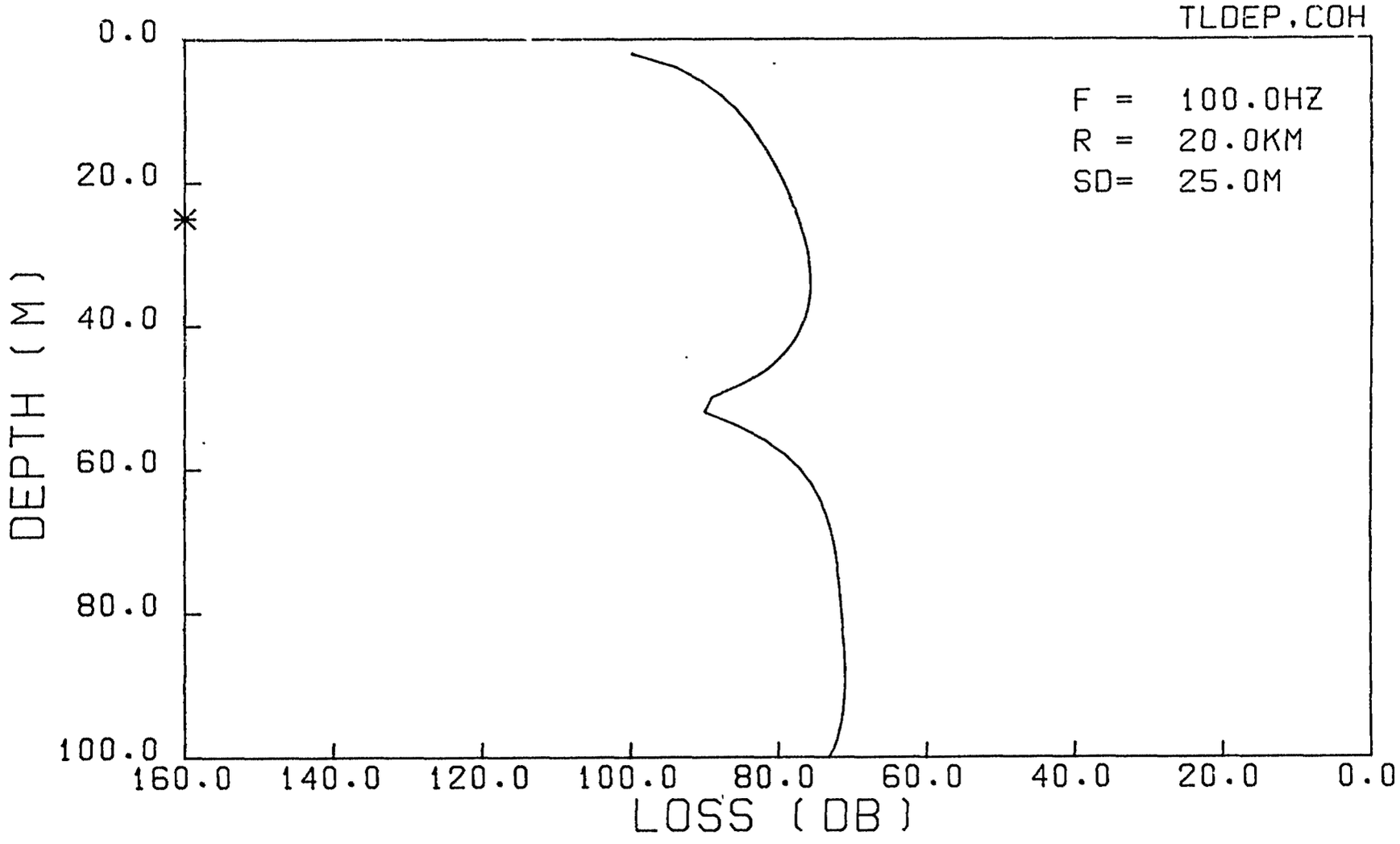

FIG. B11 TRANSMISSION LOSS VERSUS DEPTH BY COHERENT ADDITION OF MODES

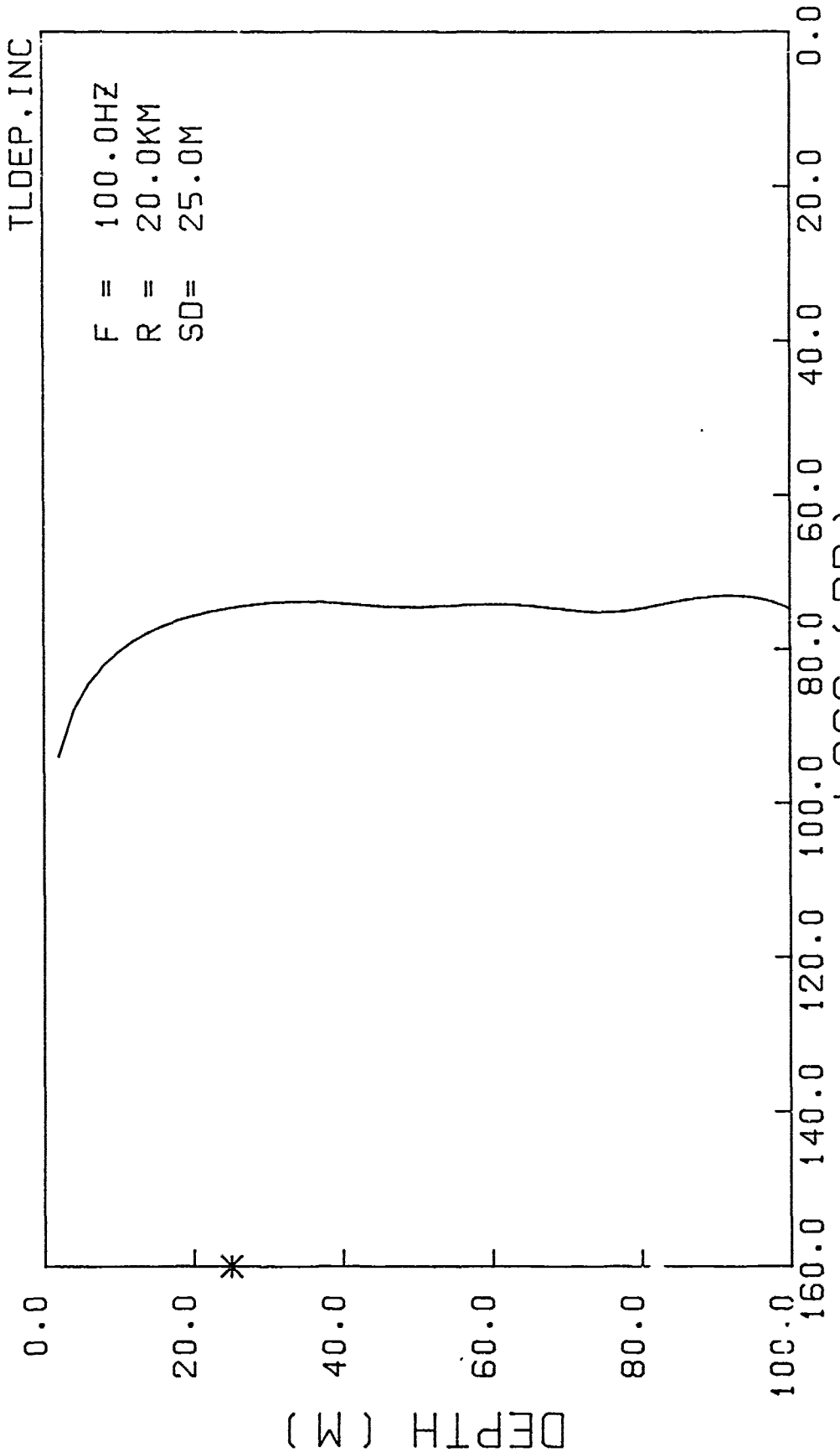

FIG. B12 TRANSMISSION LOSS VERSUS DEPTH BY INCOHERENT ADDITION OF MODES

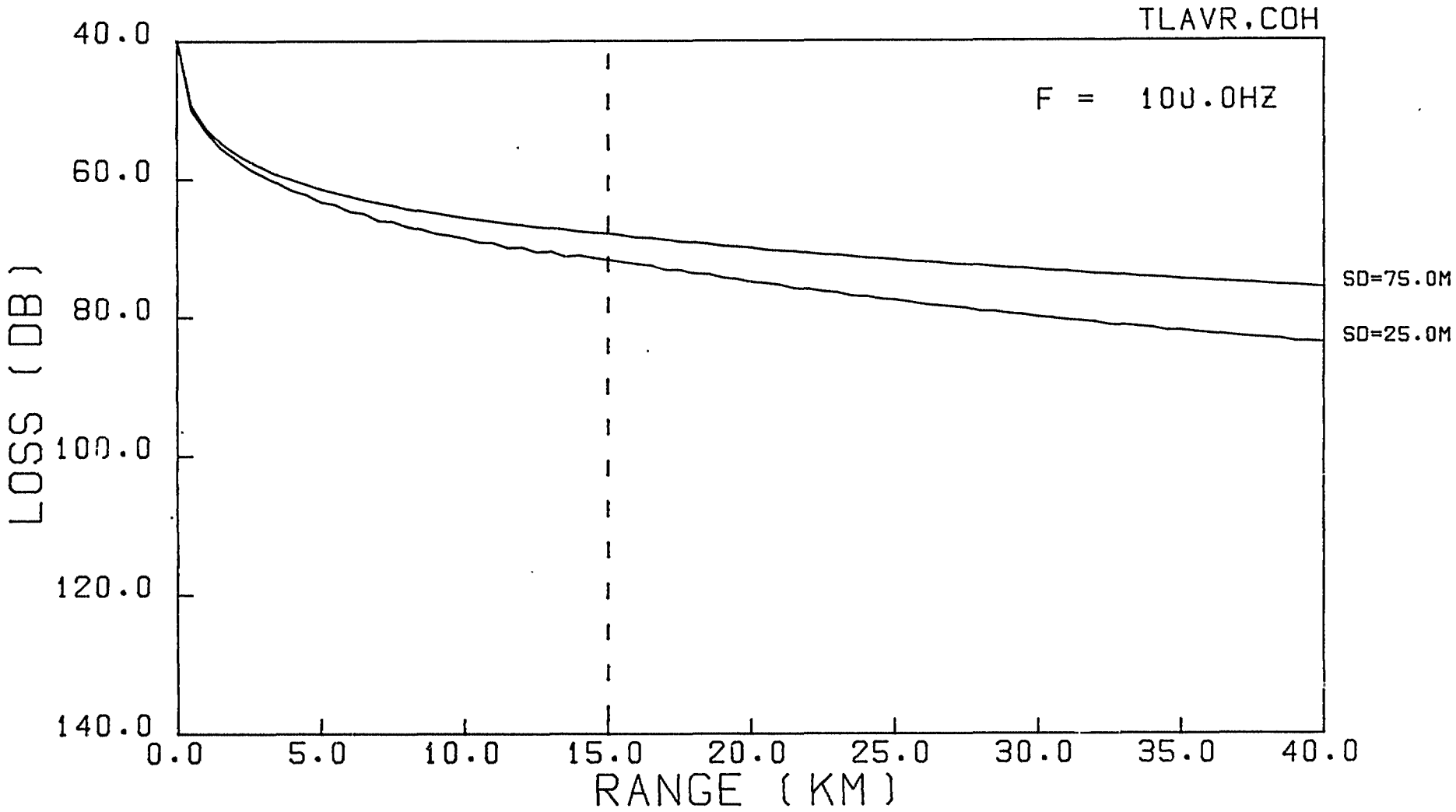

FIG. B13 DEPTH-AVERAGED LOSS VERSUS RANGE BY COHERENT ADDITION OF MODES

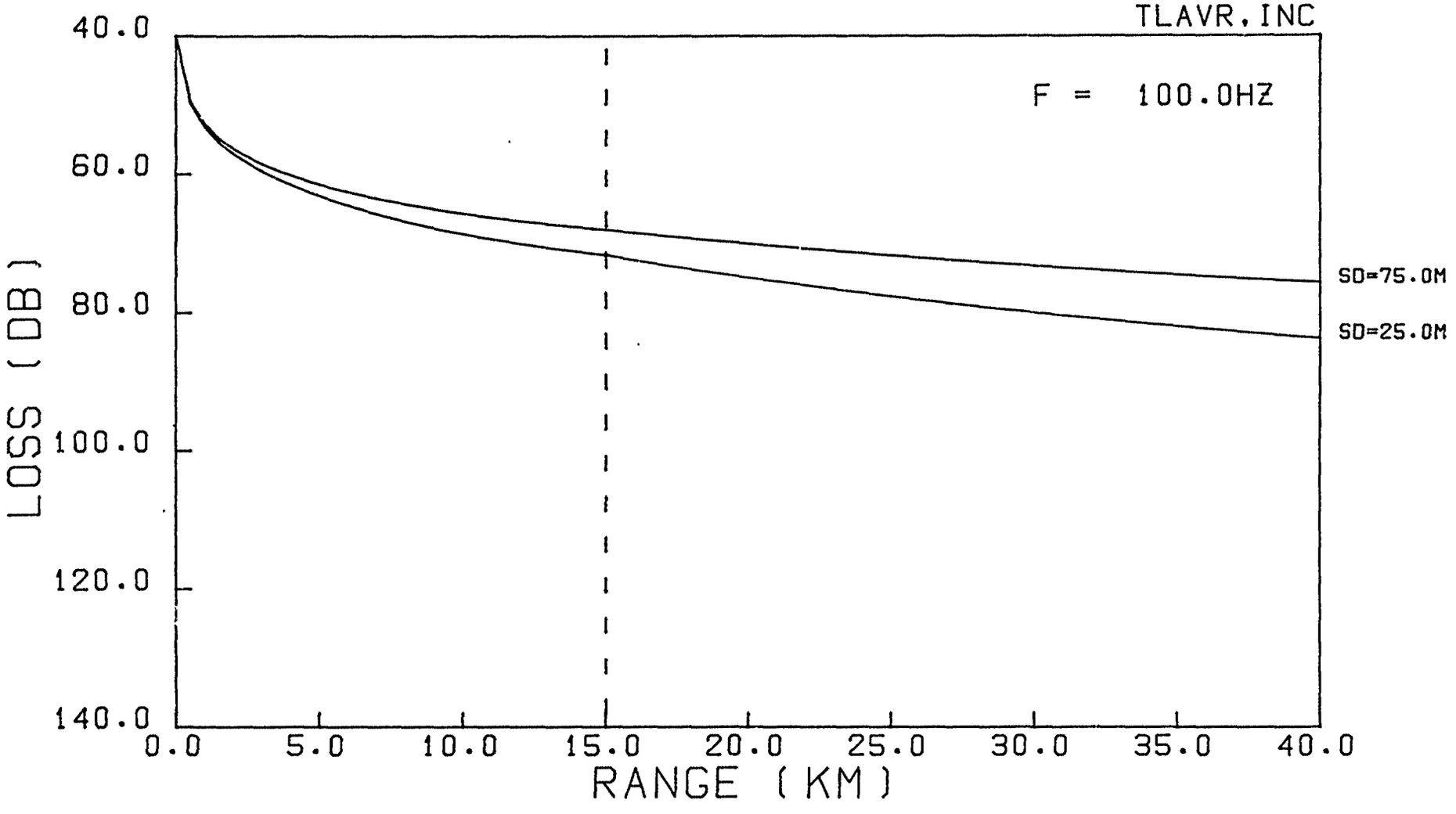

FIG. B14 DEPTH-AVERAGED LOSS VERSUS RANGE BY INCOHERENT ADDITION OF MODES

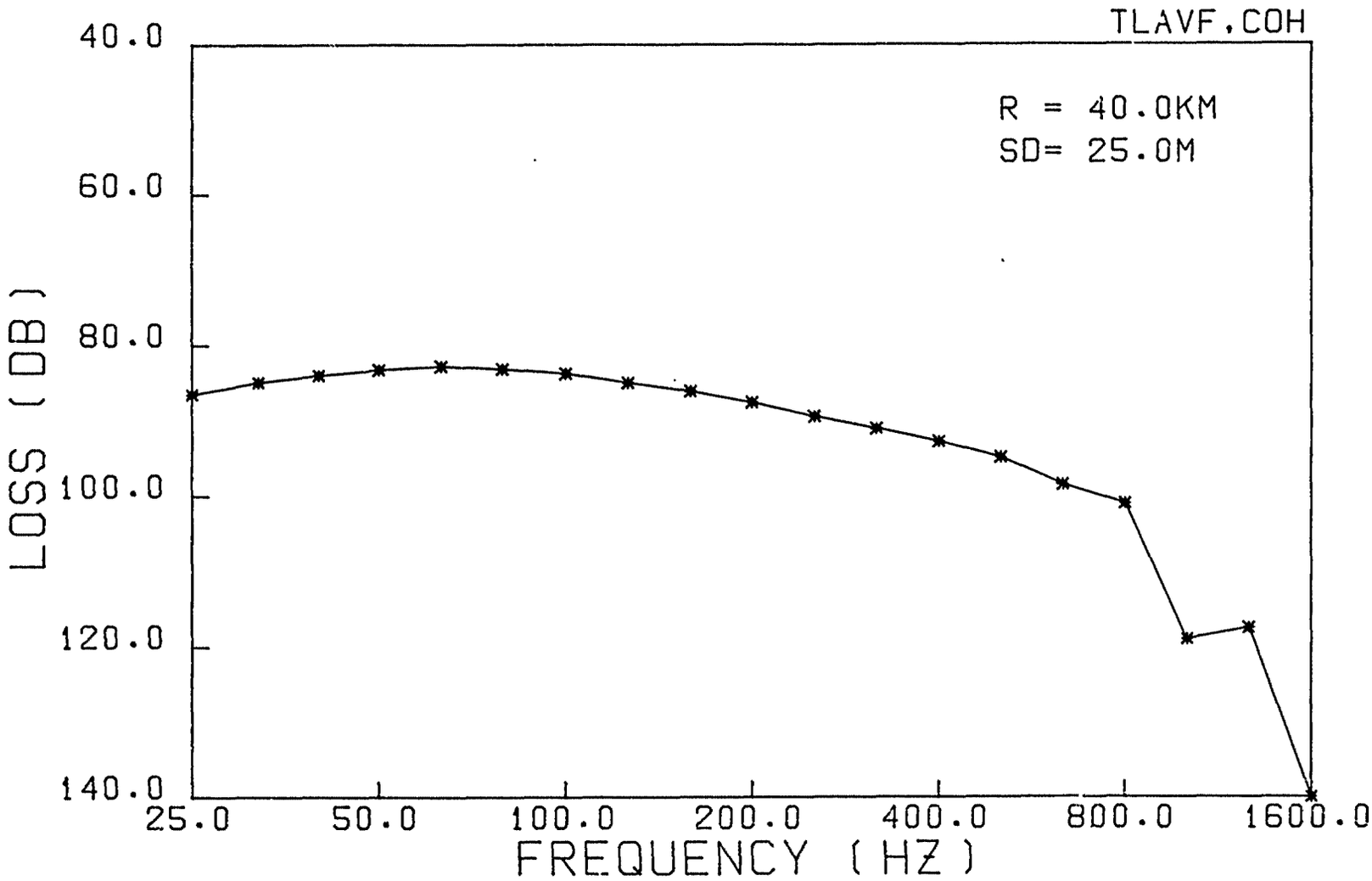

FIG. B15 DEPTH-AVERAGED LOSS VERSUS FREQUENCY BY COHERENT ADDITION OF MODES

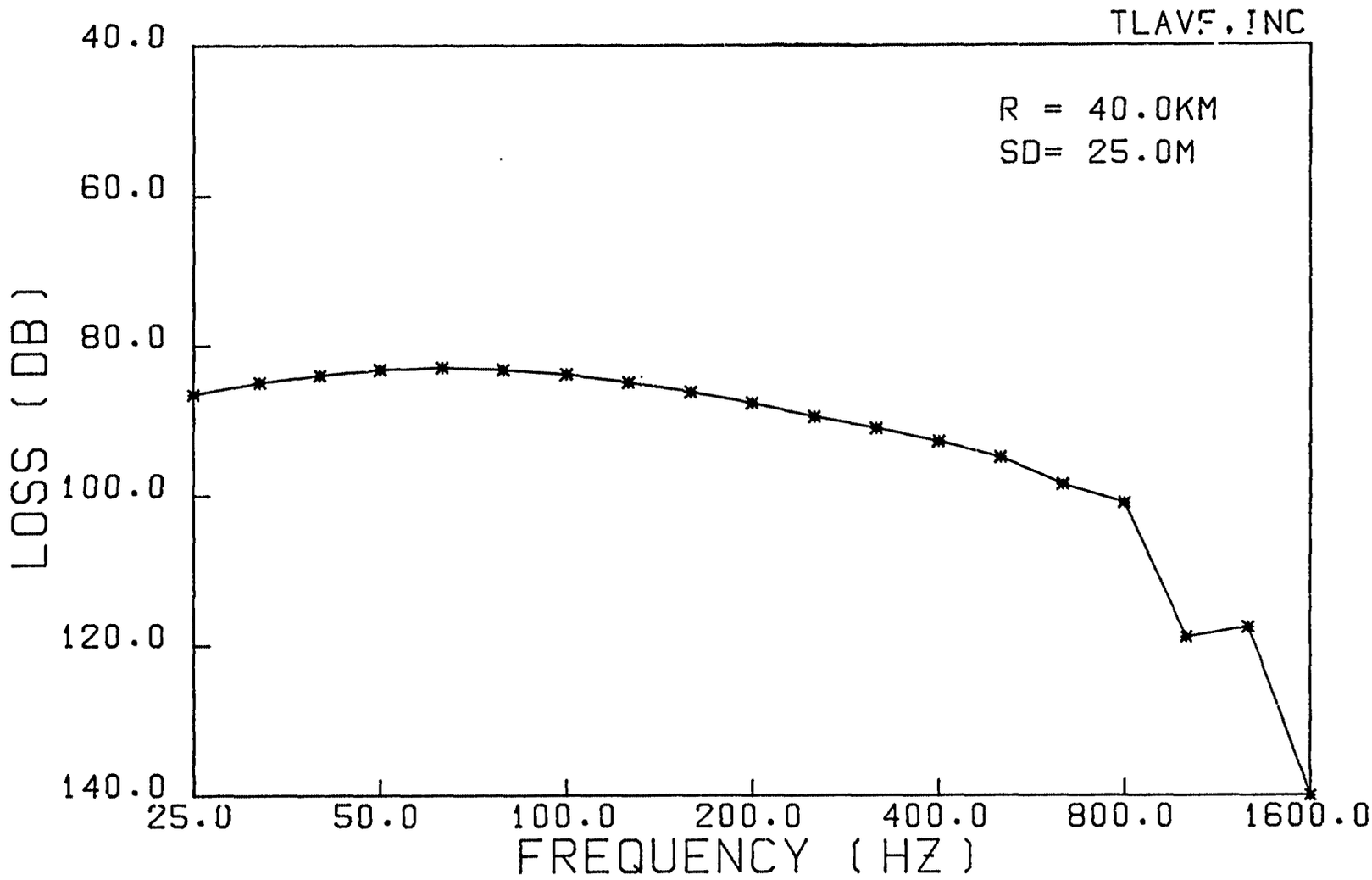

FIG. B16 DEPTH-AVERAGED LOSS VERSUS FREQUENCY BY INCOHERENT ADDITION OF MODES

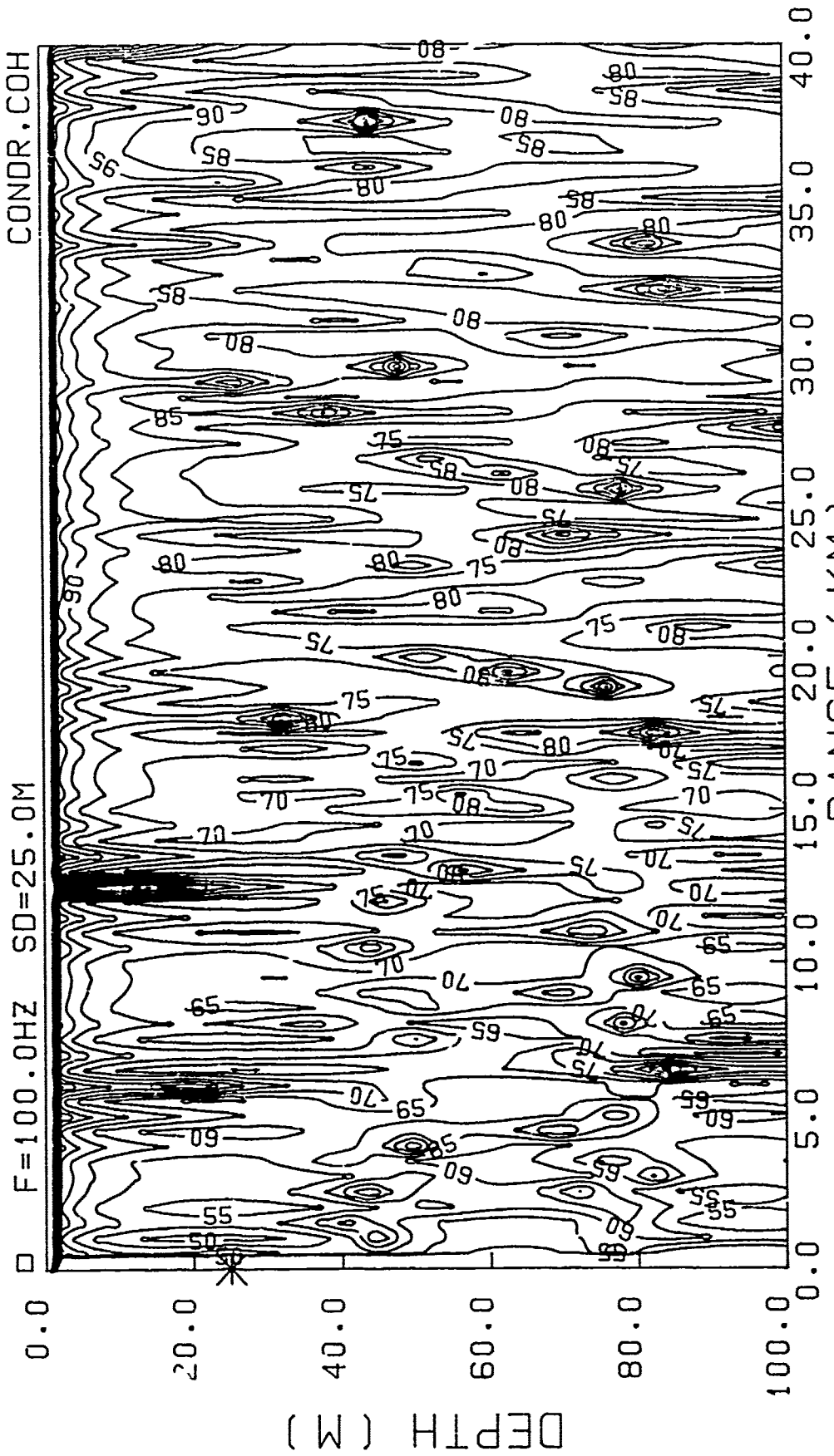

FIG. B17 CONTOURED LOSS VERSUS DEPTH AND RANGE BY COHERENT ADDITION OF MODES

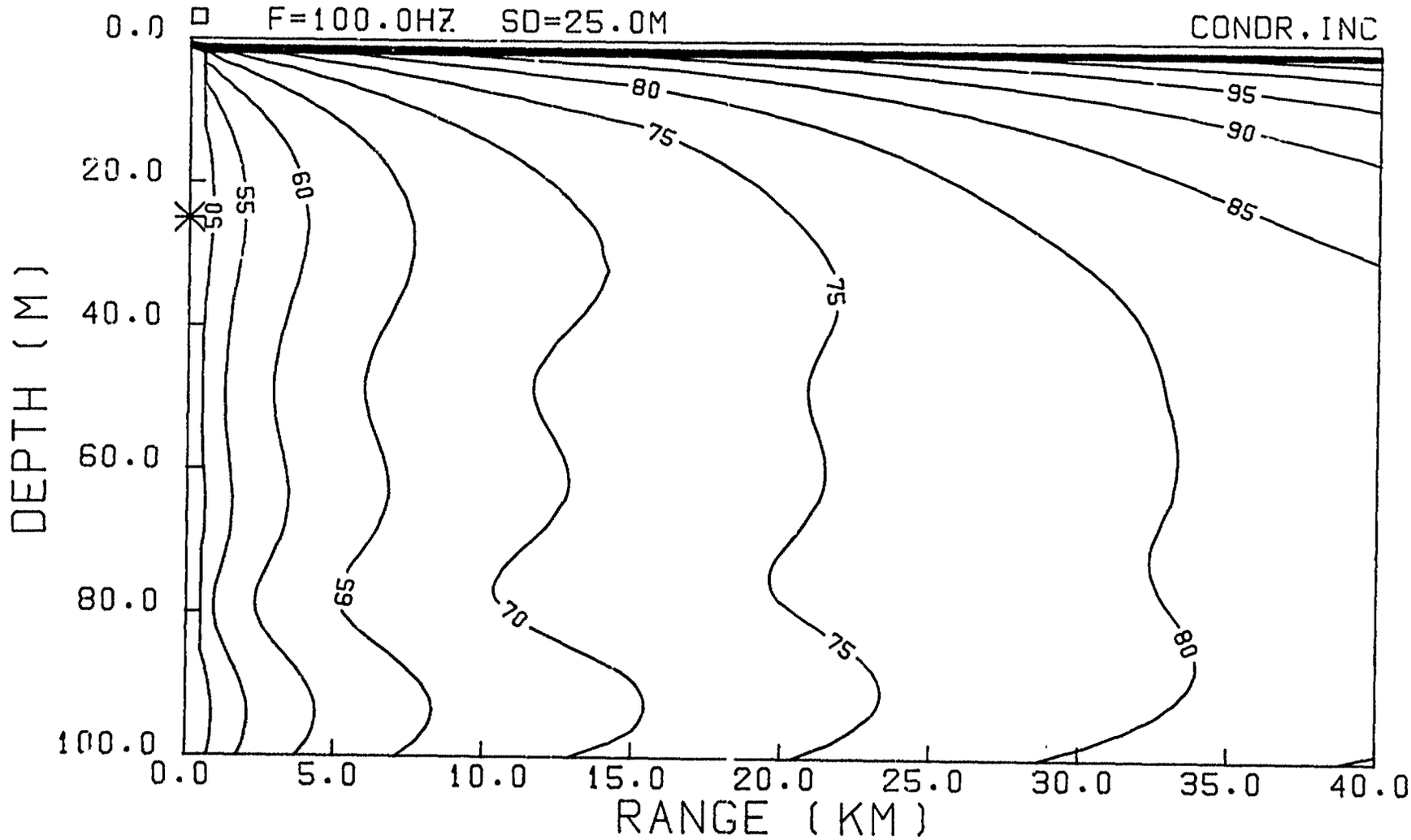

FIG. B18 CONTOURED LOSS VERSUS DEPTH AND RANGE BY INCOHERENT ADDITION OF MODES

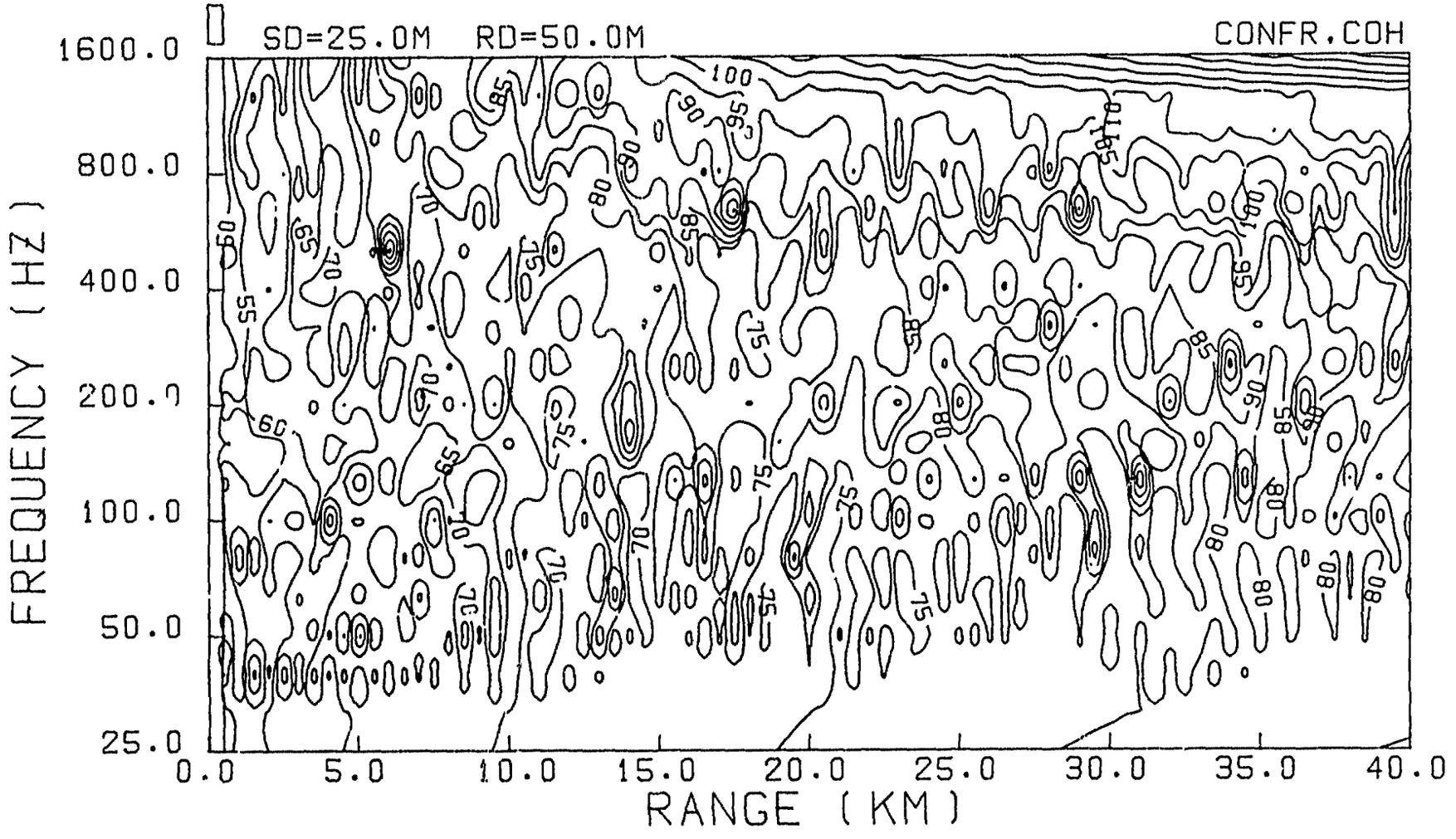

FIG. B19 CONTOURED LOSS VERSUS FREQUENCY AND RANGE BY COHERENT ADDITION OF MODES

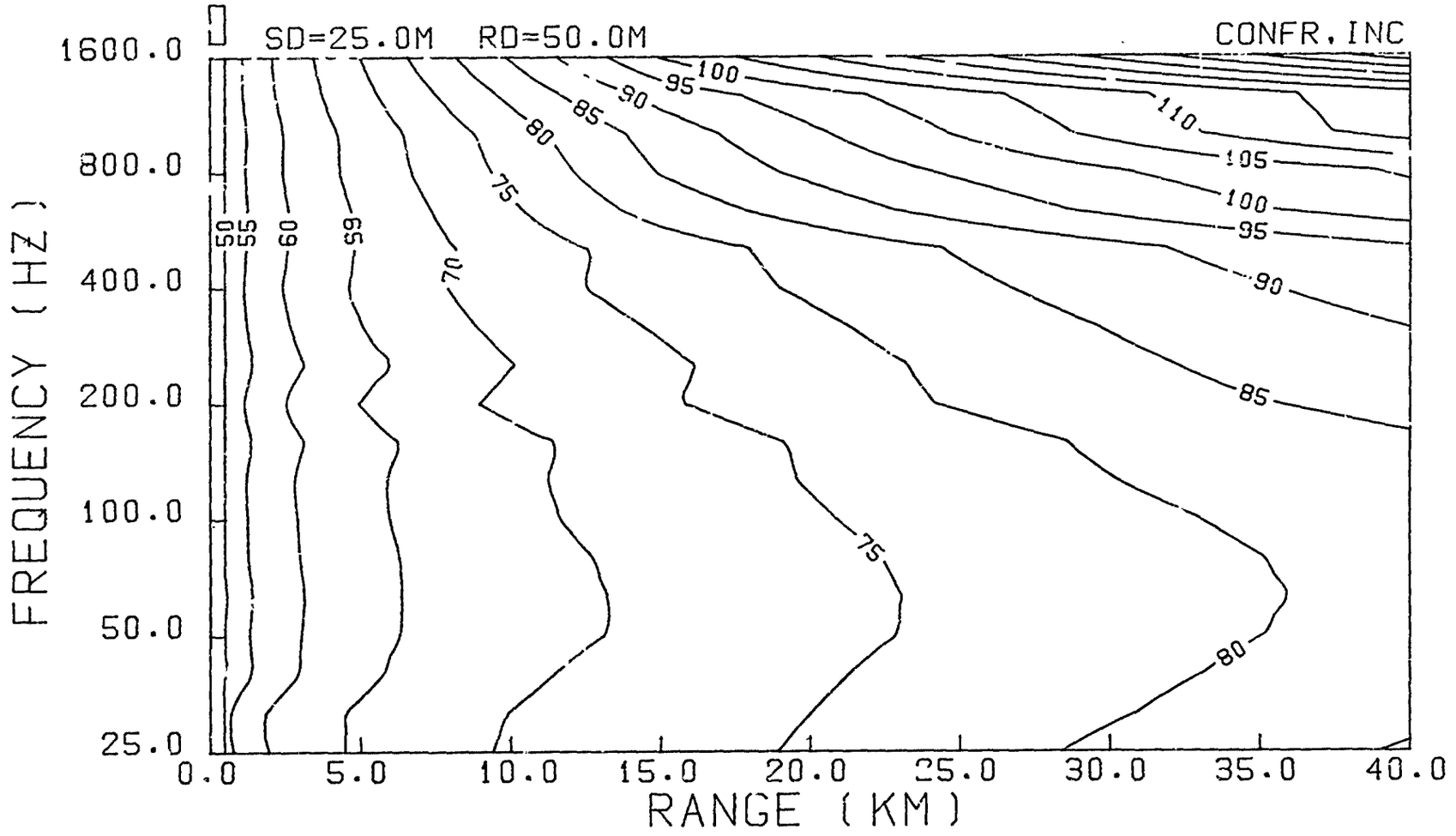

FIG. B20 CONTOURED LOSS VERSUS FREQUENCY AND RANGE BY INCOHERENT ADDITION OF MODES

APPENDIX C

PROGRAM DESCRIPTION AND FLOW DIAGRAMS

INTRODUCTION

The SNAP program consists of seven absolute elements:

a) SNAP.A50
b) SNAP.A100
c) SNAP.A200
d) SNAP.GRIDDER
e) SNAP.CONTOURER-FR
f) SNAP.CONTOURER-DR
g) SNAP.ADDRIVER

The only difference between the first three elements (a, b, and c) is the number of points used for sampling the acoustic field over the water column (see Appendix A). The last four elements (d, e, f, and g) are automatically executed whenever a contour option is requested.

All absolute elements run on a UNIVAC 1106 computer. The symbolic elements are written in the UNIVAC 1100 FORTRAN V language, with the exception of three elements written in the UNIVAC 1100 NUALGOL language. The TFOR, the FOR, and the NUALG compilers are used, together with the UNIVAC 1100 System Library and the FORTRAN V Library. The plotting is done utilizing the UNI*TEKX software package developed at SACLANTCEN *[C.1]*, and plot outputs can be displayed both on the video-terminals and on the CALCOMP 960 table-plotter.

The required storage allocation for the SNAP programs is given in Table C1.

TABLE C1

PROGRAM STORAGE ALLOCATION

PROGRAM	DECIMAL LOCATIONS
SNAP.A50	49672
SNAP.A100	51332
SNAP.A200	59780
SNAP.GRIDDER	25483*
SNAP.CONTOURER-FR	30867*
SNAP.CONTOURER-DR	34156*
SNAP.ADDRIVER	2354

Size at map time. The main program is an ALGOL program and the actual size will dynamically increase at execution time depending on the amount of data to be contoured.

C.1 SNAP.A50,SNAP.A100,SNAP.A200

These programs are written entirely in FORTRAN V and all routines are compiled with the TFOR compiler. The programs are segmented in order to keep their size to a minimum. Arrays and variables are used and re-used as the calculations loop through the various options and step through the various segments in range. Both SDF data files and binary written files are used, their number depending on the number of plots requested. All files are temporary files. Intermediate results needed for producing the plots are saved in binary written files using the UNIVAC NTRAN I/O processing technique.

The programs have a modular structure, which means that new options can be added or the existing ones removed without too much programming effort.

The map instructions used for producing an absolute element are:

```
@MAP,IN    C,ABS
SEG A
IN SNAP.DRIVER,.FILE,.RANGE
IN SNAP.COHRNT,.INCRNT
IN SNAP.ASIZE
IN NBFO4$
LIB UNI*TEKX.
CLASS FOR68
SEG B*,(A)
IN SNAP.INPUT
SEG C*,(A)
IN SNAP.MODE
SEG E*,(A)
IN SNAP.TLRAN
SEG G*,(A)
IN SNAP.TLAVR
SEG H*,(A)
IN SNAP.TLDEP
SEG H1*,(A)
IN SNAP.ANGLE
SEG H2*,(A)
IN SNAP.PHASE
SEG H3*,(A)
IN SNAP.CONDR
SEG H3B*,(A)
IN SNAP.CONFR
SEG H4*,(A)
IN SNAP.TLAVF
SEG H5*,(A)
IN SNAP.PROFL
SEG H6*,(A)
IN SNAP.MODES
SEG I*,(E,G,H,H1,H2,H3,H3B,H4)
IN SNAP.MODFUN
SEG L*,(E,G,H,H1,H2,H4,H5)
IN SNAP.PLOTT
IN SNAP.XAXLOG
SEG N*,(L,H6)
IN SNAP.XAXLIN,.YAXLIN
END
```

The flow of logic through the various routines and the links to the contouring programs are illustrated in Fig. C1, and a brief functional description of each subroutine is given below:

ANGLE calculates field intensity versus arrival angle. Print and plot outputs are produced only for those modes having real arrival angles.

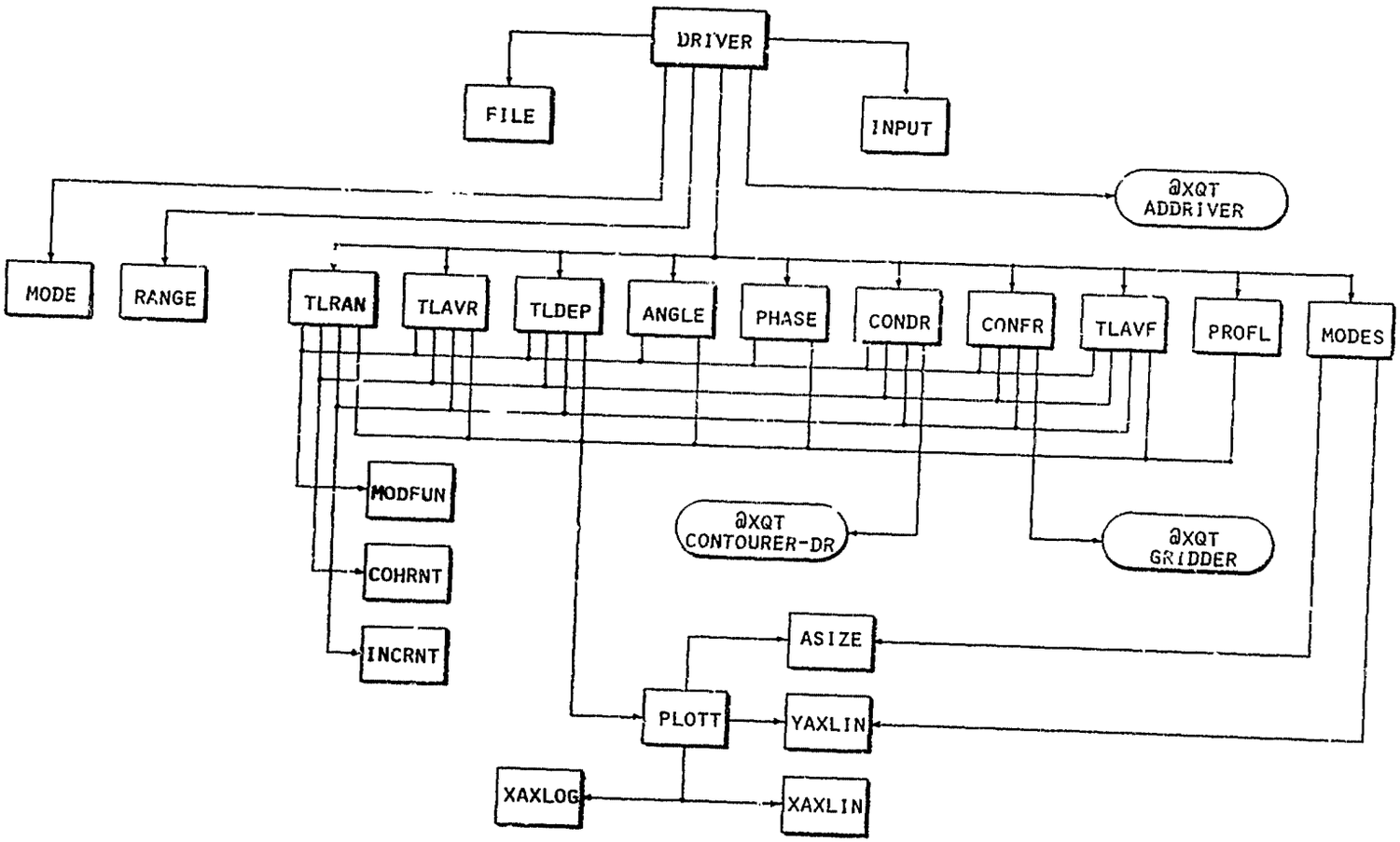

FIG. C1 SUBROUTINE FLOW DIAGRAM OF THE SNAP.A50, SNAP.A100, AND SNAP.A200 PROGRAMS

ASIZE chooses the correct sheet size for plotted output (A0 to A4 of the International Organization for Standardization paper sizes).

COHRNT calculates transmission loss by coherent addition of modes. Range-dependent parameters, such as wave numbers, mode amplitudes, attenuation coefficients, and water depth are interpolated here, while calculations loop through the various range steps.

CONDR provides transmission loss versus depth and range to be contoured by program SNAP.CONTOURER-DR. For each combination of frequency, source depth, and calculation-type specification (COH,INC) given in the input, this subroutine creates two temporary files. The first is a SDF data file that contains the control statement @XQT SNAP.CONTOURER-DR followed by some identifiers and contour parameters. When calculations have terminated, the control statement and all of the data contained in this file are automatically added to the run stream. The second file is a binary-written, random-access, data file containing the transmission losses to be contoured. Values are calculated on a rectangular equidistant grid in depth and range, where the depth covered is always from 0 to H_o.

CONFR provides transmission loss as a function of frequency and range to be gridded by program SNAP.GRIDDER and then contoured by program SNAP.CONTOURER-FR. For each combination of source/receiver depth and calculation-type specification (COH,INC) given in the input, this subroutine creates two temporary files. The first is a SDF data file that contains the control statement @XQT SNAP.GRIDDER, followed by some identifiers and contour parameters. When calculations have terminated, the control statement and all of the data contained in this file are automatically added to the run stream. The second file is a binary-written, random-access, data file containing the transmission losses to be contoured. Since values are generally calculated on a non-equidistant grid (arbitrary frequency spacing), the data have to be mapped onto an equidistant grid before carrying out the contouring. This latter transformation is performed by program SNAP.GRIDDER by interpolation.

DRIVER is the main program. It controls the looping through frequencies and segments in range for the various computational and output options. It also prints out a table showing the type of input and the type of calculation requested for each option.

FILE deals with the initial assignment of data files and with the filling of some arrays. As the calculations step through the various segments in range the files are updated accordingly.

INCRNT calculates transmission loss by incoherent addition of modes. Range-dependent parameters, such as wave numbers, mode amplitudes, attenuation coefficients, and water depth are interpolated here while calculations loop through the various range steps.

INPUT reads both the environmental and the computational input data. The environmental data are checked and stored into a binary file. Self-explanatory messages are provided for some of the most common input errors.

MODE calculates eigenvalues (wave numbers), normalized eigenvectors (mode functions), and attenuation coefficients for all modes, and stores the mode functions into a binary-written file. This subroutine also prints the environmental input for which calculations are done, together with some basic modal properties.

MODES produces print and plot of the normalized mode functions.

MODFUN reads mode amplitude values from a file created by subroutine MODE and stores appropriate values in arrays.

PHASE calculates phase distribution over depth.

PLOTT contains the plot routines for all options except MODES, CONDR, and CONFR.

PROFL produces a plot of the input sound-speed profile.

RANGE calculates for each option the number of sample points in range falling within a particular segment.

TLAVF provides depth-averaged transmission loss versus frequency.

TLAVR provides depth-averaged transmission loss versus range.

TLDEP provides transmission loss versus depth.

TLRAN provides transmission loss versus range.

XAXLIN draws the x-axis with centred title, with tick marks, and with data values on a linear scale.

XAXLOG draws the x-axis with centred title, with tick marks, and with data values on a logarithmic scale.

YAXLIN draws the y-axis with centred title, with tick marks, and with data values on a linear scale.

C.2 SNAP.GRIDDER

This program takes an arbitrarily-placed set of data points and fits them onto a rectangular equidistant grid by performing a two-dimensional interpolation.

There are NX points in the X direction [NX = (rmax-rmin)/delr + 1] and NY points in the Y direction (NY = number of input frequencies). The program produces two temporary files. The first is a SDF data file containing the control statement @XQT SNAP.CONTOURER-FR followed by some identifiers and control parameters. After the gridding is done, the control statement and all of the data contained in this file are automatically added to the run stream. The second file is a binary-written file that contains the gridded data.

The execution of the program is automatically triggered by programs SNAP.A50, SNAP.A100, and SNAP.A200 if the programs are executed in batch mode, otherwise it is triggered by program SNAP.ADDRIVER.

The main program is written in NUALGOL and is compiled with the NUALG compiler, while the subroutines are written in FORTRAN V and are compiled with the FOR compiler.

Subroutines ZGRID and SMOOTH have been developed at the Department of Energy, Mines, and Resources, Ottawa, Canada *[C.2]*.

The map instructions used for producing the absolute element are:

```
@MAP,IS    C,SNAP.GRIDDER
IN SNAP.GRIDDER,.ZGRID,.SMOOTH,.READF
END
```

Figure C2 illustrates the flow of logic through the various subroutines and the link to the contouring program.

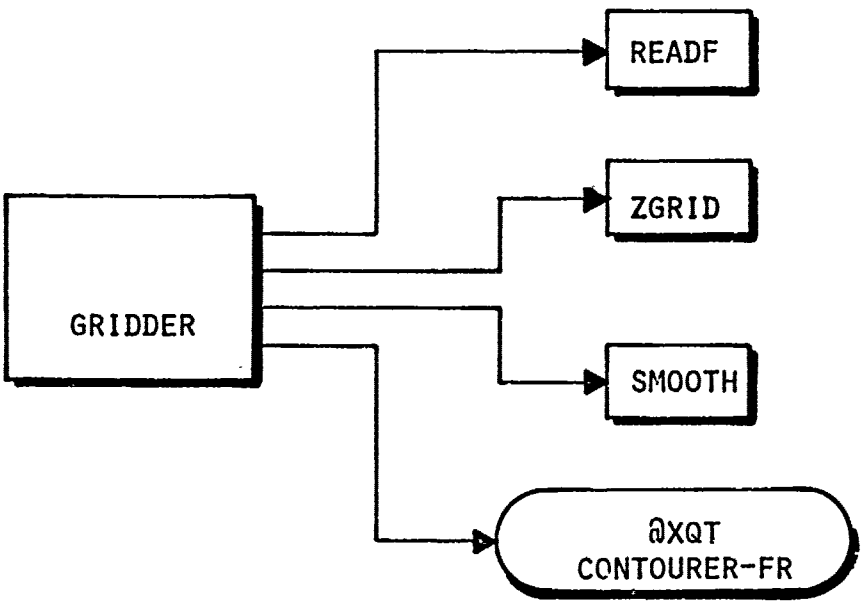

FIG. C2 SUBROUTINE FLOW DIAGRAM OF PROGRAM SNAP.GRIDDER

Below is given a brief functional description of each subroutine:

GRIDDER is the main program. It reads the contour parameters and the data to be contoured from two files produced by subroutine CONFR; it also calls the subroutines needed for mapping the data onto a rectangular, equidistant grid.

READF is a subroutine that makes it possible for an ALGOL program to read FORTRAN-written files, in this case the SDF data files written by subroutine CONFR.

SMOOTH smoothes the surface established over the rectangular, equidistant grid.

ZGRID performs two-dimensional interpolation from arbitrarily-spaced data points onto a rectangular equidistant grid. A combination of a two-dimensional Laplacian and Spline interpolation is used and all frequency values are converted to a logarithmic scale before the interpolation is made.

C.3 SNAP.CONTOURER-FR

This program contours data on an equidistant grid and produces a plot. The execution of the program is automatically triggered by program SNAP.GRIDDER.

The main program is written in NUALGOL and it is compiled with the NUALG compiler. The subroutines, on the other hand, are written in FORTRAN V and are compiled with the FOR compiler.

The map instructions used for producing the absolute element are:

```
@MAP,IN    C,SNAP.CONTOURER-FR
IN  SNAP.CONTOURER-FR
IN  SNAP.XAXLIN-C,.YAXLOG-C
IN  SNAP.ASIZE-C
IN  SNAP.CONSEG,.DOUBLE,.CONTUR,.PLOTNY,.ARC
LIB  UNI*TEKX.
END
```

Subroutines ARC, CONSEG, CONTUR, DOUBLE, and PLOTNY have been developed at the Department of Energy, Mines, and Resources, Ottawa, Canada *[C.2]*.

The flow of logic through the various subroutines is illustrated in Fig. C3, and a brief functional description of each subroutine is given below:

ARC creates a series of smooth-flowing arcs from a series of straight-line segments.

ASIZE-C chooses the correct sheet size for plotted output (A0 to A4 of the International Organization for Standardization paper sizes).

CONSEG calls DOUBLE and CONTUR to subdivide the grid and contour the surface in segments.

CONTOURER-FR is the main program. It reads the files created by program SNAP.GRIDDER and calls the subroutines needed for producing the contour plot.

CONTUR calculates contours as strings of data points and plots them.

DOUBLE halves the grid using cubic polynomials.

PLOTNY plots an ordinary, heavy, or dotted line segment.

XAXLIN-C draws the x-axis with centred title, with tick marks, and with data values on a linear scale.

YAXLOG-C draws the y-axis with centred title, with tick marks, and with data values on a logarithmic scale

C.4 SNAP CONTOURER-DR

This program contours data on an equidistant grid and produces a plot. The execution of the program is automatically triggered by either SNAP.A50, SNAP.A100, SNAP.A200, or SNAP.ADDRIVER. The main program is written in NUALGOL and is compiled with the NUALG compiler. The subroutines, on the other hand, are written in FORTRAN V and are compiled with the FOR compiler.

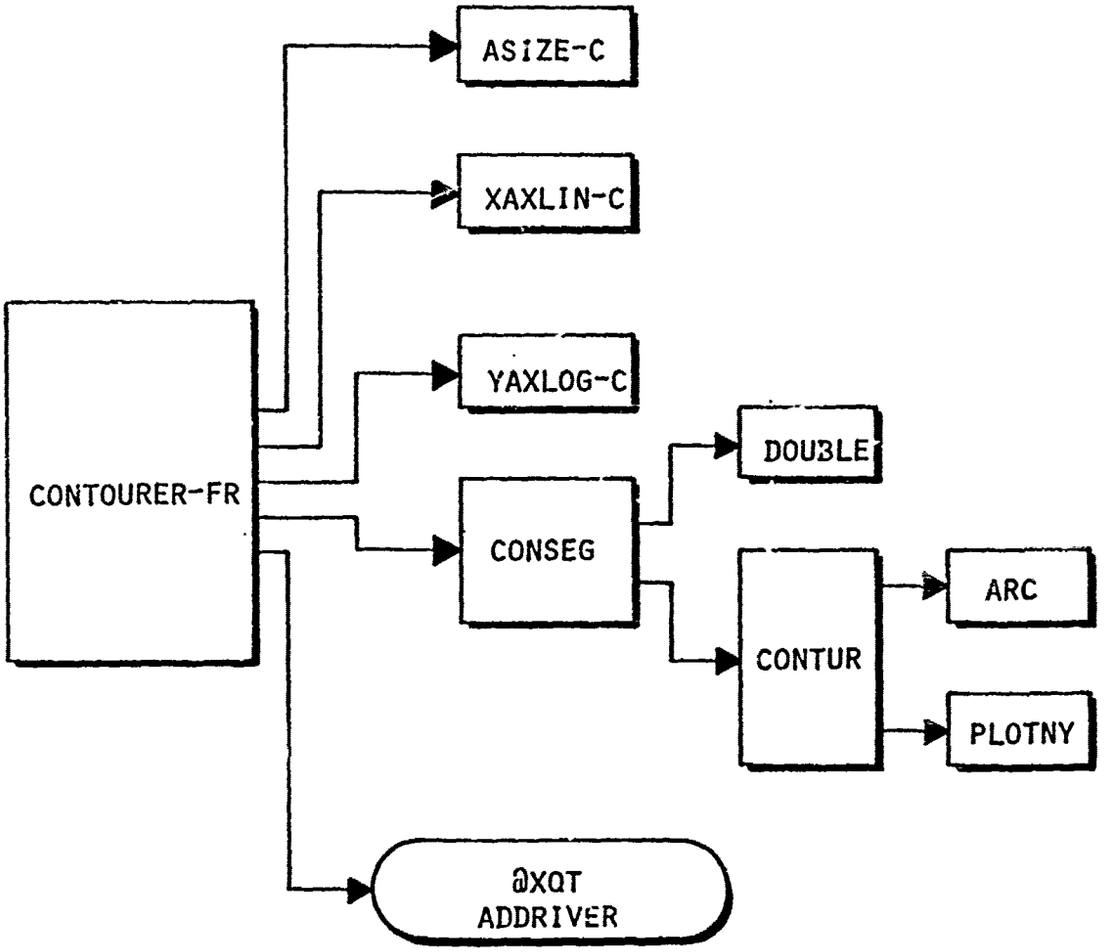

FIG. C3 SUBROUTINE FLOW DIAGRAM OF PROGRAM SNAP.CONTOURER-FR

The map instructions used for producing the absolute element are:

```
@MAP,IN     C,SNAP.CONTOURER-DR
IN  SNAP.CONTOURER-DR,.READF
IN  SNAP.XAXLIN-C,.YAXLIN-C
IN  SNAP ASIZE-C
IN  SNAP.CONSEG, DOUBLE,.CONTUR,.PLOTNY,.ARC
LIB UNI*TEKX.
END
```

Subroutine READF is the same as described for program SNAP.GRIDDER, while subroutines ARC, CONSEG, CONTUR, DOUBLE, PLOTNY, and XAXLIN-C are the same as described for program SNAP.CONTOURER-FR.

A brief functional description of the remaining two subroutines is given below.

CONTOURER-DR is the main program. It reads the contour parameters and the data to be contoured from two files created by subroutine CONDR and calls the subroutines for producing the contour plot.

YAXLIN-C draw the y-axis with centred title, with tick marks, and with data values on a linear scale.

Figure C4 illustrates the flow of the logic through the various subroutines.

C.5 SNAP.ADDRIVER

This program adds to the run stream the SDF data files produced by subroutines CONDR and CONFR of programs SNAP.A50, SNAP.A100, and SNAP.A200. The files are added one at the time, the next one being added only after some plot options for the previous one have been selected via the terminal keyboard.

The program is used only when SNAP.A50, SNAP.A100, and SNAP.A200 are executed in demand mode. In batch mode the SDF data files are immediately added to the run stream by subroutines CONDR and CONFR.

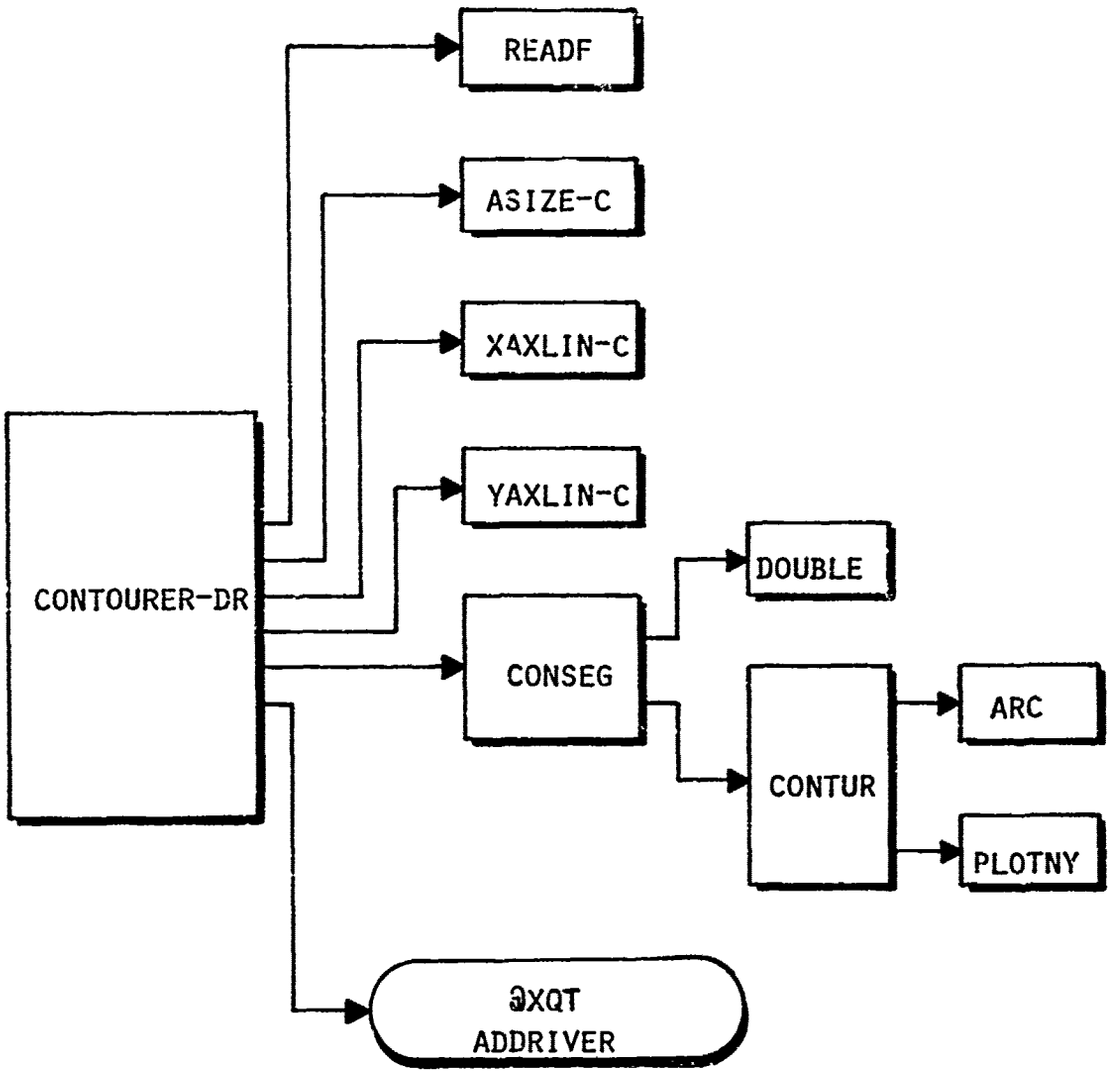

FIG. C4 SUBROUTINE FLOW DIAGRAM OF PROGRAM SNAP.CONTOURER-DR

The map instructions used for producing an absolute element are:

```
@MAP,IS     C,SNAP.ADDRIVER
IN SNAP.ADDRIVER
END
```

REFERENCES

C.1 GOUDRIAAN, E. UNI*TEKX: Univac/Tektronix graphics system for 1100 series computers, Tektronix terminals and Calcomp plotters. (Internal Users' Guide). La Spezia, Italy, SACLANT ASW Research Centre, 1976.

C.2 TAYLOR, J. et al. Computer routines for surface generation and display, Manuscript Report No. 16. Ottawa, Canada, Department of Energy, Mines, and Resources, 1971.

APPENDIX D

FEATURES OF THE RANGE-INDEPENDENT VERSION OF SNAP

INTRODUCTION

The range-independent version of SNAP has been derived from the general-purpose range-dependent version in order to create a smaller and faster program version for handling the many propagation conditions in which range dependence is of minor importance. The range-independent version (SNAP1) works essentially as the range-dependent version (SNAP) with only one range segment. However, the elimination of the range-dependent features from SNAP results in a simpler program structure, a smaller program size, and in somewhat shorter running times. Since very few changes have been made to the essential features of the model, the description given in the main text also applies to this range-independent version, with the few changes and additions given below.

D.1 PROGRAM STRUCTURE AND SIZE

The program description given in Appendix C also applies to the SNAP1 version if all references to range segments are disregarded and if SNAP1 is read for SNAP throughout. An extra output option (GROUP) has been added, leading to a slight modification of the subroutine flow diagram, as shown by the dashed lines in Fig. D1.

By virtue of less file writing and reading (input/output on temporary files) the running time has been reduced by up to 25% depending on the type of calculation requested.

The program size has been reduced slightly for the three main programs, as shown below, but the contouring routines are unchanged.

PROGRAM NAME	DECIMAL LOCATIONS
SNAP1.A50	47901 (-1771)
SNAP1.A100	48601 (-2731)
SNAP1.A200	49971 (-9809)

Actually, the SNAP1 program may take any size from 20 k to 50 k depending on the number of output options attached. Thus, the smallest size of 20 k is obtained by limiting the possible outputs to plotting of sound-speed profile (PROFL), of model depth functions (MODES), and of transmission loss versus range (TLRAN).

D.2 GROUP VELOCITY CALCULATIONS

The calculation of group velocity versus frequency for the various modes has been added as an output option to SNAP1. The group velocity U_n for the n'th mode is determined by

$$U_n = \frac{\partial \omega}{\partial k_n} \quad ,$$

where ω is the source frequency ($\omega = 2\pi f$) and k_n the horizontal modal wave number. In the program this derivative is evaluated numerically by calculating the wave numbers for two adjacent frequencies $f_o \pm 1/100$ Hz, with f_o being the centre frequency.

Examples of group velocity calculations are given in Figs. D2 and D3. Generally, dispersion curves are displayed for up to ten modes per graph, and the number of frequencies and modes for which calculations are carried out is determined by the input parameters [NF] and [MMIN,MMAX], respectively.

The specific examples given in Figs. D2 and D3 are based on the same environmental input as used earlier for illustrating the various output options of SNAP. Thus, Fig. D2 shows dispersion curves for the deep-water environment used in Ch. 4 of the main text, while the environment used in Fig. D3 is identical to the first segment of the shallow-water

case described in Appendix B. In both cases, the number of frequency samples were around 50 and the running time per graph less than 10 minutes. A low-frequency cut-off is a common feature to all modes. Furthermore, the shallow-water case (Fig. D3) shows a clear minimum (the Airy phase) on all dispersion curves close to modal cut-off.

D.3 PROGRAM EXECUTION

The necessary information for running the range-independent SNAP model is as given in Appendix A if SNAP1 is read for SNAP throughout and the following few changes to the inputs are made.

Three program versions are available: SNAP1.A50, SNAP1.A100, and SNAP1.A200. The standard program version, SNAP1.A50, can be executed by preparing a run stream as shown in Fig. D4. The @RUN card is followed by two instructions for copying the contents of file SNAP1*SNAP1 into file OWNPROJID*SNAP1. This is done to avoid interference with other users of the model. The copying should be done only once, hence the dashed lines around the two statements. Now, the executable program versions are catalogued under the user's own project identifier (OWNPROJID), but the file name is still SNAP1. *In fact, it is essential to the automatic program execution that the file name SNAP1 is kept unchanged.* As seen from Fig. D4, the @XQT statement is followed directly by the input data prepared according to the directions given in Tables D1-D5. Finally, an @EOF card indicates termination of the data stream.

The environment handled by SNAP1 is shown in Fig. D5, and all inputs are given in Tables D1-D2, with some additional information listed in Tables D3-D5. Compared with the SNAP inputs, the specification of number of segments in range and segment length has been removed from Table D1, while the new output option GROUP has been added in Table D2.

SUMMARY

The range-independent SNAP version documented here is both smaller and faster than the original version. Furthermore, the program structure is less complicated, making it easier to implement this model on a different computer system. The range-independent SNAP version will in the near future be combined with a surface-noise model as a first step towards creating a complete sonar-performance prediction model based on wave theory.

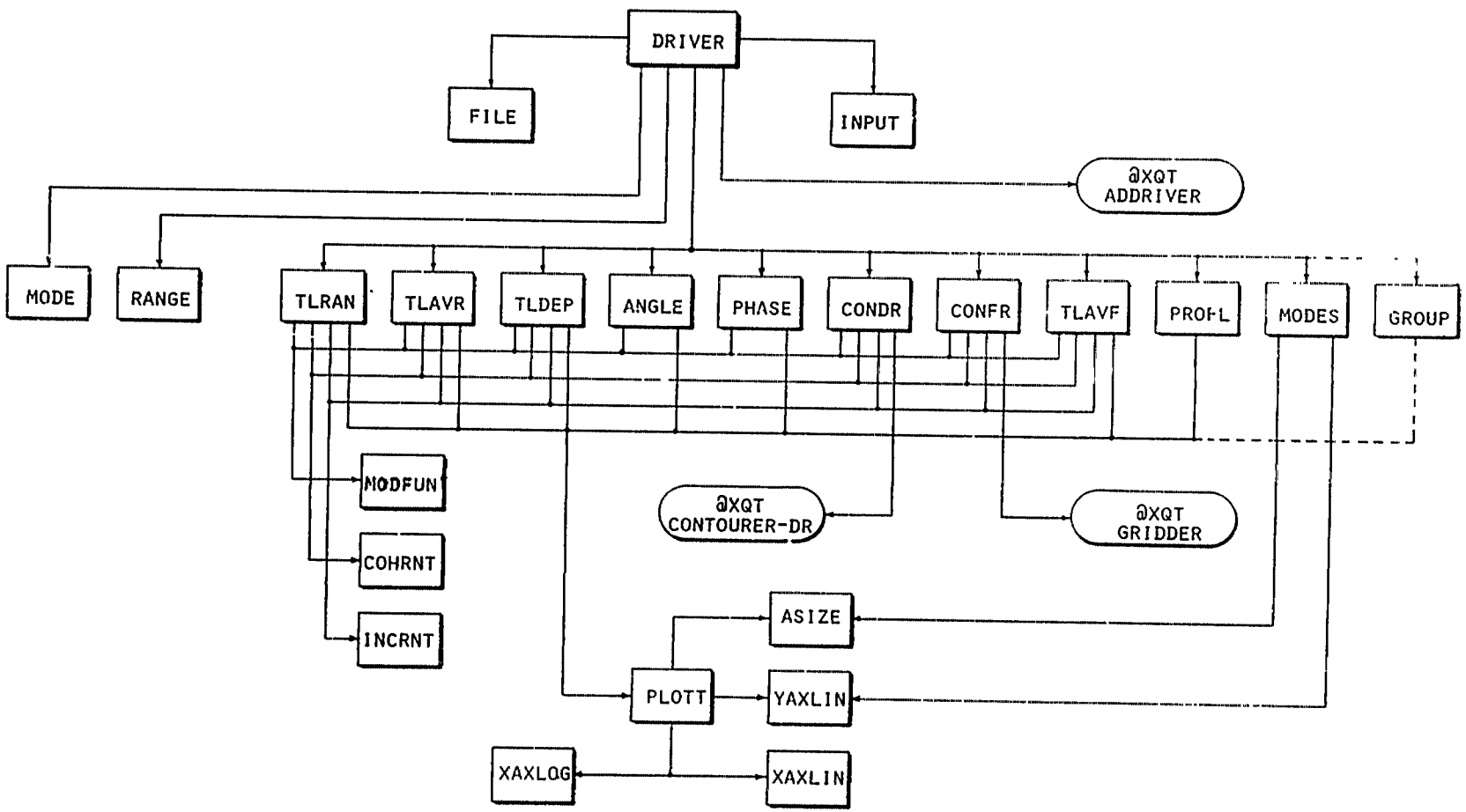

FIG. D1 SUBROUTINE FLOW DIAGRAM OF THE SNAP1.A50, SNAP1.A100, AND SNAP1.A200 PROGRAMS

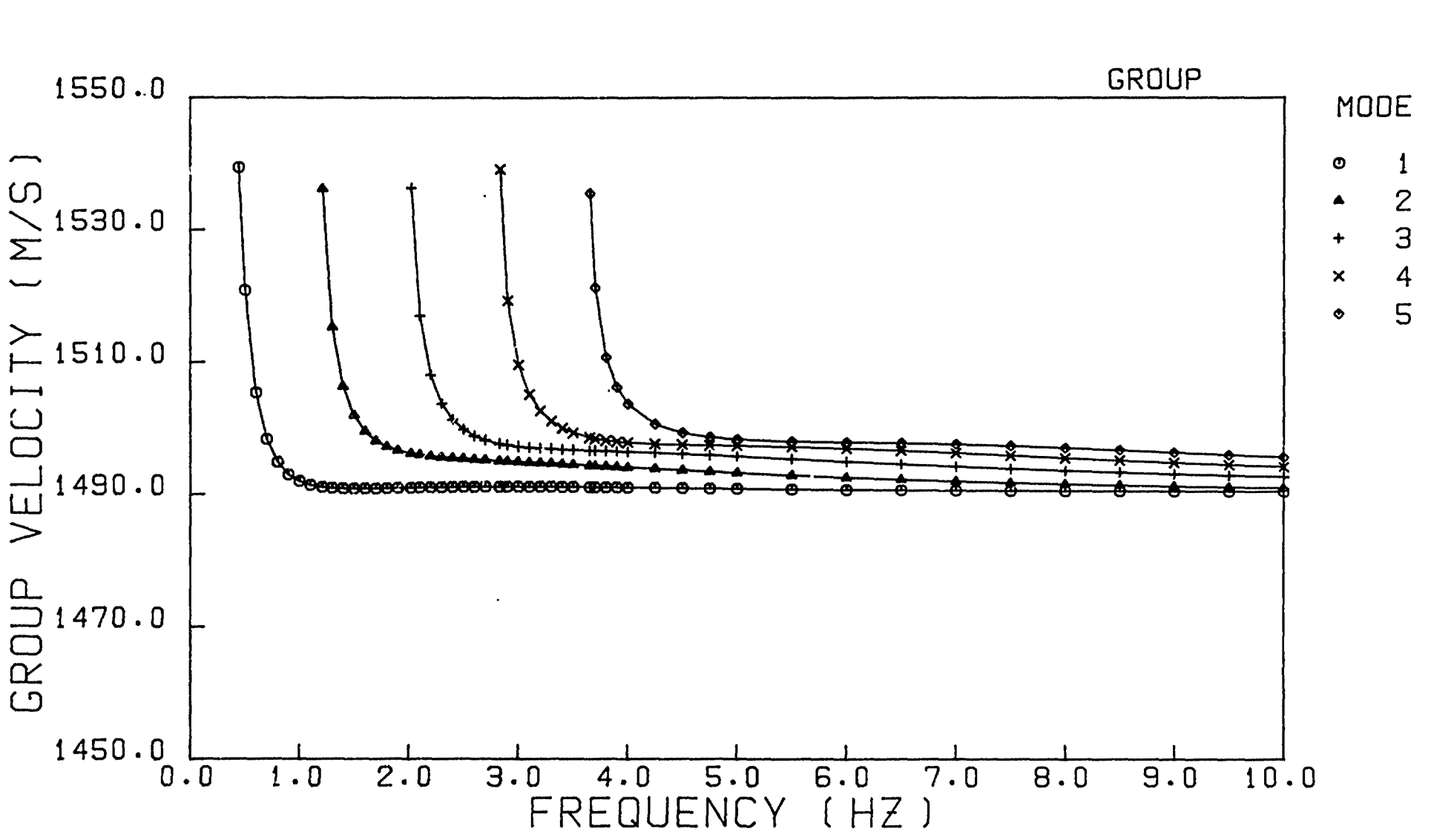

FIG. D2 GROUP VELOCITY VERSUS FREQUENCY (DEEP WATER)

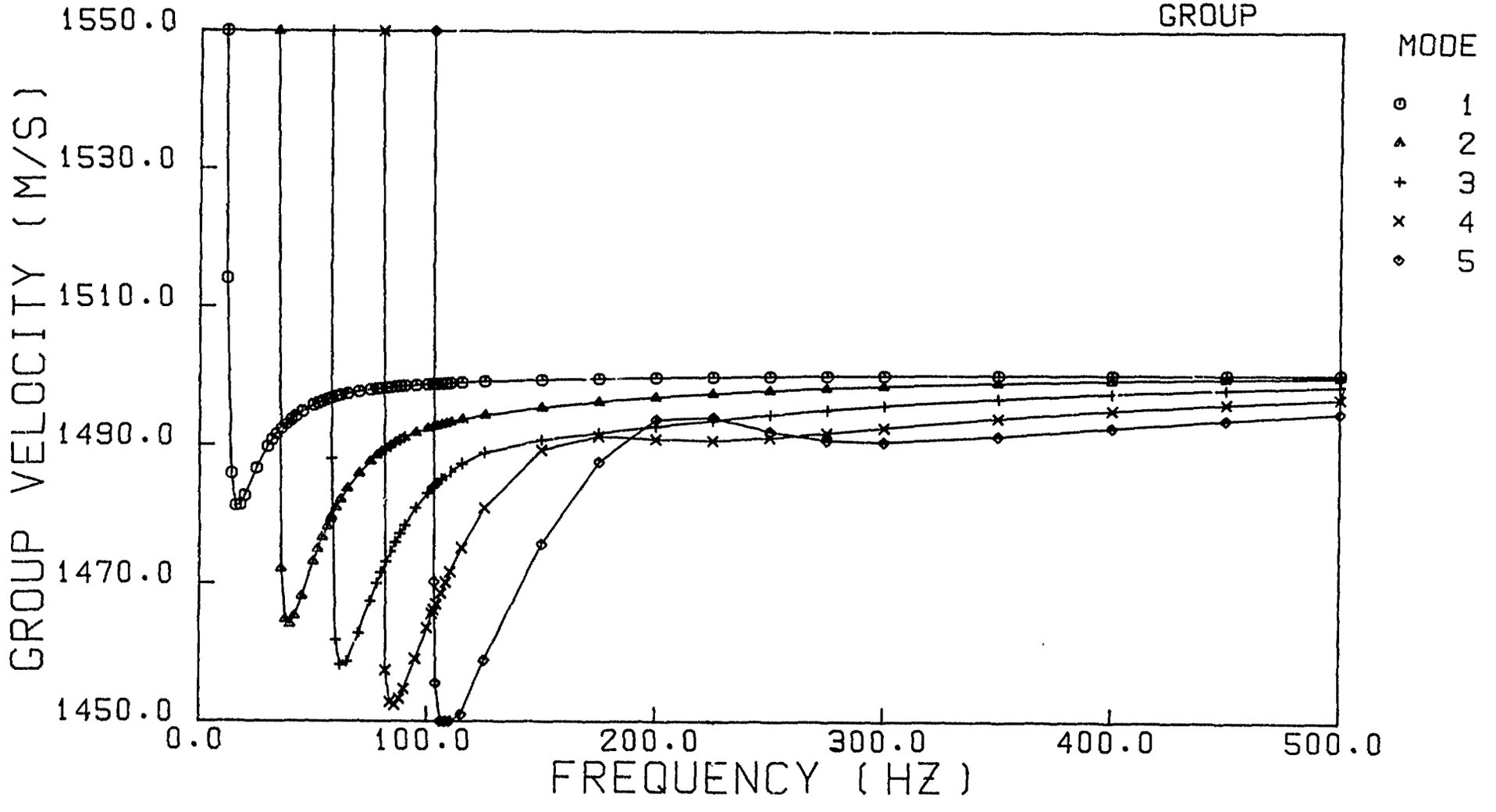

FIG. D3 GROUP VELOCITY VERSUS FREQUENCY (SHALLOW WATER)

```
@RUN  .....,.....,OWNPROJID,..
@ASG,UP   SNAP1.
@COPY,A   SNAP1*SNAP1.,SNAP1.
@XQT  SNAP1.A5Ø
Input data from
Tables D1 and D2
@EOF
```

FIG. D4 RUN STREAM FOR PROGRAM EXECUTION

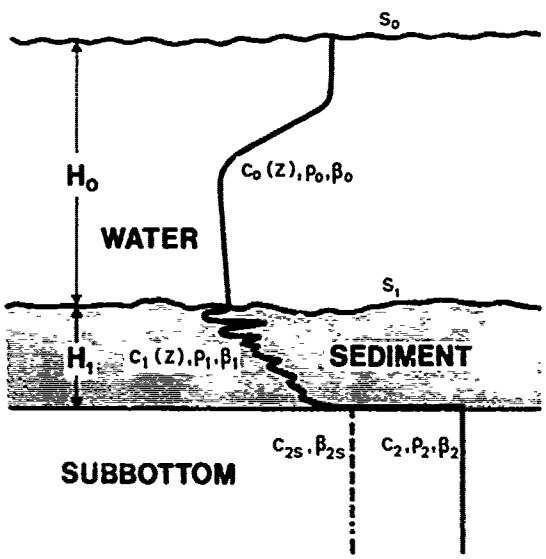

FIG. D5 ENVIRONMENT HANDLED BY THE SNAP1 MODEL

TABLE D1 SUMMARY OF SNAP1 INPUTS (PART I)

INPUT PARAMETER	EXPLANATION	UNIT	LIMITS
TITLE	Text on plots	-	≤ 80 characters
NF	No. of source frequencies	-	NF ≤ 100
F(1),·····F(NF)	Source frequencies	Hz	F > 0
MMIN,MMAX	MMIN: First mode to be calculated MMAX: Last mode to be calculated	- -	1 ≤ MMIN ≤ MMAX ≤ 500
LI0,LI1	LI0: No. of discretization points in water LI1: No. of discretization points in sediment	- -	0 < LI0+LI1 ≤ 2500
H0,S0,S1	H0: Water depth in first segment S0: RMS roughness of sea surface S1: RMS roughness of sea bottom	m m m	H0 > 0 S0 ≥ 0 S1 ≥ 0
Z0(1),C0(1)	Z0(1): First sound-speed profile depth (≡ 0) C0(1): First sound-speed profile value in water	m m/s	- -
⋮	⋮	⋮	⋮
Z0(n),C0(n)	Z0(n): Last sound-speed profile depth (≡ H0) C0(n): Last sound-speed profile value in water	m m/s	2 ≤ n ≤ 100
H1,R1,B1	H1: Thickness of sediment layer R1: Density of sediment B1: Compressional wave attenuation in sediment	m g/cm³ dB/λ	H1 ≥ 0 R1 > 0 B1 ≥ 0
Z1(1),C1(1)	Z1(1): First sound-speed profile depth (≡ 0) C1(1): First sound-speed profile value in sediment	m m/s	- -
⋮	⋮	⋮	⋮
Z1(m),C1(m)	Last sound-speed profile depth (≡ H1) Last sound-speed profile value in sediment	m m/s	2 ≤ m ≤ 100
R2,B2,C2	R2: Density of subbottom B2: Compressional attenuation in subbottom C2: Compressional speed in subbottom	g/cm³ dB/λ m/s	R2 > 0 B2 ≥ 0 C2 > 0
B2S,C2S	B2S: Shear attenuation in subbottom C2S: Shear speed in subbottom	dB/λ m/s	$0 \leq B2S < 0.75\,B2\left(\frac{C2}{C2S}\right)^2$ 0 ≤ C2S << C1(H1)

TABLE D2 SUMMARY OF SNAP1 INPUTS (PART II)

1) ANGLE,PLT,PRT XAXIS x_1,x_2,x_3,x_4 YAXIS y_1,y_2,y_3,y_4 rmin,rmax,delr sd(1),rd(1) ⋮ sd(n),rd(n)	2) CONDR,INC,COH,PLT rmin,rmax,delr zmin,zmax,delz sd(1) ⋮ sd(n)	3) CONFR,INC,COH,PLT rmin,rmax,delr zmin,zmax,delz sd(1),rd(1) ⋮ sd(n),rd(n)	4) GROUP,PLT,PRT
5) MODES,PLT,PRT	6) PHASE,PLT,PRT rmin,rmax,delr sd(1) ⋮ sd(n)	7) PROFL,PLT	8) TLAVF,INC,COH,PLT,PRT rmin,rmax,delr sd(1) ⋮ sd(n)
9) TLAVR,INC,COH,PLT,PRT rmin,rmax,delr sd(1) ⋮ sd(n)	10) TLDEP,INC,COH,PLT,PRT rmin,rmax,delr sd(1) ⋮ sd(n)	11) TLRAN,INC,COH,PLT,PRT rmin,rmax,delr sd(1),rd(1) ⋮ sd(n),rd(n)	

TABLE D3 DEFINITION OF INPUT CODES USED IN PART II

INPUT CODE	EXPLANATION
ANGLE	Field intensity vs arrival angle
CONDR	Contoured transmission loss vs depth and range
CONFR	Contoured transmission loss vs frequency and range
GROUP	Group velocity vs frequency
MODES	Individual mode functions vs depth
PHASE	Phase of acoustic field vs depth
PROFL	Sound speed vs depth
TLAVF	Depth-averaged transmission loss vs frequency
TLAVR	Depth-averaged transmission loss vs range
TLDEP	Transmission loss vs depth
TLRAN	Transmission loss vs range
INC	Incoherent addition of modes
COH	Coherent addition of modes
PLT	Plotted output
PRT	Printed output
XAXIS	Identifier for horizontal axis
YAXIS	Identifier for vertical axis

TABLE D4 DEFINITION OF INPUT PARAMETERS USED IN PART II

INPUT PARAMETER	EXPLANATION	UNIT	LIMITS
x_1, x_2, x_3, x_4	x_1: Lowest data value on horizontal axis x_2: Highest data value on horizontal axis x_3: No. of data units per centimeter[1] x_4: Distance between tick marks in data units[2]	see Table D5	
y_1, y_2, y_3, y_4	y_1: Lowest data value on vertical axis y_2: Highest data value on vertical axis y_3: No. of data units per centimeter[1] y_4: Distance between tick marks in data units[2]	see Table D5	
rmin, rmax, delr	rmin: Minimum range for loss calculation rmax: Maximum range for loss calculation delr: Range increment[3]	km km km	$\emptyset \leq$ rmin $\leq$ rmax delr $\geq \emptyset$
zmin, zmax, delz	zmin: Minimum contour level zmax: Maximum contour level delz: Level increment[4]	dB dB dB	$\emptyset \leq$ zmin $\leq$ zmax delz $\geq \emptyset$
sd(1), rd(1)	sd(1): First source depth rd(1): First receiver depth	m m	$\emptyset <$ sd $\leq$ H$\emptyset$ $\emptyset <$ rd $\leq$ H$\emptyset$
⋮	⋮	⋮	⋮
sd(n), rd(n)	sd(n): Last source depth rd(n): Last receiver depth	m m	n $\leq$ 1$\emptyset$

[1]For logarithmic frequency axes this argument indicates the length of an octave in centimeters.

[2]For logarithmic frequency axes this argument indicates the number of subdivisions per octave ($x_4 \geq 1$). Ex: x_4=3 results in tick marks every 1/3 of an octave.

[3]No. of range steps cannot exceed 500.

[4]No. of contour level steps cannot exceed 51.

TABLE D5 DEFAULT AXIS VALUES

OPTION	X-AXIS								Y-AXIS							
	x_1		x_2		x_3		x_4		y_1		y_2		y_3		y_4	
ANGLE	$\emptyset$	deg	4$\emptyset$	deg	2	deg/cm	5	deg	4$\emptyset$	dB	14$\emptyset$	dB	5	dB/cm	2$\emptyset$	dB
CONDR	rmin	km	rmax	km	2	km/cm	5	km	$\emptyset$	m	H$\emptyset$	m	5	m/cm	2$\emptyset$	m
CONFR*	rmin	km	rmax	km	2	km/cm	5	km	F_{min}	Hz	F_{max}	Hz	2	cm/oct	1	-
GROUP	F_{min}	Hz	F_{max}	Hz	25	Hz/cm	1$\emptyset\emptyset$	Hz	145$\emptyset$	m/s	155$\emptyset$	m/s	5	m/s/cm	2$\emptyset$	m/s
MODES	-$\emptyset$.2	**	$\emptyset$.2	**	.12	**/cm	$\emptyset$.2	**	$\emptyset$	m	H$\emptyset$+H1	m	5	m/cm	2$\emptyset$	m
PHASE	-18$\emptyset$	deg	18$\emptyset$	deg	18	deg/cm	45	deg	$\emptyset$	m	h$\emptyset$	m	5	m/cm	2$\emptyset$	m
PROFL	145$\emptyset$	m/s	165$\emptyset$	m/s	1$\emptyset$	m/s/cm	25	m/s	$\emptyset$	m	H$\emptyset$+H1	m	5	m/cm	2$\emptyset$	m
TLAVF*	F_{min}	Hz	F_{max}	Hz	3	cm/oct	1	-	4$\emptyset$	dB	14$\emptyset$	dB	5	dB/cm	2$\emptyset$	dB
TLAVR	rmin	km	rmax	km	2	km/cm	5	km	4$\emptyset$	dB	14$\emptyset$	dB	5	dB/cm	2$\emptyset$	dB
TLDEP	$\emptyset$	dB	16$\emptyset$	dB	3	dB/cm	2$\emptyset$	dB	$\emptyset$	m	H$\emptyset$	m	5	m/cm	2$\emptyset$	m
TLRAN	rmin	km	rmax	km	2	km/cm	5	km	4$\emptyset$	dB	14$\emptyset$	dB	5	dB/cm	2$\emptyset$	dB

*Option with logarithmic frequency axis.

**$(m^2/kg)^{\frac{1}{2}}$.

NB: The unit for loss is dB re 1 meter.

APPENDICES E AND F ARE OF SPECIALIZED INTEREST TO A LIMITED NUMBER OF USERS AND ARE THEREFORE PUBLISHED SEPARATELY AS SACLANTCEN SPECIAL MEMORANDA, M-91 AND M-92 RESPECTIVELY.

INITIAL DISTRIBUTION

MINISTRIES OF DEFENCE	Copies
MOD Belgium	2
DND Canada	10
CHOD Denmark	8
MOD France	8
MOD Germany	15
MOD Greece	11
MOD Italy	10
MOD Netherlands	12
CHOD Norway	10
MOD Portugal	5
MOD Turkey	5
MOD U.K.	16
SECDEF U.S.	61

NATO AUTHORITIES	
Defence Planning Committee	3
NAMILCOM	2
SACLANT	10
SACLANTREPEUR	1
CINCWESTLANT/COMOCEANLANT	1
COMIBERLANT	1
CINCEASTLANT	1
COMSUBACLANT	1
COMMAIREASTLANT	1
SACEUR	2
CINCNORTH	1
CINCSOUTH	1
COMNAVSOUTH	1
COMSTRIKFORSOUTH	1
COMEDCENT	1
COMMAR IRMED	1
CINCHAN	1

SCNR FOR SACLANTCEN	Copies
SCNR Belgium	1
SCNR Canada	1
SCNR Denmark	1
SCNR Germany	1
SCNR Greece	1
SCNR Italy	1
SCNR Netherlands	1
SCNR Norway	1
SCNR Portugal	1
SCNR Turkey	1
SCNR U.K.	1
SCNR U.S.	2
SECGEN Rep.	1
NAMILCOM Rep.	1

NATIONAL LIAISON OFFICERS	
NLO Canada	1
NLO Denmark	1
NLO Germany	1
NLO Italy	1
NLO U.K.	1
NLO U.S.	1

NLR TO SACLANT	
NLR Belgium	1
NLR Canada	1
NLR Germany	1
NLR Greece	1
NLR Italy	1
NLR Norway	1
NLR Portugal	1
NLR Turkey	1

Total initial distribution	232
SACLANTCEN STI Library	10
SACLANTCEN STI Stock	38
Total number of copies	280